African Journal of Biotechnology

Volume 15 Number 8, 24 February 2016

ISSN 1684-5315

Academic Journals

ABOUT AJB

The African Journal of Biotechnology (AJB) (ISSN 1684-5315) is published weekly (one volume per year) by Academic Journals.

African Journal of Biotechnology (AJB), a new broad-based journal, is an open access journal that was founded on two key tenets: To publish the most exciting research in all areas of applied biochemistry, industrial microbiology, molecular biology, genomics and proteomics, food and agricultural technologies, and metabolic engineering. Secondly, to provide the most rapid turn-around time possible for reviewing and publishing, and to disseminate the articles freely for teaching and reference purposes. All articles published in AJB are peer-reviewed.

Contact Us

Editorial Office: ajb@academicjournals.org

Help Desk: helpdesk@academicjournals.org

Website: http://www.academicjournals.org/journal/AJB

Submit manuscript online http://ms.academicjournals.me/

Editorial Board

African Journal of Biotechnology

Table of Content: Volume 15 Number 8 24 February, 2016

ARTICLES

academicJournals

Vol. 15(8), pp. 214-220, 24 February, 2016
DOI: 10.5897/AJB2014.13783
Article Number: 3709FA357324
ISSN 1684-5315

http://www.academicjournals.org/AJB

African Journal of Biotechnology

Full Length Research Paper

Antiproliferative activity of protein extracts from the black clam (*Chione fluctifraga*) on human cervical and breast cancer cell lines

Hiesu García-Morales[1], Luis Enrique Gutiérrez-Millán[1], Miguel A.Valdez[2], Armando Burgos-Hernández[3], Teresa Gollas-Galván[4] and María G. Burboa[1]*

[1]Posgrado en Biociencias, Departamento de Investigaciones Científicas y Tecnológicas (DICTUS), Universidad de Sonora, Hermosillo, Sonora, 83000, México.
[2]Departamento de Física, Universidad de Sonora, Hermosillo, Sonora, 83000, México.
[3]Departamento de Investigación y Posgrado en Alimentos, Universidad de Sonora, Hermosillo, Sonora, 83000, México.
[4]CTAOA, Centro de Investigaciones en Alimentación y Desarrollo A.C, Carretera a la Victoria Km 0.6, Hermosillo, Sonora, 83304, México.

Received 6 March, 2014; Accepted 13 October, 2015

The wide diversity of the marine environment has been an important resource for the discovery of new bioactive agents from marine organisms. The aim of this study was to obtain protein extracts from the clam *Chione fluctifraga* and determine its antiproliferative activity against cervical and breast cancer cells. The extracts were obtained by ammonium sulfate fractionation, gel filtration and ion exchange chromatography. Antiproliferative activity was evaluated by 3-(4,5-dimethylthiazol-2-yl)-2,5-diphenyltetrazolium bromide assay (MTT). The results showed that 3F3 had antiproliferative effect against HeLa and MDA-MB-231 cell lines with IC_{50} values of 138.035 and 157.19 µg/ml, respectively, and 2F2 showed IC_{50} values of 67.46 µg/ml on HeLa cells. These results suggest that protein extracts from *C. fluctifraga* might be potential anticancer agents.

Key words: Protein extracts, clam, antiproliferative activity, breast cancer, cervical cancer.

INTRODUCTION

Cancer is a worldwide health issue; it is not just one disease but a variety of different diseases, which have in common uncontrolled cell proliferation. There are more than 100 different types of cancer, most of them take the name of the organ or cell in which they begin to grow (Hawkins, 1992; Martinez et al., 2003). Breast and cervical cancer are the main cancer related cause of death in women around the world. The high prevalence of these types of cancer is due to a lack of strategies that allow detection at early cancer stages (Palacio-Mejía et al., 2009; Gök et al., 2011). Chemotherapy is the most commonly used treatment against cancer, however some

*Corresponding author. E-mail: mburboa@correom.uson.mx. Tel: (662) 2592169. Fax: (662) 2592197.

patients develop resistance against the drugs and this has become a major problem in the past years. Resistance to treatment can be caused by a large variety of factors, which include individual variations between patients and genetic differences among tumor cells (Gottesman, 2002; Jordan and Wilson, 2004; Bhutia and Maiti, 2008). The discovery of new compounds from natural sources has been very important in pharmaceutical science research. The past decade has seen an increase in the number of compounds obtained from the screening of diverse marine invertebrates, such as soft corals, tunicates and mollusks, that are advancing to preclinical trials (Liang et al., 2008; Simmons et al., 2005; Amador, 2003; Bhatnagar and Kim, 2010). Examples of anticancer agents extracted from marine organisms include bryostatin-1, a macrocyclic lactone from *Bugula neritine*, with antitumor activity; ziconotide, a peptide from cone snail, is an N-type calcium-channel blocker in chronic pain treatment; ectenaisdin 743 is a tetrahydroisoquinolone alkaloid, isolated from *Ectinascidia turbinate*, with cytotoxic activity. It has been previously reported that the peptide dolastatin, obtained from the marine mollusk *Dollabella auricularia*, possesses an impressive growth inhibition of cancer cells. Another example is Kahalalide F, a cyclic depsipeptide obtained from *Elysia rufescens*; this peptide shows antitumor activity against colorectal, lung and prostate cancer cells, being lysosomes the cellular target (Haefner, 2003; Amador, 2003; Aneiros and Garateix, 2004; Faircloth and Cuevas, 2006; Bhatnagar and Kim, 2010).

Many peptides with different biological activities such as antioxidant (Wenyan et al., 2012), immune-regulatory (Lixin et al., 2005), antihyperglycemia and antihyperlipemia activity (Tsai et al., 2008) have been isolated from the clam *Meretrix meretrix*; polypeptide Mer2, MGP_{0501} and MGP_{0405} inhibits cell proliferation of several cancer cell lines; Mere-15 shows antitumor activity *in vitro* and *in vivo;* the protein (MML) shows growth inhibition in several cancer cell lines such as breast, colon and hepatic (Leng et al., 2005; Ning et al., 2009; Wang et al., 2012). Two peptides, 18 and 16 kDa, with cytotoxic activity *in vitro* against HeLa cells have been purified from *Arca subcrenata* (Song et al., 2008). The Gulf of California has a great diversity of clams, such as the black clam (*Chione fluctifraga*), that represent a popular seafood and a very important income source for the community (Martinez-Cordova and Martinez-Porchas, 2006). The aim of the present study was to evaluate the capability of *C. fluctifraga's* protein extract to inhibit the cellular growth on HeLa and MDA-MB-231 cultured cells.

MATERIALS AND METHODS

Materials

The clams (*C. fluctifraga*) were obtained from the experimental unit of the University of Sonora (Kino Bay, Sonora). All the reagents were obtained from Sigma-Aldrich (St. Louis, MO, USA).

Preparation of the crude extract

The clams were cut into small pieces and homogenized with 0.01 M phosphate buffer (0.1 M NaCl, pH 7.2) in a 1:3 ratio (w/v). The homogenate was centrifuged at 3000 *x g*. The supernatant was fractionated by ammonium sulfate precipitation up to 60% saturation. After 12 h of stirring the precipitate was collected by centrifugation (3000 *x g*, 10 min) and the pellet was suspended in phosphate buffer and collected as the crude extract.

Preparation of protein extract

The crude extract was passed through a Sephadex G-25 column (1.5 × 50 cm) pre-equilibrated with 0.01 M phosphate buffer (0.1 M NaCl, pH 7.2) at a flow rate of 1 ml/min and the absorbance was monitored at 280 nm. The fraction collected was dialyzed against 0.025 M Tris-HCl and then loaded onto a HiPrep 16/10 Q XL column (BioRad) pre-equilibrated with 0.025 M Tris-HCl pH 8.2. The column was eluted with a linear gradient 0 to 1 M NaCl prepared in Tris-HCl buffer at a flow rate of 1 ml/min, each fraction was collected at a volume of 5 ml and detection was performed at 280 nm. Fractions were lyophilized then dialyzed and antiproliferative activities were determined.

Measurement of protein content

The protein concentration was measured by the BCA method using the BCA protein assay kit (Pierce, USA) and bovine serum albumin as standard.

Tricine-SDS-PAGE

The extraction process was monitored by electrophoresis tricine-SDS-PAGE (Schägger, 2006) using a Bio-Rad Mini-Protean II electrophoresis unit (Bio-Rad, CA, USA) with an acrylamide concentration of 16% for the running gel. The protein bands were detected by silver stain.

Cell culture

The breast cancer cell (MDA-MB-231), cervical cancer cell (HeLa) and a human retinal pigment epithelial cell line (ARPE-19) were obtained from American Type Culture Collection (Rockrville, MD). HeLa and ARPE-19 cell were grown in Dulbecco´s Modified Eagle Medium (DMEM) supplemented with 10% fetal bovine serum (GIBCO, BRL, Grand Island, NY), 1% penicillin-streptomycin and 1% gentamicin; MDA-MB-231 was grown in DMEM supplemented with 15% fetal bovine serum, 2 mM glutamine, 1% penicillin-streptomycin, 1% gentamicin and 1% non-essential amino acids (SIGMA-Aldrich, St. Louis, MO, USA) and were maintained at 37°C under humidified atmosphere with 5% CO_2.

Antiproliferative assay

MDA-MB-231, HeLa and ARPE-19 cells were cultured in a 96 wells microplate (1×10^4 cell/ml) for 24 hours; then 50 µl of the extracts were added in serial concentrations, PBS or Cisplatin as controls, and incubated for 48 h. At the end of the incubation period, 10 µl of MTT (3-(4,5-Dimethylthiazol-2-yl)-2,5-diphenyltetrazolium bromide)

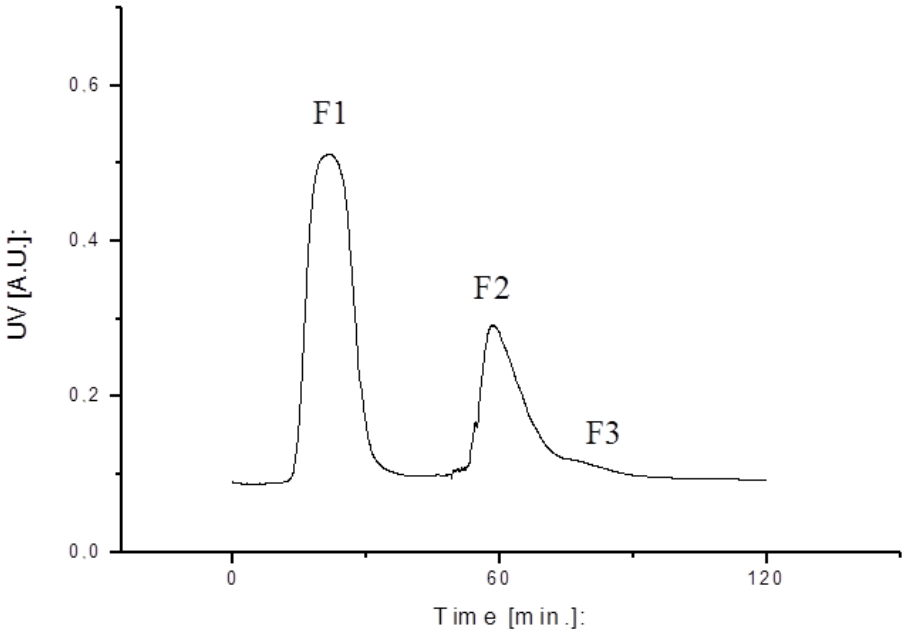

Figure 1. Fractionation of crude extract by gel filtration chromatography on a Sephadex G-25 column. Column specification: 1.5 x 50 cm; the elution was performed with 0.1M phosphate buffer at a flow rate of 1 ml/min. The elution was monitored at 280 nm.

solution (SIGMA-Aldrich, St. Louis, MO, USA) were added to each well and the microplate was incubated for 4 h to allow the formation of formazan by the viable cell. The formazan crystals were dissolved in 150 µl of solubilization solution. The absorbance was read on an ELISA reader (Beckman Coulter AD 340) at 570 nm. The percentage of growth inhibition was calculated as [(values from experimental conditions) – (values from control conditions)] × 100 / (Values from untreated control).

Statistical analysis

The experimental data were expressed as the mean ± standard deviation. Statistical analysis was carried out using the GraphPad PRISM 6 program (GraphPad Software, Inc., San Diego, CA), statistical significance ($p < 0.05$) was determined using a Student´s t-test.

RESULTS AND DISCUSSION

Marine organisms represent a large source of new compounds with biological activities. Direct extraction is one way to obtain bioactive compounds from marine organisms; this approach is widely used for isolated and purified biologically active peptides (Chen et al., 2013). Figure 1 shows the crude extract's chromatogram. Three fractions were obtained after passing the crude extract through the Sephadex column. The separation is given based on the size, the high molecular weight proteins were obtained in the first fraction and afterwards the low molecular weight ones. The fractions that resulted (F1, F2, and F3) from gel filtration chromatography were separated by ion-exchange chromatography through elution with a NaCl gradient on a HiPrep 16/10 QXL column, ten fractions were obtained as follows: four fractions from F1, three fractions from F2 and three fractions from F3 (Figure 2). Antiproliferative activity of all fractions was tested using the MTT assay, a well-established *in vitro* model for citotoxicity against cancer cell lines that has been used as a conventional technique for the screening of new compounds with antiproliferative activity (Song et al., 2008). F1 showed a antiproliferative effect of 87% of over MDA-MB-231 cell and 43.17% over HeLa cell. F3 shows inhibition of the cellular growth of 64.36 and 70% on HeLa and MDA-MB-231 cell, respectively (Figure 3). When a high concentration of the extract is required to inhibit the cellular growth on 50% of the population, it is considered a low cytotoxicity (Hsu et al., 2010). The concentrations used ranged from 0.054 to 1.97 mg/ml, inhibition on cancer cell line has been reported with 1 mg/ml of extracts (Picot et al., 2006; Liang et al., 2008). The fractions did not inhibit cellular proliferation beyond 60% on the human retinal pigment epithelial cells (ARPE-19). Ten fractions were obtained by ion-exchange chromatography, on the antiproliferative evaluation of these samples (Table 1), the fraction 3F3 showed to inhibit the proliferation of HeLa and MDA-MB-231 cell with IC_{50} values of 138.035 and 157.19 µg/ml respectively and 2F2 fraction showed IC_{50} values of 67.46 µg/ml over HeLa cells. Wang et al. (2012) have

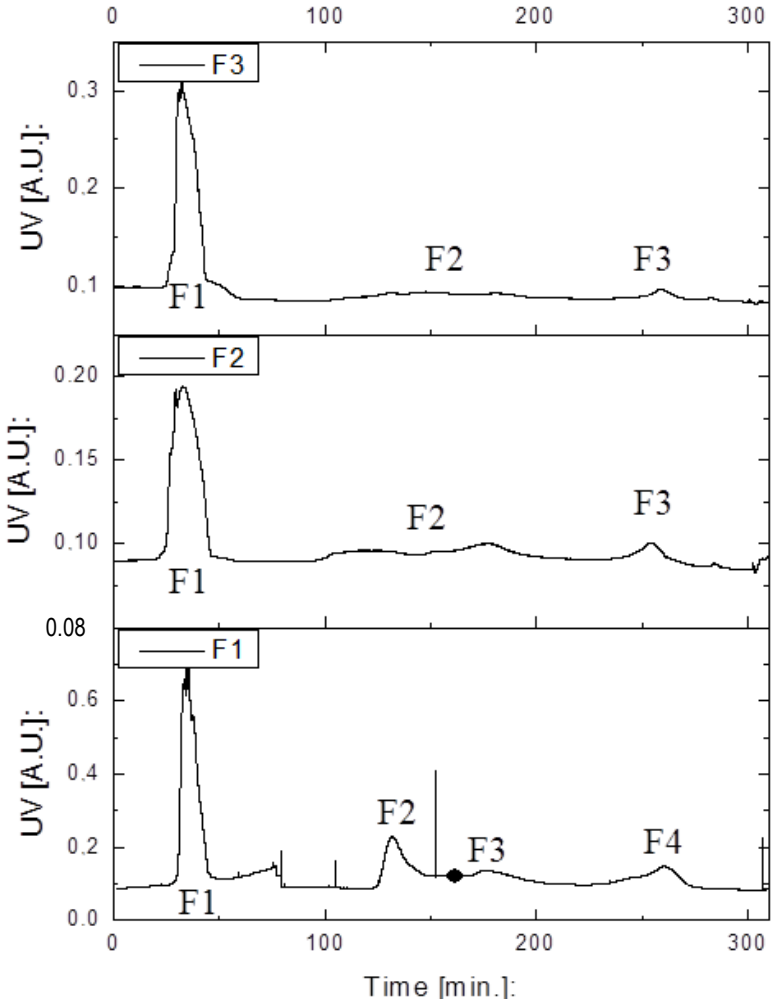

Figure 2. Fractionation by anion exchange chromatography on a HiPrep 16/10 QXL column. The elution was performed with a linear gradient of NaCl (0-1 M) in 25 mM Tris-HCl buffer at a flow rate of 1ml/min. The elution was monitored at 280 nm. F1: Fraction 1 from gel filtration chromatography; F2: Fraction 2 from gel filtration chromatography and F3: Fraction 1 from gel filtration chromatography.

reported IC_{50} values of 84.9 and 215.3 µg/ml over A549 and CCRF-CEM cells, for *Syngnathus acus's* protein purified by ion-exchange cromatography; from *A. subcrenata* two fractions have shown cytotoxic activity against HL-60 (IC_{50}: 123.2 µg/ml) and HeLa cells (IC_{50}: 38.2 µg/ml) (Song et al., 2008).

Several biologically active peptides from marine organisms have been identified and have shown different activities including antioxidant, antimicrobial, antiproliferative and antihypertensive actions (Kim et al., 2013). Some of these compounds are in the process of entering clinicals trials. Peptides from marine sources (Jaspamide, aplidine, didemnin, MML, Mere 15 and dolastatin) induce cell death with different mechanisms, including apoptosis, disruption of microtubular function; interaction with tubulin, alteration of microtubule assembly, or angiogenesis inhibition (Bai et al., 1990; Zheng et al., 2011). Also some of these compunds can bind the vinca alkaloids or the colchine-binding domain inhibiting the polimerization of microtubules (Simmons et al., 2005; Amador, 2003). Several bands with molecular weights between 45 and 18 kDa were observed in the electrophoresis gel (Figure 4). Several compounds derived from marine organisms that have been evaluated on pre-clinical and clinical trials as potential anticancer drug are low molecular weight compounds (Ning et al., 2009).

Cyplisin, a 56 kDa protein isolated from *Aplysia punctate,* has shown citotoxicity against several cancer cell lines; MML, a 40 kDa protein from *M. meretrix,* has inhibitory effects on the proliferation of human hepatoma,

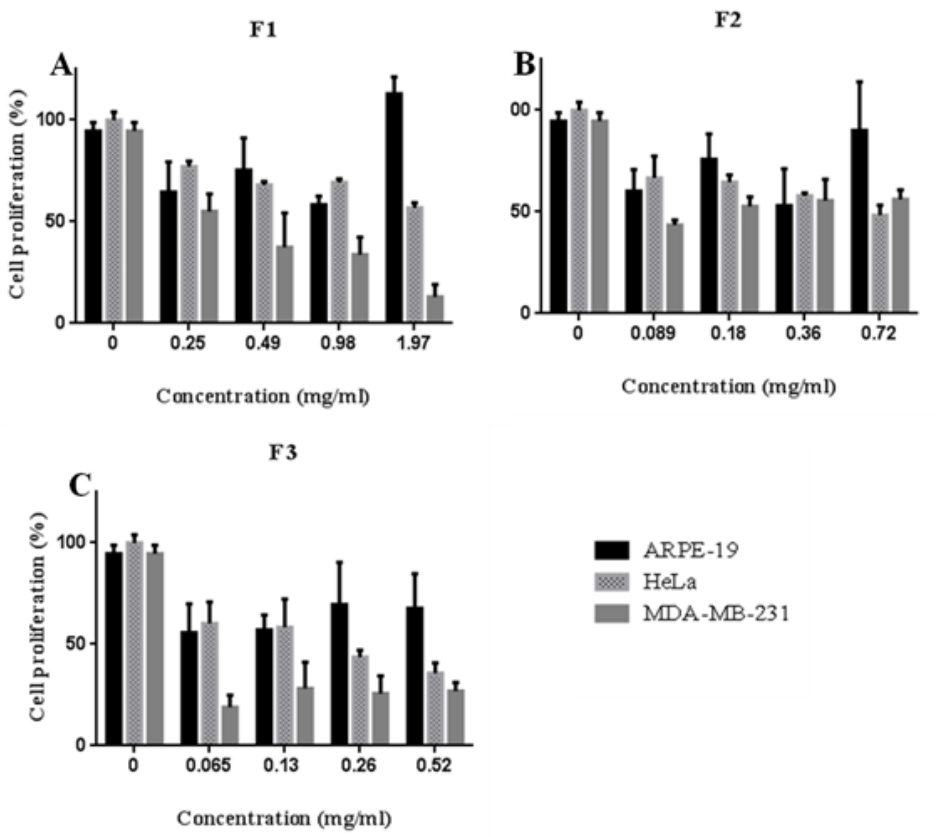

Figure 3. The inhibitory effect of fractions obtained by gel filtration chromatography. The cancer cell lines were treated with the indicated concentrattion of protein and cell proliferation was determinated by MTT assay. A: Fraction 1; B: Fraction 2; C: Fraction 3.

Table 1. Antiproliferative activity of fractions obtained by anion exchange chromatography against different cell lines (IC_{50} µg/ml ± SD).

Fraction	IC_{50} (µg/ml)		
	ARPE-19	HeLa	MDA-MB-231
1 F1	345.76 ± 0.0092	ND	105.89 ± 0.036*
1 F2	174.42± 0.0074	ND	101.83 ± 0.0068*
1 F3	281.29 ± 0.082	ND	150.35 ± 0.0005
1 F4	497.84 ± 0.167	ND	187.02 ± 0.0066*
2F1	260.18 ± 0.022	227.18 ± 0.13	ND
2F2	146.22 ± 0.030	67.46 ± 0.0026*	ND
2F3	235.94 ± 0.053	143.02 ± 0.0024*	ND
3F1	1339.91 ± 1.42	119.35 ± 0.013	1667.70 ± 1.075
3F2	1201.5 ± 0.21	155.09 ± 0.032*	186.67 ± 0.057*
3F3	240.54 ± 0.022	138.035 ± 0.0017*	157.19 ± 0.052

ND: No determinate; 1F1: Fraction 1 from F1; 1F2: Fraction 2 from F1; 1F3: Fraction 3 from F1; 1F4: Fraction 4 from F1; 2F1: Fraction 1 from F2; 2F2: Fraction 2 from F2; 2F3: Fraction 3 from F2; 3F1: Fraction 1 from F3; 2F3: Fraction 2 from F3; 3F3: Fraction 3 from F3. (*) Significant difference between the normal cell and cancer cell line at $p<0.05$ as analyzed by Student´s t-test.

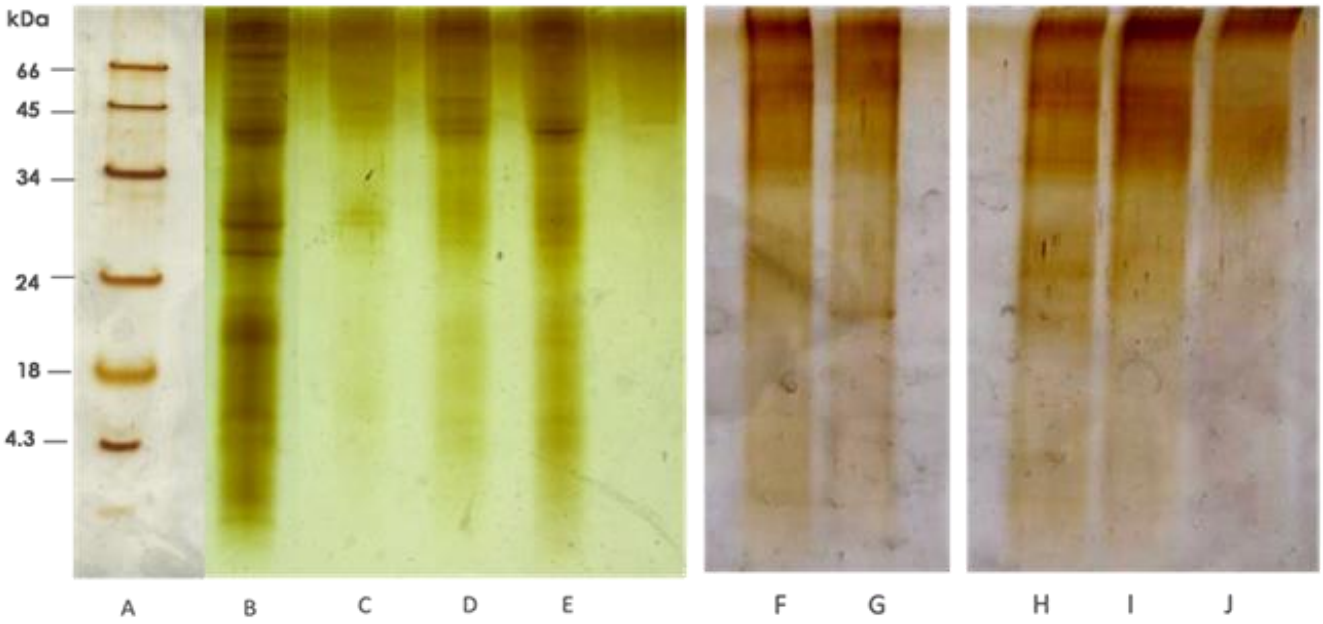

Figure 4. Tricine-SDS-PAGE of fractions obtained by anion exchange chromatography; protein bands were detected by silver stain. Lane A: Low range molecular weight marker; B: Fraction 1 from F1; C: Fraction 2 from F1; D: Fraction 3 from F1; E: Fraction 4 from F1; F: Fraction 1 from F2; G: Fraction 2 from F2; H: Fraction 1 from F3; I: Fraction 2 from F3; J: Fraction 3 from F3.

apparently increasing the permeability of the cell membrane and inhibiting tubulin polymerization. Also, peptides with antiproliferative activity, such as MGP_{0405} and MGP_{0501} (9.6 and 15.8 kDa, respectively), have been reported (Hoarau et al., 2002; Lixin et al., 2005; Nakano et al., 2006; Takahashi et al., 2008; Zheng et al., 2011; Wang et al., 2012). Takahashi et al. reported a protein with antimicrobial activity of 58 kDa from clam (*Ruditapes philippinarum*) and Hoarau found fractions of 20 to 28 kDa with detoxify activity. It has been reported that bioactive peptides or small proteins are highly influenced by their molecular weight and structure, which are affected by the isolation process; different approaches for isolation can lead to different bioactive agents (Guo-fang et al., 2011; Wang et al., 2012).

In the present study, the *in vitro* antiproliferative activity of protein extracts from *C. fluctifraga* was evaluated for the first time, the importance of these results is evidenced by previous reports of many anticancer chemical entities found by the screening of natural sources, such as marine organisms. Our results suggest that protein extracts from *C. fluctifraga* could induce cellular growth inhibition against HeLa and MDA-MB-231 cells, however further studies are needed.

Conflict of interests

The author(s) did not declare any conflict of interest.

REFERENCES

Amador ML (2003). Progress in the development and acquisition of anticancer agents from marine sources. Ann. Oncol. 14:1607–1615.

Aneiros A, Garateix A (2004). Bioactive peptides from marine sources: pharmacological properties and isolation procedures. J. Chromatogr. B. Anal. Technol. Biomed. Life Sci. 803:41–53.

Bai RL, Pettit GR, Hamel E (1990). Binding of dolastatin 10 to tubulin at a distinct site for peptide antimitotic agents near the exchangeable nucleotide and vinca alkaloid sites. J. Biol. Chem. 265:17141–17149.

Bhatnagar I, Kim S-K. (2010). Marine antitumor drugs: status, shortfalls and strategies. Mar. Drugs 8:2702–2720.

Bhutia SK, Maiti TK (2008). Targeting tumors with peptides from natural sources. Trends Biotechnol. 26:210–217.

Chen L, Song L, Li T, Zhu J, Xu J, Zheng Q, Yu R (2013). A new antiproliferative and antioxidant peptide isolated from Arca subcrenata. Mar. Drugs 11:1800–1814.

Faircloth G, Cuevas C(2006). Kahalalide F and ES285: potent anticancer agents from marine molluscs. Prog. Mol. Subcell. Biol. 43: 363–379.

Gök M, Rozendaal L, Berkhof J, Visser O, Meijer CJLM, van Kemenade FJ (2011). Cytology history preceding cervical cancer diagnosis: a regional analysis of 286 cases. Br. J. Cancer 104:685–692.

Gottesman MM (2002). Mechanism of cancer drug resistance. Annu. Rev. Med. 53:615–627.

Guo-fang D, Fang-fang H, Zui-su Y, Di YU, Yong-fang Y (2011). Anticancer Activity of an Oligopeptide Isolated from Hydrolysates of Sepia Ink. Chin. J. Nat. Med. 9:151–155.

Haefner B (2003). Drugs from the deep: marine natural products as drug candidates. Drug Discov. Today 8:536–544.

Hawkins MJ (1992). National Cancer Institute. JNCI J. Natl. Cancer Inst. 84:1699–1702.

Hoarau P, Garello G, Gnassia-Barelli M, Romeo M, Girard J-P (2002). Purification and partial characterization of seven glutathione S-transferase isoforms from the clam Ruditapes decussatus. Eur. J. Biochem. 269:4359–4366.

Hsu H-F, Wu Y-C, Chang C-C, Houng J-Y (2010). Apoptotic effects of bioactive fraction isolated from *Glossogyne tenuifolia* on A549 human lung cancer cells. J. Taiwan Inst. Chem. Eng. 1–7.

Jordan MA, Wilson L (2004). Microtubules as a target for anticancer drugs. Nature 4:253–265.

Kim E-K, Kim Y-S, Hwang J-W, Lee JS, Moon S-H, Jeon B-T, Park P-J (2013). Purification and characterization of a novel anticancer peptide derived from *Ruditapes philippinarum*. Process Biochem. 48:1086–1090.

Leng B, Liu X-D, Chen Q-X (2005). Inhibitory effects of anticancer peptide from Mercenaria on the BGC-823 cells and several enzymes. FEBS Lett. 579:1187–1190.

Liang C-H, Wang G-H, Liaw C-C, Lee M-F, Wang S-H, Cheng D-L, Chou T-H (2008). Extracts from *Cladiella australis*, *Clavularia viridis* and *Klyxum simplex* (soft corals) are capable of inhibiting the growth of human oral squamous cell carcinoma cells. Mar. Drugs 6:595–606.

Lixin Z, Xiao F, Lijun H (2005). Antitumor and immune regulation activities of the extracts of some Chinese marine invertebrates. Chin. J. Oceanol. Limnol. 23:110–117.

Martinez JD, Parker MT, Fultz KE, Ignatenko AN, Gerner EW (2003). Molecular biology of cancer. In Burger's Medicinal Chemistry and Drug Discovery, D. J. Abraham, ed. (John Wiley & Sons, Inc.), pp. 1–50.

Martinez-Cordova LR, Martinez-Porchas M (2006). Polyculture of Pacific white shrimp, *Litopenaeus vannamei*, giant oyster, *Crassostrea gigas* and black clam, *Chione fluctifraga* in ponds in Sonora, Mexico. Aquaculture 258:321–326.

Nakano T, Matsushima-Hibiya Y, Yamamoto M, Enomoto S, Matsumoto Y, Totsuka Y, Watanabe M, Sugimura T, Wakabayashi K (2006). Purification and molecular cloning of a DNA ADP-ribosylating protein, CARP-1, from the edible clam *Meretrix lamarckii*. Proc. Natl. Acad. Sci. U. S. A. 103:13652–13657.

Ning X, Zhao J, Zhang Y, Cao S, Liu M, Ling P, Lin X (2009). A novel anti-tumor protein extracted from *Meretrix meretrix* Linnaeus induces cell death by increasing cell permeability and inhibiting tubulin polymerization. Int. J. Oncol. 35:805–812.

Palacio-Mejía LS, Lazcano-Ponce E, Allen-Leigh B, Hernández-Avila M (2009). Diferencias regionales en la mortalidad por cáncer de mama y cérvix en México entre 1979 y 2006. Salud Publica Mex. 51:208–219.

Picot L, Bordenave S, Didelot S, Fruitierarnaudin I, Sannier F, Thorkelsson G, Berge J, Guerard F, Chabeaud A, Piot J (2006). Antiproliferative activity of fish protein hydrolysates on human breast cancer cell lines. Process Biochem. 41:1217–1222.

Schägger H (2006). Tricine-SDS-PAGE. Nat. Protoc. 1:16–22. Available at: http://www.ncbi.nlm.nih.gov/pubmed/17406207 [Accessed July 15, 2011].

Simmons TL, Andrianasolo E, Mcphail K, Flatt P, Gerwick WH (2005). Minireview Marine natural products as anticancer drugs. Mol. Cancer Ther. 4:333–342.

Song L, Ren S, Yu R, Yan C, Li T, Zhao Y (2008). Purification, characterization and in vitro anti-tumor activity of proteins from Arca subcrenata Lischke. Mar. Drugs 6:418–430.

Takahashi KG, Kuroda T, Muroga K (2008). Purification and antibacterial characterization of a novel isoform of the Manila clam lectin (MCL-4) from the plasma of the Manila clam, *Ruditapes philippinarum*. Comp. Biochem. Physiol. B. Biochem. Mol. Biol. 150: 45–52.

Tsai J-S, Chen J-L, Pan BS (2008). ACE-inhibitory peptides identified from the muscle protein hydrolysate of hard clam (*Meretrix lusoria*). Process Biochem. 43:743–747.

Wang C, Liu M, Cheng L, Wei J, Wu N, Zheng L, Lin X (2012). A novel polypeptide from *Meretrix meretrix* Linnaeus inhibits the growth of human lung adenocarcinoma. Exp. Biol. Med. 237:442–450.

Wenyan X, Chen C, Xiaoshuang L, Bo W, Ying S, Maocang Y, Xiaoying Z (2012). Meretrix Meretrix: Active Components and Their Bioactivities. Life Sci. J. 9:756–762.

Zheng L-H, Wang Y-J, Sheng J, Wang F, Zheng Y, Lin X-K, Sun M (2011). Antitumor peptides from marine organisms. Mar. Drugs 9: 1840–1859.

academicJournals

Vol. 15(8), pp. 221-235, 24 February, 2016
DOI: 10.5897/AJB2014.14358
Article Number: 2B4DAA857327
ISSN 1684-5315

http://www.academicjournals.org/AJB

African Journal of Biotechnology

Full Length Research Paper

Toxicity effects of ethanol extract of *Simarouba versicolor* on reproductive parameters in female Wistar rats

Marlene S. Oliveira[1], Maria Zenaide L. C. M. Fernandes[2], Ana Lys B. B. Mineiro[3], Rosimeire F. dos Santos[2], Gregório E. N. Viana[6], Josana M. Coelho[4], Sahâmia M. Ribeiro[4], Ana Paula G. P. Cunha[5], Joselene F. Costa[5] and Rozeverter M. Fernandes[6]

[1]Medicinal Plants Research Center, Federal University of Piauí, Teresina/PI, Brazil.
[2]Department of Biochemistry and Pharmacology, Federal University of Piauí, Teresina/PI, Brazil.
[3]Department of Veterinary Clinic and Surgery, Federal University of Piauí, Teresina/PI, Brazil.
[4]Department of Medicine, Federal University of Piauí, Teresina/PI, Brazil.
[5]Veterinary Medicine, Federal University of Piauí, Teresina/PI, Brazil.
[6]Department of Veterinary Morphophysiology, Federal University of Piauí, Teresina/PI, Brazil.

Received 9 December, 2014; Accepted 12 November, 2015

***Simarouba versicolor* is popularly known as pau-paraiba. It belongs to the Simaroubaceae family and is found in the Northeast of São Paulo and in some parts of the states of Pará and Mato Grosso do Sul. It is known that this and other species from this genus have several activities: insecticides, anti-inflammatory, antitumor, anthelmintic, among others. The effects of ethanolic extract of the bark of *S. versicolor* (Sv-EtOH) on the reproductive system of rats were investigated; also the influence of estrogenic and/or antiestrogenic activity, estrous cycle, pregnancy, lactation and offspring development was observed. In the experimental protocols with ethanolic extract of *S. versicolor*, the doses were 10, 20 and 40 mg/kg. To evaluate estrogenic and anti-estrogenic activity, uterotrophic assay and histopathology of the uterus were performed. In the estrous cycle tests, animals were treated daily, for 30 days, to count number of cycles and record the biochemical profile. During pre-implantation and post-implantation, the effect of the extract on pregnancy, lactation and development of the progeny was observed. Uterotrophic assay exhibited anti-estrogenic activity at extract doses of 10, 20 and 40 mg/kg. The animals exposed to all doses had no changes in their estrous cycle, pregnancy, lactation and biochemical profile. All results were within normal range; however, creatinine concentration increased significantly at all doses as compared to the control. The ethanol extract of *S. versicolor* presented antiestrogen activity, low systemic toxicity and had no reproductive toxicity at investigated doses.**

Key words: *Simarouba versicolor*, reproduction, rats.

INTRODUCTION

Medicinal plants are important and they supply raw materials to synthetize medicines, besides being used as therapeutics. The use of plants is overvalued traditionally based on their medicinal benefits, and often they are the only therapeutic resource of many communities and ethnic groups (Tresvenzol et al., 2006; Garcia et al., 2010). Herbal remedies are often indiscriminately ingested during pregnancy due to popular belief that

natural products are not harmful to health. Therefore, it is necessary to carry out toxicity studies with respect to this class of users. Thus, reproductive toxicity evaluation tests comprise the exposure of sexually mature animals before conception, during prenatal development and after birth (Lourenço et al., 2009).

Among the commonly used plants, *Simarouba versicolor*, from Simaroubaceae family, stands out in folk medicine. Its bark and fruit are used as anthelmintic and the infusion of its bark has anti poisonous effect (Pires et al., 2006). Furthermore, they may be useful in the treatment of dyspepsia, diarrhea and fever. *S. versicolor* inhibits acetylcholinesterase enzyme (Carvalho, 2008), and causes an outbreak of cattle poisoning in Agua Clara County, Mato Grosso do Sul (Carvalho et al., 2013). Regarding its acute toxicity, Fernandes et al. (2004) determined the median lethal dose (DL_{50}) of the aqueous extract of *S. versicolor* in mice; it was approximately 185.88 and 68.80 mg/kg administered through oral and intraperitoneal routes, respectively. Mesquita (2009), studying an anticancer substance (glaucarubinona, extremely active on cancer cells) obtained from hexane extract of the bark and root of *S. versicolor*, saw that the substance gave significant results.

Mesquita (1997), through chromatographic analysis of chloroform and ethyl acetate fractions removed from the wood of *S. versicolor*, isolated two quassinoids, excelsina and 11-ethyl-amarolídio, where excelsina was first isolated in this genus. Arriaga et al. (2002), through hexane, chloroform, ethyl acetate and methanol extracts, isolated a mixture of quassinoids triterpenoids and steroids, in addition to kaempferol flavonoid and squalenic derivatives from roots, branches and fruits of this plant. According to Almeida et al. (2007), quassinoids present in *S. versicolor* show a wide range of biological activities, such as antitumor, antimalarial, antioxidant, amebicides, antiviral and also a male anti-fertility, a fact that aroused the interest in studying *S. versicolor* effect on female reproduction.

From this perspective, this study aimed to investigate the effects of *S. versicolor* bark ethanolic extract (Sv-EtOH) on the reproductive system of rats, observing the influence of estrogenic and/or antiestrogenic activity, estrous cycle, pregnancy, lactation and progeny development, as well as the effects of this extract on biochemical profile, histologic and morphometric aspects of system reproductive female Wistar rats.

MATERIALS AND METHODS

Animals

Female rats (*Rattus norvegicus*, Wistar variety) were provided by the Central Biotherium of the Federal University of Piauí. Animals were kept in standard cages at controlled temperature (24 ± 1°C) in a 12 h light/dark cycle; there was free access to water and feed. Experimental protocols were approved by the Ethics Committee in Animal Experimentation of the Federal University of Piauí (EAEC-PI 029/11).

Chemicals and drugs

The following constituted the chemicals and drugs used in this study: dimethylsulfoxide (DMSO) - DYNAMIC, BRAZIL), estradiol cyprionate (Pfizer), Tamoxifen (DEG, CHINA), sodium thiopental and corn oil. For protocols application, the extract was diluted in DMSO and distilled water.

Preparation of the ethanol extract

Barks of *S. versicolor* were collected in Angical (6°05'41°28'), Piauí, Brazil. A voucher of the plant was identified and deposited in the Herbarium Graziela Barroso acquis (TEPB) of the Federal University of Piauí, Teresina, Piauí under number TEPB-20.883. It was dried in a forced air circulation drying oven for three days at 45 ± 1°C. After complete drying, the material was crushed in a Willi type mill. The ethanol extract was obtained by placing 1 kg of plant feedstock into ethanol for four days at room temperature in cold maceration followed by filtration. After four successive extractions, it was homogenized and placed in a rotary evaporator at 45 ± 1°C coupled to a thermostatic bath, followed by lyophilization. The ethanol extract lyophilized was diluted in dimethylsulfoxide and distilled water (DMSO = 6%).

Uterotrophic test

To uterotrophic assay, 100 immature Wistar rats (21 ± 1 postnatal day), weighing from 40 - 55 g, were divided into 10 groups of 10 animals treated after 22 to 28 post-natal days (once per day). Treatments were performed according to Table 1, wherein the extract (Sv-EtOH) vehicle was distilled water and dimethyl sulfoxide (6%); for estradiol, it was corn oil and for tamoxifen, distilled water. After treatment, animals were euthanized with an overdose of sodium thiopental (100 mg/kg, ip). They had uterus and ovaries removed, dissected and weighed on an analytical balance (0.001g) and then Formalin fixed (10% buffered formaldehyde). After 24 h, organs were re-sectioned for histology processing: they were dehydrated with alcohol (70 to 100%), diaphanized in xylene, submitted to impregnation and included in paraffin. Tissue fragments were cut with 5.0 µM thickness in a microtome, stained with hematoxylin-eosin and examined by light microscopy. Uterine sections were submitted to morphometric analysis using computerized image analyzer (Qwin Leica D-1000, version 2.1.0: Cambridge, UK). Five to six fields of uterine epithelium of each animal were captured and measured using Image-Pro Plus, version 4.5.0 Windows 98/NT/200.

Test involving estrous cycle

To evaluate the effect of Sv-EtOH treatment on the estrous cycle of rats, 32 mice were randomly assigned into 4 groups of 8 animals of

*Corresponding author. E-mail: pessoasipauba@yahoo.com.br

Table 1. Experimental design of uterotrophic assay with ethanol extract of *Simarouba versicolor* in rats.

Number	Groups	Dosage	Routes of administration
10	Negative control (H_2Od + DMSO)	10 mL/kg	o.a.
10	Sv-EtOH 10	10 mg/kg	o.a.
10	Sv-EtOH 20	20 mg/kg	o.a.
10	Sv-EtOH 40	40 mg/kg	o.a.
10	Estradiol	5 µg/kg	i.m.
10	Tamoxifen	4 mg/kg	i.m
10	Estradiol + Tamoxifen	5 µg/kg + 4 mg/kg	o.a + i.m
10	Sv-EtOH 10 + Estradiol	10 mg/kg + 5µg/kg	o.a. + i.m
10	Sv-EtOH 20 + Estradiol	20 mg/kg + 5µ/kg	o.a. + i.m
10	Sv-EtOH 40 + Estradiol	40 mg/kg + 5µ/kg	o.a. + i.m

Distilled water (H_2Od); dimethylsulfoxide (DMSO) = dilution vehicle, n = number of animals; o.a = oral admnistration; im = intramuscular.

Table 2. Experimental design of treatment with ethanol extract of *S. versicolor* to evaluate its effect on estrous cycle of female rats.

Number	Groups	Dosage	Routes of administration
8	G1 - Control (H_2Od + DMSO)	10 mL/kg	o.a.
8	G2 - Sv-EtOH 10	10 mg/kg	o.a.
8	G3 - Sv-EtOH 20	20 mg/kg	o.a.
8	G4 - Sv-EtOH 40	40 mg/kg	o.a.

Distilled water (H_2Od); dimethylsulfoxide (DMSO) = dilution vehicle; number of animals (n); oral administration (o.a.).

90 days and weighing from 180 – 250 g, having regular estrous cycle. From the beginning of estrus, animals were treated for 30 consecutive days according to the protocol outlined on Table 2.

Daily, rats were submitted for vaginal lavage with saline solution of 0.9% (50 µL release and immediate recovery). Then, fresh confectioned smears were used to verify cycle phase. This was observed in light microscopy at 40x magnification. Phases were determined according to Hankness and Wagner (1993) (diestrus, proestrus; onset of estrus; end of estrus and meta-oestrus). Estrus visualization was considered as the starting point of each estrous cycle, which was recorded during each individual cycle phase.

After treatment, animals were euthanized with sodium pentobarbital overdose (100 mg/kg, i.p.). Then, there was blood and serum collection, which was stored for later evaluation of the biochemical profile: glutamic oxalacetic transaminase (TGO), transaminase glutamic pyruvate (TGP), triglycerides, urea, creatinine, total cholesterol and total protein. Colorimetric method was performed to determine contents in a Quick Lab (Drake) equipment.

Assays involving pregnancy and lactation

Mating

Nulliparous females were placed with adult males in the dark phase of the cycle consisting of 1 male for 2 females. In the morning after mating, vaginal lavage was performed looking for evidence of sperms. Smears were evaluated by optical microscopy (10 - 40x). The presence of vaginal plug or sperm in vaginal washes confirmed copulation, and it is considered the first day of pregnancy.

Preimplantation period (1st to 7th day of pregnancy)

In this protocol, 32 pregnant rats with 160-250 weights were divided into 4 groups of 8 animals. Rats were treated with extract (10, 20 and 40 mg/kg) from the first to seventh day of pregnancy, as well the control group (distilled water and 6% DMSO/10 g body weight). During the treatment, animals were weighed daily. After eight days, progenitors were euthanized (sodium thiopental 100 mg/kg, ip), observing organ weights, pre-implant and visible signs of toxicity losses: piloerection, fur loss, shivers, salivation, convulsions, hypo activity, reduction of normal feed intake, weight loss, and presence of diarrhea. Liver, kidneys, adrenals, uterus and ovaries had their absolute masses weighed in analytical balance.

Pre-implant losses were determined according to the following formula: pre-implant losses = (number of corpus luteum - number of implants/number of corpus luteum) × 100. Corpus luteum was counted with Lupa Olympus SZ40 and implants with naked eye.

Gestational period (1st to 20th day of pregnancy)

In this experiment, 32 pregnant rats, weighing 160-250 g, divided into 4 groups (n = 8) were housed in individual cages and treated daily from the first to the twentieth day of gestation with control (vehicle), SvEtOH 10, 20 and 40 mg/kg.

Females' weight gain was evaluated daily and extract doses

were adjusted. On the 20th day of gestation, females were anesthetized (ketamine 50 mg + xylazine 5 mg) and submitted to cesarean for removal and evaluation of the pregnant uterus and its contents. Fetuses and implantation sites were counted and weighed individually, so were gravid uterus, fetus and placenta. Fetuses were examined and analyzed macroscopically looking for anomalies and/or congenital malformations. After caesarian, animals were euthanized by overdose of anesthetic association (1 mL/100 g/bw/ip) to remove and weigh the following organs: ovaries, liver, kidneys, spleen, heart, lung and adrenal glands, which had their relative masses calculated. Corpus luteum and implantations sites were counted. Reproductive parameters were evaluated using the following formulas:

Implementation contents = (number of deployments/number of corpora luteum) x 100

Resorption index = (number of resorption*/number of implants) x 100

*Number of resorption = (number implants) - (number of fetuses)

Pre-implant losses = (number of corpus luteum - number of implants/number of corpus luteum) x 100

Post-implant losses = (number of implants - number of births/number of implants) x 100

Piloerection, fur loss, shivers, salivation, convulsions, hypo activity, reduction of normal feed intake, weight loss, abortion and presence of diarrhea were used as systemic toxicity indicators (Muller et al., 2013).

Post-implantation, lactation and development of progeny period

Pregnant rats divided into 4 groups of 5 animals, weighing 160-250, were treated once daily with 10, 20 and 40 mg/kg of Sv-EtOH and with the vehicle; administrations started on the 8th day of pregnancy, beginning of fetus post-implantation period. Treatment was stopped only on progeny birth (21 ± 1 day of pregnancy), and continued on the day after birth until the 21th day of lactation (weaning).

On the 18th day of pregnancy, progenitors were separated into individual cages until delivery and inspected twice daily until offspring birth (1st postnatal day). On 21st postnatal day, pups were separated and placed in new cages (Muller et al., 2009) and progenitors were euthanized (Thiopental, 100 mg/kg/i.p.) for organ gathering. During pregnancy and breastfeeding were observed: weight gain, duration of pregnancy, birth rate, number of births, viability thereof, besides indicators of systemic toxicity (Muller et al., 2013). Birth delivery, birth rates and viability were determined according to US-EPA (1996) formulas:

Childbirth index = (number of females who delivered/number of females with evidence of pregnancy) x 100

Index birth = (number of births/number of litters) x 100

Index viability = (number of live young on the fourth day post-natal/number of live births) x 100

Post-implant losses = (number of implants – number of births/number of implants) × 100

Progeny was observed twice daily as the evolution of characteristics: emergence of fur (5 to 7 days), bilateral eyelid opening (12 to 16 days), displacement of pinna (6 to 8) and opening of vaginal canal in female puppies (about 35 days), based on Mello (2007).

Statistical analysis

For tests conducted during pre and post-implantation periods, pregnancy and uterotrophic data were expressed as mean standard error of the mean (SEM). Statistical analyses were performed with Graphpad PRISM ® software, version 5.0, by ANOVA (One Way), followed by Tukey post-test; significance was set at $p<0.05$. Comparison of data in the same group was made by paired student's test with significance of $p<0.05$.

Estrous cycle length data were analyzed and processed using SPSS (Statistical Package for Social Sciences) software for Windows, version 15. Initially, a descriptive analysis of the sample was done by calculating the average. Thereafter, Kolmogorov-Smirnov test was applied to test the normality of the results. When the data set to compare the results met the requirements for applying parametric statistics, we used the parametric analysis of variance (ANOVA). When application of non-parametric statistics was necessary, comparison between groups was performed using Kruskal-Wallis test. A significance level of 0.05 was adopted.

RESULTS

Uterotrophic assay

Rats treated with SV-EtOH at all doses tested did not show any increase in relative masses of uterus, which is similar to negative control, that shows no estrogenic activity. On the other hand, the group treated with estradiol (positive control) showed a significant increase in the relative mass of uterus ($p <0.05$) as compared to negative control and treated group.

Nevertheless, in anti-estrogenic activity test of females treated with Sv-EtOH and estradiol in all the doses, there was an inhibition of uterine growth and statistically significant differences ($p <0.05$) compared to animals treated only with estradiol (Figure 1). Their behavior was equal to groups treated with tamoxifen and tamoxifen + estradiol, which showed a significant inhibition ($p <0.05$) in uterine relative masses compared to those treated with estradiol.

Histological evaluation of uterine epithelium in estrogenic activity tests showed that rats treated with estradiol had 90% eosinophilic inflammatory infiltration of mean intensity reaching muscular layer (Table 3 and Figure 1a). In contrast, animals treated with 10 and 20 mg/kg of Sv-EtOH had a percentage less of eosinophilic infiltration (60 and 50%, respectively). Animals treated with 40 mg/kg presented 100% of eosinophilic infiltration in lamina propria with moderate intensity and swollen mucosal epithelial cells (Table 3).

Antiestrogenic activity in the groups treated with Sv-EtOH + estradiol at doses of 10 and 20 mg/kg (Figure 1d, e and 1f) revealed eosinophilic infiltration of moderate intensity reaching muscle layer with 90 and 100%, respectively. Different behavior was observed at 40 mg/kg, which inhibited infiltration by 50% (Table 3).

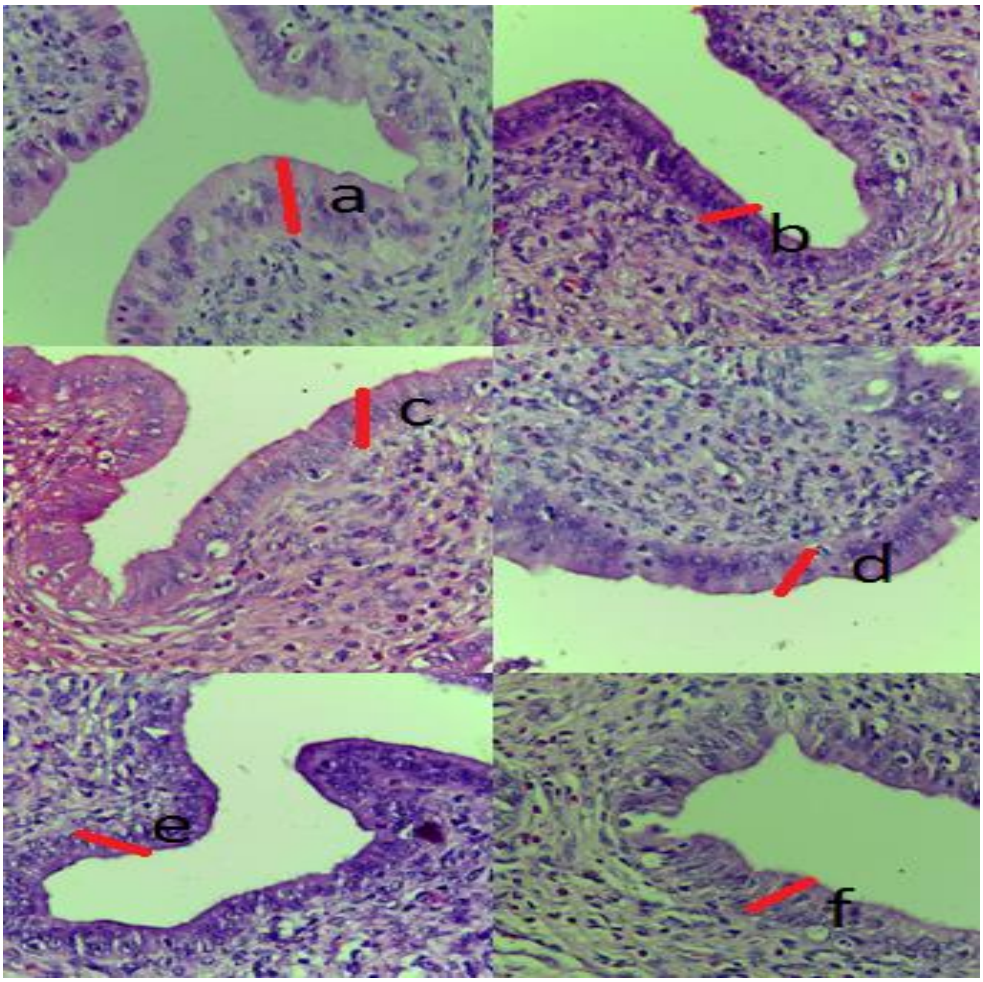

Figure 1. Photomicrographs showing longitudinal sections of the endometrium of rats: **a**, treated with estradiol (5µg); **b**, treated with tamoxifen (4 mg/kg); **c**, treated with estradiol + tamoxifen **d**, **e**, **f**, treated with estradiol + Sv-EtOH (10, 20, 40 mg / kg), respectively.

Table 3. Histopathological uterus of female rats treated with ethanolic extract of *S. versicolor* when compared with negative and positive controls in uterotrophic assay.

Number	Groups	Uterus histopathology	Percentage
10	Negative control (ad + DMSO)	Normal	100
10	Sv-EtOH 10	Eosinophilic inflammatory infiltration of the lamina propria and muscle layer	40
10	Sv-EtOH 20	Eosinophilic infiltrate of moderate intensity reaching the muscle layer	50
10	Sv-EtOH 40	Eosinophilic infiltration of lamina propria of moderately severe intensity and swelling of epithelium cells mucosa	100
10	Estradiol	Eosinophilic infiltration of moderate intensity reaching the muscle layer.	90
10	Tamoxifen	Normal	100

Table 3. Contd.

10	Tamoxifen + Estradiol	Eosinophilic inflammatory infiltrate of lamina propria and muscle layer.	70
10	Sv-EtOH 10 + Estradiol	Eosinophilic inflammatory infiltrate of moderate intensity reaching the muscle layer	90
10	Sv-EtOH 20 + Estradiol	Eosinophilic infiltration of the lamina propria of moderate moderately severe intensity reaching the muscle layer and swelling of the epithelial cells of the mucosa	100
10	Sv-EtOH 40 + Estradiol	Eosinophilic infiltrate of moderate intensity reaching the muscle layer	50

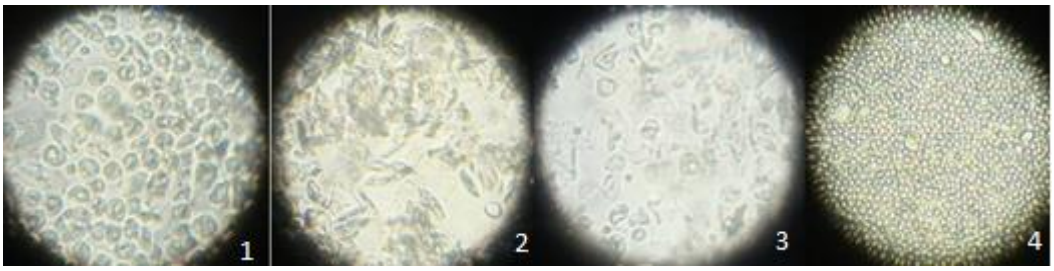

Figure 2. Vaginal smears of rats treated with Sv-EtOH showing the four phases of estrous cycle (400x); proestrus (1), estrus (2), metaestrus (3), diestrus (4). Source: Author.

Rats treated only with tamoxifen showed normal and undeveloped epithelium similar to negative control (Figure 1b). However, 70% of animals treated with tamoxifen + estradiol presented eosinophilic infiltration in the simple columnar epithelium of the lamina propria with moderate intensity and swollen mucosa epithelial cells (Figure 1c).

Regarding morphometry of uterine epithelium in antiestrogen activity (Figure 1d, e and f), Sv-EtOH at all doses was able to inhibit the increased thickness of estradiol-induced uterine epithelium, behaving like tamoxifen alone and associated with estradiol. The group treated with estradiol had values significantly higher than the other groups (Figure 4 and Figure 1a).

Evaluation of estrous cycle

The four phases of the estrous cycle (Figure 2) were observed through smear vaginal realized during 30 days of treatment. The estrus, being the most characteristic phase, was regarded as the starting point of each cycle; it duration ranged from 1 to 7 days in this experiment. The number of estrous cycles recorded during 30 days for treated groups did not differ significantly ($p>0.05$) compared with the control group. Control average was 6.00 ± 0.26 estrous cycles, and groups treated with Sv-EtOH (10, 20 and 40 mg/kg) presented 5.13 ± 0.39; 4.62 ± 0.39; 4.37 ± 0.65 estrous cycles, respectively (Figure 5).

Cycle duration for group treated with Sv-EtOH (10, 20, 40 mg/kg) was not significant ($p>0.05$), but it was observed that the estrous cycle length is dose dependent. Control group average was 4.83 ± 1.18 and for those treated with Sv-EtOH (10, 20, 40 mg / kg) it ranged from 5.57 ± 1.88, 6.16 ± 2.35, 8.16 ± 1.17, respectively.

Concerning the regularity of cycles, those that exceeded the duration of 5 days were considered irregulars. The total number of estrous cycles was 159, with 77.36% regular and 22.64% irregular. Control group exhibited 87.5% of regular cycles and 12.5% of irregular cycles. Animals treated with Sv-EtOH (10, 20, 40 mg / kg) had frequencies of 73.17, 67.56 and 78.78% for regular estrous cycles and 26.82, 32.43 and 21.21% for irregulars, respectively.

Biochemical analysis

During treatment with Sv-EtOH at 10, 20, 40 mg/kg for 30 days, no clinical signs of toxicity nor mortality were observed. The treatment did not induce changes in the biochemical profile of TGP, TGO, urea, total cholesterol,

Table 4. Effect of ethanolic extract of *S. versicolor* on biochemical parameters of Wistar rats treated for 30 days.

Parameters	Control	Treatments (Sv-EtOH)		
	H_2Od + DMSO	10 mg/kg	20 mg/kg	40 mg/kg
TGP (U/L)	67.37 ± 4.55	55.75 ± 7.34	71.87 ± 15.4	87.00 ±14.0
TGO (U/L)	164.8 ± 10.8	130.3 ± 64.7	98.62 ± 5.19	81.50 ± 7.9
Urea (mg/dL)	48.25 ± 0.79	47.00 ± 1.09	46.00 ± 2.36	60.12 ± 5.9
Creatinine (mg/dL)	0.625 ± 0.037	1.00 ± 0.05***	0.92 ±0.05***	0.87±0.025**
Total cholesterol (mg/dL)	77.50 ± 33,0	56.00 ± 21.33	50.62 ± 8.12	44.37± 11.1
Triglycerides (mg/dL)	25.37± 4.14	30.75± 3.61	31.62 ± 5.72	30.37± 5.70
Total protein (mg/dL)	6.72 ± 0.17	6.088 ± 0.34	6.11± 0.23	5.86 ±0.075

The data express mean (± SEM). **p <0.01, ***p <0.001 (One way ANOVA/Tukey).

triglycerides and total protein, since the parameters were within the reference range, as to the values observed in control animals. The only exception is observed for the dosage of creatinine in animals treated with Sv-EtOH at doses of 10, 20, 40 mg/kg, which increased significantly at 1.00, 0.92, 0.87 (mg/dL), respectively, as compared to those of control animals (Table 4).

Trial involving pregnancy and lactation

Pre-implantation period

The administration of Sv-EtOH (10, 20 and 40 mg/kg) during pre-implantation period (1st to 7th day of pregnancy), as compared to control, had no effect on body weight gain of the mother (Figure 6).

Absolute (g) and relative masses (%) of organs (uterus, ovaries, kidney, adrenal, lung, heart, liver and spleen) from progenitor treated with extract during pre-implantation did not differ significantly (p>0, 01) when compared to control (Table 5).

Pre-implant losses, numbers of corpus luteum and number of deployments found in dams treated with Sv-EtOH (10, 20 and 40 mg/kg) during pre-implantation did not differ from control group (Table 6).

Pregnancy

Administration of Sv-EtOH during gestation did not affect body weight gain of progenitor, and did not differ significantly from control (Figure 7). During this period, absolute (g) and relative masses of uterus, ovaries, adrenals, kidneys, lungs, heart, liver and spleen were not significantly different (P>0.05) (Table 7). In the reproductive parameters evaluated, deployment rate was 100% for animals treated with 10 and 40 mg/kg and 99.03% at 20 mg/kg. Females treated with 10, 20 and 40 mg/kg had resorption rate, pre-implant loss, and post implant loss of 2.50 ± 1.63 to 2.60 ± 1.75; 1.56 ± 1.56 to 2.50 ± 1.63; 1.56 ± 1.56 to 2.50 ± 1.63, respectively, not significantly different from control group.

Post-implantation period (8th to 21st days of lactation) and evaluation of progeny

Administration of Sv-EtOH, at all doses, during gestation did not affect body weight gain of progenitors, and did not differ significantly from control (Figure 8). Absolute (g) and relative masses (%) of organs (uterus, ovaries, kidneys, adrenals, lungs, heart, liver, and spleen) from progenitors treated with Sv-EtOH (10, 20 and 40 mg/kg) on post-implantation period (8th day of pregnancy to weaning) did not differ significantly when compared to control (Table 8).

Childbirth and birth rates were 100 and 98.05%, respectively. Animals treated with Sv-EtOH at different doses in post-implementation period did not differ significantly in relation to pregnancy duration, number of born alive offspring and offspring viability compared to control (Figure 3). The Sv-EtOH administration during lactation, at all doses, interfered significantly reducing weight gain of progenitors as compared to the control (Figure 9).

Evaluation of the progeny: Analysis of daily observations on indicative characteristics of physical development expected in normal offspring from mothers treated with Sv-EtOH (10, 20 and 40 mg/kg) for 45 days did not show significant differences, compared to the control (Table 9).

DISCUSSION

Estradiol, predominant estrogen, is synthesized on ovaries and secreted by granulosa cells of mature follicles, as well by placenta during pregnancy. Secretion in the systemic circulation acts on alpha and beta estrogen receptors. It is important to note that epithelial cells and uterine stroma express ER in early development and adulthood, and therefore both tissues are susceptible to estrogens in these phases (Brown et al., 1999; Brolio et al., 2010). Whereas, estrogens are

Table 5. Evaluation of the absolute (g) and relative masses (%) of organs from progenitors treated with the ethanolic extract of *S. versicolor* during pre-deployment period (1st to 7th day) as compared to the control.

Variables	Control (n=8)	Treatment (Sv-EtOH)		
		10 mg/kg (n=8)	20 mg/kg (n=8)	40 mg/kg (n=8)
Body weight (g)	194.08 ± 12.45	170.14 ± 4.93	171.58 ± 4.72	193.42 ± 13.21
Absolute mass				
Uterus	0.412 ± 0.044	0.474 ± 0.012	0.447 ± 0.035	0.528 ± 0.049
Kidneys	1.636 ± 0.083	1.446 ± 0.034	1.619 ± 0.079	1.562 ± 0.093
Ovary D	0.040 ± 0.002	0.036 ± 0.001	0.031 ± 0.004	0.103 ± 0.067
Ovary L	0.041 ± 0.005	0.039 ± 0.002	0.038 ± 0.004	0.073 ± 0.039
Adrenal	0.084 ± 0.037	0.047 ± 0.002	0.053 ± 0.005	0.051 ± 0.005
Lung	1.330 ± 0.086	1.234 ± 0.036	1.163 ± 0.053	1.377 ± 0.096
Heart	0.702 ± 0.035	0.672 ± 0.015	0.650 ± 0.021	0.733 ± 0.046
Liver	8.604 ± 0.534	8.593 ± 0.327	7.119 ± 1.075	8.405 ± 0.484
Spleen	0.815 ± 0.121	0.897 ± 0.073	0.799 ± 0.094	0.798 ± 0.087
Relative mass				
Uterus	0.204 ± 0.022	0.260 ± 0.009	0.247 ± 0.018	0.263 ± 0.015
Kidneys	0.806 ± 0.029	0.796 ± 0.030	0.895 ± 0.030	0.782 ± 0.017
Ovary D	0.020 ± 0.001	0.020 ± 0.001	0.017 ± 0.002	0.047 ± 0.029
Ovary L	0.020 ± 0.002	0.022 ± 0.001	0.021 ± 0.002	0.034 ± 0.017
Adrenal	0.042 ± 0.019	0.026 ± 0.001	0.029 ± 0.002	0.026 ± 0.003
Lung	0.655 ± 0.037	0.676 ± 0.015	0.645 ± 0.025	0.687 ± 0.018
Heart	0.346 ± 0.015	0.368 ± 0.006	0.361 ± 0.013	0.367 ± 0.011
Liver	4.212 ± 0.133	4.712 ± 0.172	3.934 ± 0.578	4.226 ± 0.162
Spleen	0.398 ± 0.055	0.494 ± 0.044	0.448 ± 0.060	0.403 ± 0.041

Data express means ± standard error (ANOVA / Tukey).

Table 6. Effect of ethanolic extract of *S. versicolor* during pre-implantation (1st to 7th days) on pre-implant losses, number of corpus luteum and number of deployments compared to control.

Variables	Control	Treatment (Sv-EtOH)		
		10 mg/kg	20 mg/kg	40 mg/kg
Corps luteum	9.75 ± 0.52	10.75 ± 0.81	10.62 ± 0.68	10.62 ± 0.59
Deployments	9.12 ± 0.66	9.37 ±0.65	10.0. ±0.53	10.12 ± 0.54
Pre-implant loss (%)	6.80 ± 2.89	12.28 ±3.51	6.39 ± 2.57	4.41 ± 2.41

Data express mean (± SEM). $p < 0.05$ (ANOVA / Tukey test), n = 8.

responsible for female secondary characteristics development, they also produce a suitable environment for fertilization, implantation, embryo nutrition and parturition (Lindzey and Korach, 1999). Sv-EtOH effect on endometrium was evaluated through uterotrophic assay. Within this perspective, the extract was not able to increase the uterus mass of rats treated at doses of 10, 20 and 40 mg/kg, when compared to rats treated with estradiol alone, inferring that it has no estrogenic activity. However, Sv-EtOH (10, 20 and 40 mg/kg) associated with estradiol inhibited increase of uterus mass stimulated by estradiol. Similar behavior was observed in animals treated with estradiol association + tamoxifen, suggesting anti- estrogenic activity and indicating that the extract can prevent fertilization processes, implantation, embryo nutrition and childbirth.

Hormonal effects on cervical epithelium are still limited on literature. Valente and Sasso (1992), studying female rats cervix, observed that the proportion of collagen fibers and infiltration of eosinophils in the lamina propria was

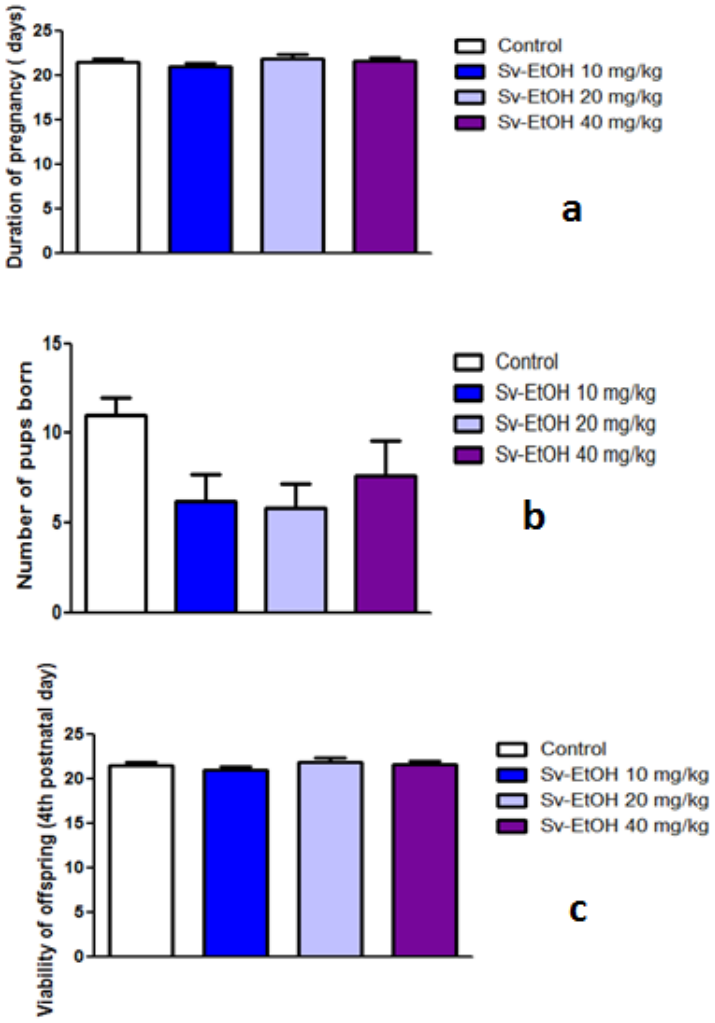

Figure 3. Evaluation of pregnancy duration (a) number of born alive offspring (b) and offspring viability (c) of progenitors treated with ethanolic extract of *S. versicolor* at post-deployment period (8th day pregnant childbirth) compared to control

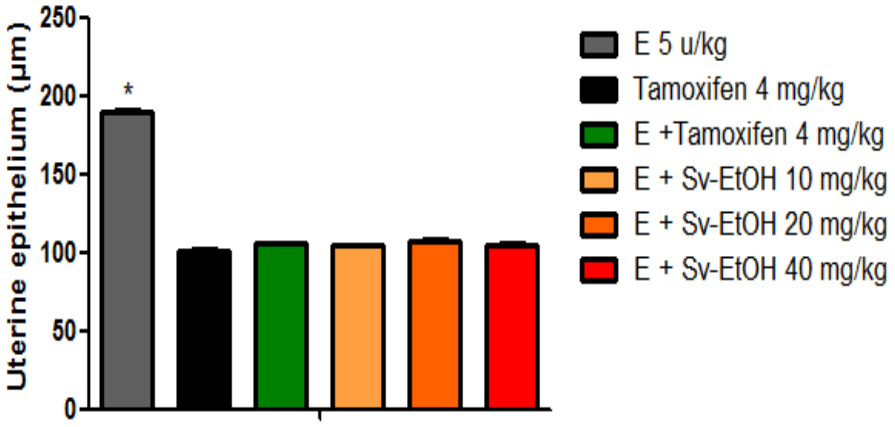

Figure 4. Effect of Estradiol, Tamoxifen, Estradiol+Tamoxifen and Estradiol + Sv-EtOH on the thickness of uterine epithelium of prepubertal rats.Data express mean ± standard error, n = 10, (One Way ANOVA / Tukey).

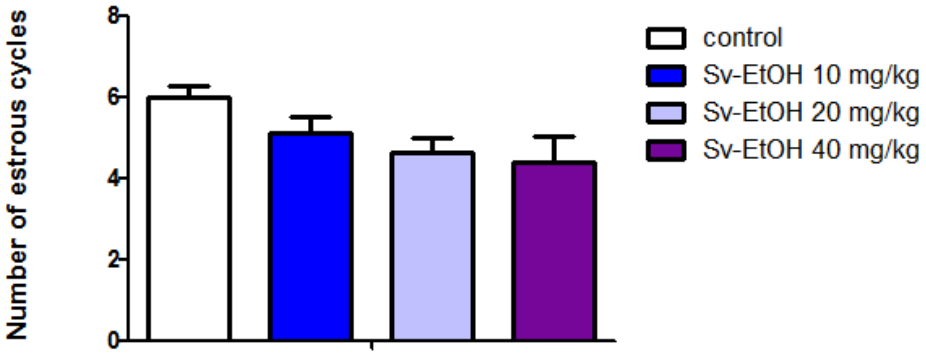

Figure 5. Effect of ethanolic extract of *S. versicolor* on the number of estrous cycles of rats treated for 30 days as compared to the control. Data express mean ± standard error, n = 8, (One Way ANOVA/Tukey).

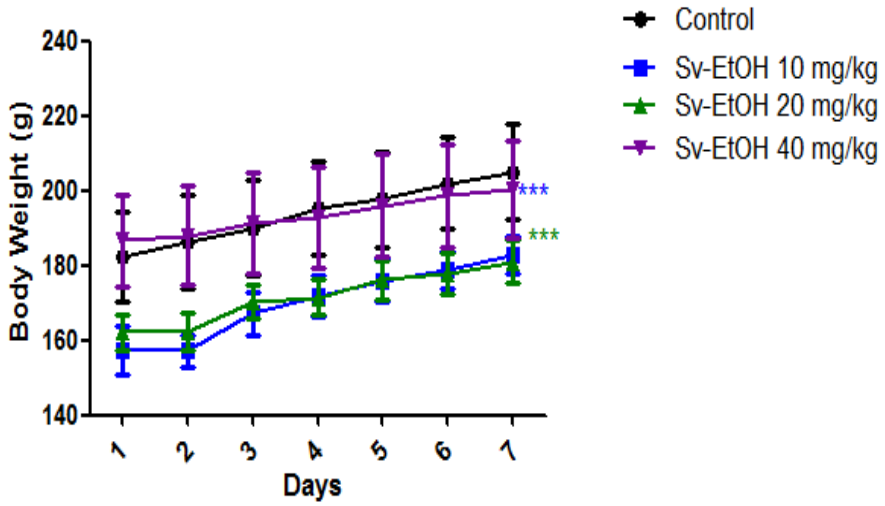

Figure 6. Weigh evolution of progenitors treated with the ethanolic extract of *Simarouba versicolor* during pre-deployment (1º to the 7º day of pregnancy), compared to control .Data express mean ± SEM, n = 8 (One Way ANOVA / Tukey) *** p <0.001 vs baseline weight.

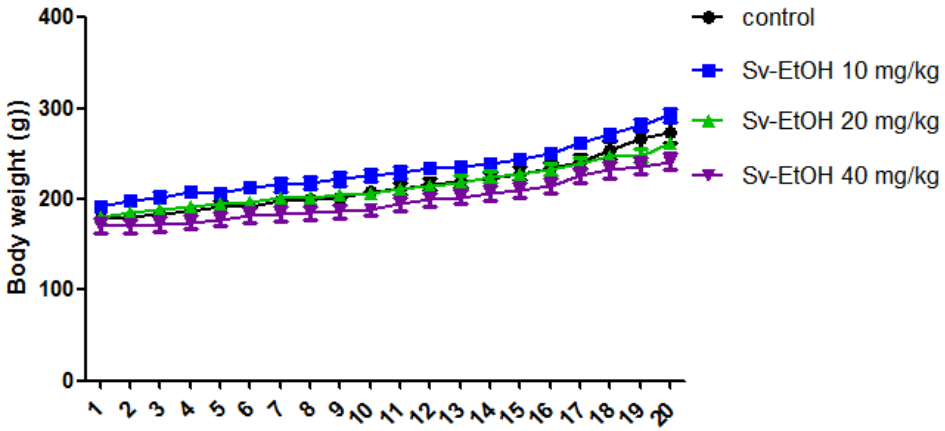

Figure 7. Weight evolution of progenitors treated with the ethanolic extract of *Simarouba versicolor* during pregnancy (1st to 20th day), compared to control. The data is expressed mean ± SEM, n = 8, (One Way ANOVA/Tukey).

Table 7. Evaluation the absolute (g) and relative masses (%) of organs from progenitor treated with ethanolic extract of *Simarouba versicolor* during pregnancy (1st to 20th day) as compared to the control.

Variables	Control (n=8)	Treatment (Sv-EtOH)		
		10 mg/kg (n=8)	20 mg/kg (n=8)	40 mg/kg (n=8)
Body weight (g)	273.25 ± 10.91	292.1 ± 7.27	261.50 ± 5.37	241.28 ± 9.74
Absolute mass				
Uterus	42.18 ± 5.019	44.47 ± 2.529	39.36 ± 2.878	45.58 ± 1.881
Kidneys	1.470 ± 0.060	1.747 ± 0.066	1.640 ± 0.069	1.430 ± 0.044
Ovary D	0.053 ± 0.006	0.064 ± 0.006	0.069 ± 0.003	0.050 ± 0.005
Ovary E	0.066 ± 0.005	0.077 ± 0.006	0.061 ± 0.005	0.059 ± 0.003
Adrenal	0.058 ± 0.005	0.056 ± 0.006	0.068 ± 0.004	0.063 ± 0.003
Lung	1.120 ± 0.067	1.224 ± 0.104	1.393 ± 0.085	1.115 ± 0.049
Heart	0.725 ± 0.040	0.865 ± 0.024	0.818 ± 0.029	0.783 ± 0.028
Liver	11.81 ± 0.437	13.17 ± 0.453	12.18 ± 0.252	11.18 ± 0.495
Spleen	0.858 ± 0.064	0.909 ± 0.032	0.977 ± 0.083	0.731 ± 0.049
Relative mass				
Uterus	15.134 ± 1.50	15.26 ± 0.860	15.10 ± 1.150	18.44 ± 0.627
kidneys	0.541 ± 0.024	0.598 ± 0.016	0.626 ± 0.018	0.595 ± 0.016
Ovary D	0.020 ± 0.003	0.022 ± 0.002	0.027 ± 0.001	0.021 ± 0.003
Ovary E	0.024 ± 0.001	0.026 ± 0.002	0.023 ± 0.002	0.025 ± 0.001
Adrenal	0.022 ± 0.003	0.019 ± 0.002	0.026 ± 0.002	0.026 ± 0.001
Lung	0.417 ± 0.037	0.415 ± 0.031	0.534 ± 0.034	0.463 ± 0.016
Heart	0.266 ± 0.012	0.297 ± 0.009	0.313 ± 0.006	0.326 ± 0.009
Liver	4.345 ± 0.135	4.515 ± 0.122	4.669 ± 0.100	4.646 ± 0.161
Spleen	0.322 ± 0.036	0.312 ± 0.012	0.372 ± 0.027	0.309 ± 0.029

The data express the mean ± standard error. ** = P <0.01 (ANOVA/Tukey).

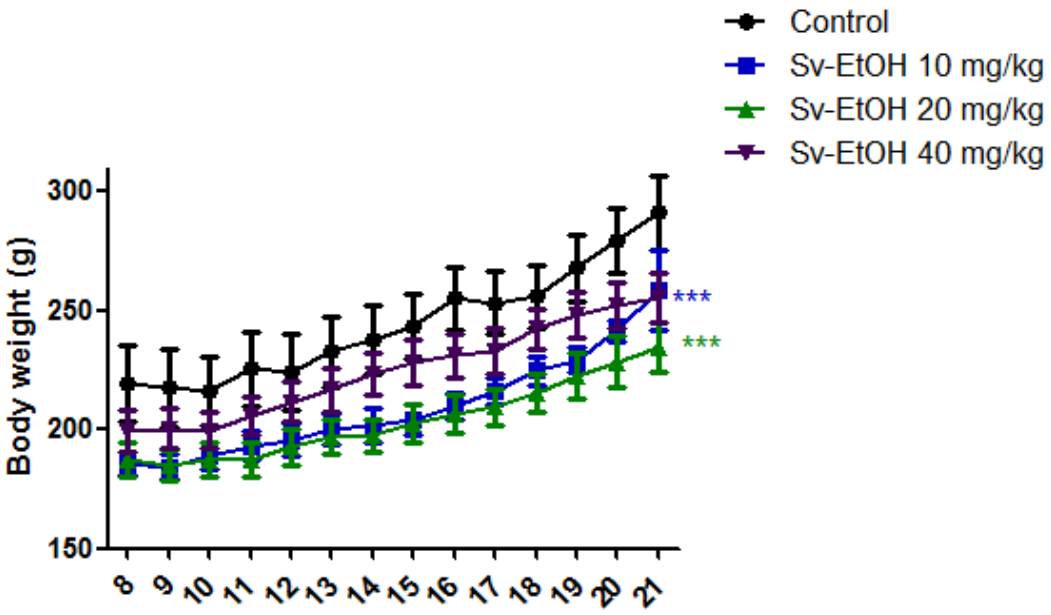

Figure 8. Weight evolution of progenitors treated with ethanolic extract of *Simarouba versicolor* on post-implantation period (8th to 21st days of pregnant) compared to control. The data is expressed mean ± SEM, n = 5, (One Way ANOVA / Tukey); p, *** p <0.001 vs. baseline weight

Table 8. Evaluation absolute (g) and relative masses (%) of organs from progenitors treated with ethanolic extract of *Simarouba versicolor* on post-implantation period (8th to 21st days of pregnancy), compared to control.

Variables	Control (n=8)	Treatment (Sv-EtOH)		
		10 mg/kg (n=8)	20 mg/kg (n=8)	40 mg/kg (n=8)
Body weight (g)	239.41 ± 14.17	209.58 ± 5.54	203.84 ± 7.81	224.71 ± 8.62
Absolute mass				
Ovary D	0.039 ± 0.004	0.035 ± 0.005	0.039 ± 0.005	0.028 ± 0.002
Ovary E	0.041 ± 0.005	1.036 ± 0.004	0.031 ± 0.005	0.046 ± 0.004
Uterus	0.252 ± 0.033	0.237 ± 0.055	0.256 ± 0.053	0.199 ± 0.018
Lung	1.497 ± 0.123	1.273 ± 0.065	1.240 ± 0.065	1.232 ± 0.015
Adrenal	0.070 ± 0.005	0.064 ± 0.006	0.062 ± 0.004	0.075 ± 0.004
kidneys	1.875 ± 0.040	1.706 ± 0.049	1.658 ± 0.064	1.912 ± 0.103
Liver	10.55 ± 0.661	8.698± 0.299	9.942 ± 0.624	10.51 ± 0.543
Spleen	0.565 ± 0.017	0.565 ± 0.036	0.559 ± 0.017	0.507± 0.023
Heart	0.790 ± 0.032	0.630 ± 0.020	0.729 ± 0.034	0.621 ± 0.025
Relative mass				
Ovary D	0.018 ± 0.002	0.018 ± 0.002	0.019 ± 0.002	0.015 ± 0.001
Ovary E	0.018 ± 0.002	0.018 ± 0.002	0.016 ± 0.003	0.024 ± 0.001
Uterus	0.114 ± 0.016	0.119 ± 0.023	0.126 ± 0.023	0.103 ± 0.010
Lung	0.668 ± 0.024	0.651 ± 0.028	0.630 ± 0.053	0.635 ± 0.012
Adrenal	0.032 ± 0.002	0.033 ± 0.003	0.032 ± 0.003	0.039 ± 0.002
Kidneys	0.847 ± 0.036	0.876 ± 0.035	0.841 ± 0.061	0.983 ± 0.036
Liver	4.721 ± 0.078	4.455 ± 0.134	5.049 ± 0.457	5.408 ± 0.206
Spleen	0.256 ± 0.013	0.288 ± 0.013	0.282 ± 0.010	0.262 ± 0.015
Heart	0.355 ± 0.009	0.323 ± 0.012	0.336 ± 0.014	0.320 ± 0.010

The data express the mean ± standard error (ANOVA/Tukey).

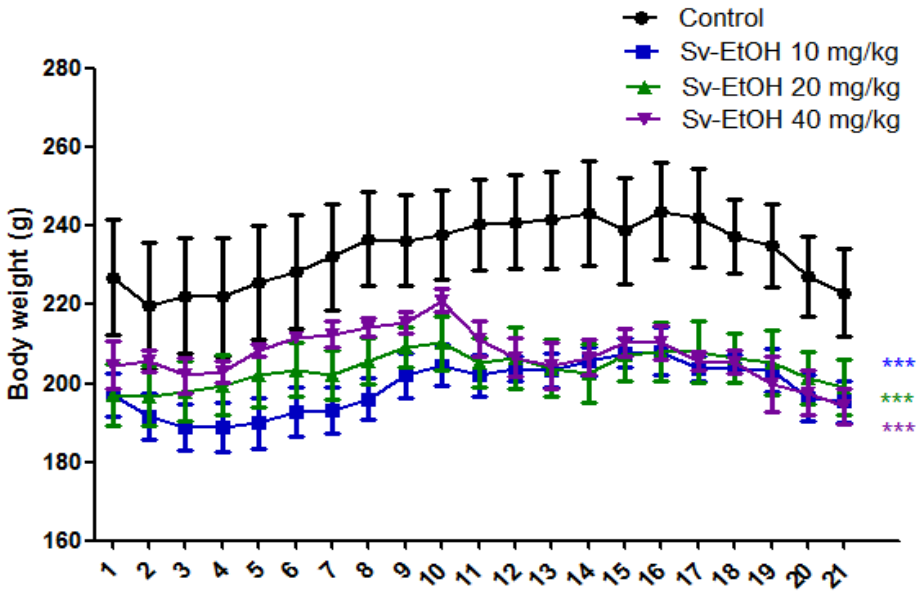

Figure 9. Weight evolution of progenitors treated with ethanolic extract of *Simarouba versicolor* on lactation period (1st to 21st days of lactation) compared to control. The data express the mean ± standard error (ANOVA One Wa /Tukey). The data is expressed mean ± SEM, n = 5, (One Way ANOVA / Tukey).

Table 9. Evaluated parameters of progeny coming from mothers treated with ethanolic extract of *Simarouba versicolor* for 45 days.

Parameters (days)	Control	Treatment (Sv-EtOH)		
		10 mg/kg	20 mg/kg	40 mg/kg
Eye opening	14.40 ± 0.51	11.16 ± 2.24	14.40 ± 0.74	11.00 ± 2.77
Detachment of ears	6.80 ± 0.37	5.83 ± 1.19	7.00 ± 0.316	5.60 ± 1.43
Appearance of hair	6.40 ± 0.24	5.33 ± 1.08	7.40 ± 0.40	5.40 ± 1.36
Opening of vaginal canal (females)	39.40 ± 1.03	33.53 ± 6.70	41.40 ± 2.01	31.80 ± 7.97

The data express mean (± SEM), p> 0.05. (ANOVA, One Way / Tukey).

higher in estrus phase (after hormonal peak of estrogen) compared to the diameter. Ramos et al. (2002) reported that uterine morphological aspects are related directly to receptors' levels of estrogen and progesterone.

However, analyzing histological sections of uterus in uterotrophic assay, animals treated with estradiol in endocervical canal presented simple cylindrical epithelium sorely infiltrated by leukocytes and stratified epithelium nonkeratinized with high concentration of eosinophils. Animals treated with tamoxifen had both epithelium endocervical and ectocervical underdeveloped compared with estradiol groups. In the treatment with estradiol + tamoxifen, simple cylindrical epithelium showed little leukocyte infiltration, low concentration of eosinophils and epithelia undeveloped compared to animals treated with estradiol alone. Likewise, it happened to groups treated with estradiol and Sv-EtOH at all doses.

Morphological and morphometric analysis confirmed that the endometrium was affected by treatments in antiestrogenic activity assay, as animals treated with estradiol + tamoxifen and estradiol + Sv EtOH (10, 20 and 40 mg/kg) presented low uterine epithelium, inhibiting estrogen action and confirming Sv-EtOH antiestrogenic activity. Events pattern in estrous cycle provide a useful normality indicator for neuroendocrine function of non-pregnant female ovaries (Andrews et al.; 2002). Sv-EtOH treatment (10, 20 and 40 mg/kg) for 30 consecutive days did not cause changes in regularity, duration and repeatability of estrous cycles as compared to the control. This indicates that the treatment did not promote disorders of hypothalamic-pituitary-ovarian axis.

Estrous cycle in female rats is regular, consists of several annual cycles and with 4 to 5 days of duration (Cobea, 1996). Due to this short period, rats are considered the ideal animals to study estrous cycle variations (Marcondes et al., 2001). However, control animals may show irregular cycles, usually in the form of cycle stretching or acyclicity (US EPA, 1996). In this study, control rats showed cycle elongation (1 day for treated groups). Although the difference between the groups was not significant ($p > 0.05$), there is a dose-dependent tendency to increase cycles duration. So far, all cycles in the 30 days consecutive period of treatment were in accordance with the literature (Santos et al., 2003; Hollenbach et al., 2008).

Cycle changes can be caused by treatment with certain substances, such as xenobiotics, that can induce acyclicity characterized by persistent estrus, diestrus or irregular standard (Goldman et al., 2007). Some changes in ovarian hormones and extra-ovarian can lead to irregularity in ovarian function causing changes in estrous cycle duration (Shivalingappa et al., 2002).

Alterations in estrous cycle extension can be a response to exposure to an agent with estrogenic property or capable of blocking ovulation. On the other hand, there are substances that can induce changes in estrous cycle at doses that do not impair fertility. Diestrus persistence indicates temporary or permanent interruption of follicular development and ovulation, inducing temporary infertility. Prolonged diestrus or anoestrus can be indicative agents (for example, polycyclic aromatic hydrocarbons) that interfere with follicle development or deplete the pool of primordial follicles or agents such as atrazine, which interrupt support of ovarian gonadotropin (US EPA, 1996; Romero, 2007). In this experiment, it was observed that in irregular cycles, the phase that lasted more was diestrous (72.2%); it is characterized by the lack of cellular elements and high concentrations of leucocytes and mucus. Estrus phase lasted for more than 12 h in 22.2% cases.

Hematological evaluation represents an important area of study on animals' health. Blood analysis helps in the diagnosis and prognosis of various diseases (Jain, 1993). Evaluation of systemic toxicity showed that oral administration of Sv-EtOH at doses of 10, 20 and 40 mg/kg for 30 days produced no behavioral changes in adult Wistar rats nor visible signs of toxicity. Chemistry profile parameters evaluated were within the normal range except for creatinine levels. There was a quantitative increase in creatinine concentration for all groups exposed to Sv-EtOH as compared to the control group. Creatinine is an important parameter for diagnosing various kidney problems. Creatinine is a non-protein nitrogenous organic compound formed from the dehydration of the muscle creatine. This serves to assess glomerular filtration rate, as blood concentration increases

with reduced renal filtration rate. The presence of this substance in blood can be used to identify renal disorders. Creatinine tends to increase slower than urea in renal disease. Thus, this parameter provides us with evidence of renal impairment in animals treated with Sv-EtOH.

Deployment is a process by which the embryo has intimate physical and physiological contact with maternal endometrium to establish pregnancy. Although there are variations of this process between species, certain basic events are similar. The fundamental characteristic of this process is the synchronized embryo development to the blastocyst stage and differentiation from uterus to receptive state. This is followed by interactions between activated blastocysts and the uterine epithelium to start deployment (Muller et al., 2009).

Progenitors exposed to Sv-EtOH (10, 20 and 40 mg/kg) during pre-implantation period did not alter weight gain. Reduction in corporal mass could reflect a variety of responses, including anorexia induced by the treatment or systemic toxicity (US EPA, 1996). In relation to absolute and relative masses of ovaries, uterus, liver, lungs, spleen, kidneys, heart and adrenal did not exhibit significant changes. There were also no physical and macroscopic changes in animals and organs exposed to Sv-EtOH. These results indicate absence of extract toxicity at investigated doses, during this period, which is probably due to short term exposure.

Gestational period is one of the most sensitive stages of reproductive cycle, which results in important responses. Today, it is known that in this period most agents cross through the placenta. Thus, it can be considered that maternal exposure to external agents may result in significant effects on a passive organism, a secondary target of these agents, which is the embryo body (Damasceno et al., 2008). During pregnancy, the exposure of mothers to the ethanol extract of *S. versicolor* at all doses did not affect the body mass gain or the absolute and relative masses of organs (uterus, ovaries, liver, heart, lung, spleen, kidney and adrenal glands). Resorption rates, pre-implant loss and post-implant loss were not significant compared to control results. Groups treated with Sv-EtOH presented implantation rates of 100%, indicating absence of maternal toxicity at doses investigated during pregnancy. Also no macroscopic signs of toxicity were observed in animals or organs.

The evaluation of absolute masses of metabolism and excretion organs is important, since liver and kidney are responsible for metabolism and elimination of xenobiotics intoxication cases, which may lead to an increase in mass (Mello, 2007). In post-implantation period, progenitors exposed to Sv-EtOH during gestation and lactation did not show changes in absolute and relative masses of organs (uterus, ovaries, liver, heart, lung, spleen, kidneys and adrenals), not differing from control animals. Exposure to Sv-EtOH did not affect weight gain of progenitors treated during gestation, compared to control animals, indicating absence of maternal toxicity in the doses investigated.

The same way, during pregnancy and lactation there were no signs of toxicity such as anorexia, shivers, diarrhea, piloerection or seizures. Rats' exposure to Sv-EtOH at different doses did not affect childbirth index (%) and birth index (%), indicating the extract is not toxic to prenatal development. Variations in gestation duration can result in alteration in childbirth labor. A significant prolongation of gestation time can be the cause of failure during childbirth mechanism and can result in death or injury of brood per dystocia.

Exposure in late pregnancy to substances with anti-estrogenic activity can interfere in estrogen action, altering both characteristics structurally and sensitivity of myometrium cells to promote childbirth (Lindzey and Korach, 1999). Administration of Sv-EtOH, at tested doses, did not affect pregnancy duration, number of born alive (cubs alive until the fourth day) and offspring viability. In this way, Sv-EtOH antiestrogenic activity did not impair estradiol action to increase oxytocin expression. It did not inhibit the production of prostaglandins in uterus in late pregnancy and did not also interfere in childbirth labor in rats treated with the extract.

Sv-EtOH at the tested doses, during lactation affected weight gain when compared to control animals. This may be an indication of toxicity but also by caloric burn in parturition and lactation periods. Although results indicate a possible extract systemic toxicity, exposure at doses investigated in pregnancy and lactation periods did not affect the overall development of offspring (detachment period of ears, fur appearance, eye opening, opening of vaginal canal and offspring viability) when compared with control group. Although, exposure route has been altered from fetal-placental membrane to breast milk, indicating a possible reduction in exposure levels to the extract components; it also suggests lack of toxicity in postnatal development because descendants of the progenitors treated with the extract.

Therefore, the ethanol extract of *S. versicolor* presented antiestrogen activity, possible systemic toxicity and showed no reproductive toxicity at the doses investigated.

Conflict of interests

The author(s) did not declare any conflict of interest.

REFERENCES

Almeida MMB, Arriaga AMC, Santos ALK, Lemos TLG, Braz-filho R, Vieira IJC (2007). Ocorrência e atividade biológica de quassinóides da última década. Química Nova 30:935-951.

Andrews P, Freyberger A, Hartmann E et al.(2002). Sensitive detection of the endocrine effects of the estrogen analogue Ethinylestradiol

using a modified enhanced subacute rat study protocol (OECD Test Guideline no 407). Arch. Toxicol. 76:194-202.
Brolio MP, Ambrosio CE, Franciolli AR, Morini AC, Guerra RR, Miglino MA (2010). A barreira placentária e sua função de transferência nutricional. Rev. Bras. Reprod. Anim. 34(4):222-232.
Brown TR, Steroids H, Overviee W (1999). In: KnobiL, E, Neil, J. D. Encyclopedia of Reroduction. San Diego: Academic press, 4:634-644.
Carvalho JIX (2008). Estudo fitoquimico e avaliação do potencial de inibição da enzima acetilcolinesterase de *Simarouba versicolor* (Simaroubaceae). Dissertação (mestrado em Química Orgânica). Universidade Federal do Ceará.
Carvalho NM, Bacha FB, Santos AC, Carvalho AQ, Faccin TC, Pott A, Lemos RAA (2013). Spontaneous and experimental intoxication of cattle by Simarouba versicolor A. St.-Hill (Simaroubaceae). Toxicon 64:55-59.
COBEA – Colégio Brasileiro de Experimentação Animal (1996). Manual para técnicos em bioterismo. 2 ed. São Paulo: H. A. Rothchild, 259p.
Damasceno DC, Kempinas WG, Volpato GT (2008). Anomalias congênitas: estudos experimentais. Belo Horizonte: Coopmed. P 102.
Fernandes MZLCM, Fernandes RM, Lopes JB, Viana GEN (2004). Determinação da toxicidade aguda da *Simarouba versicolor* em camundongos. Rev. Bras. Plantas Med. 6(2):44-47.
Garcia RC, Louredo VF, Mattedi WC, Garcia Jr RP (2010). Ensaios biológicos do Almeirão-roxo (*Cichorium intybus* L.) e barbatimão (*Styphnodendron barbatiman* MARTIUS) em ratas em menopausa cirúrgica. Revista Eletrônica de Farmácia 7:65-80.
Goldman JM, Murr AS, Cooper R (2007). The rodents estrus cycle: characterization of vaginal cytology and its utility in toxicological studies. Birth Defects Res. B Dev. Reprod. Toxicol. 80:84-97.
Hankness JE, Wagner JE(1993). Biologia e Clínica de Coelhos e Roedores. São Paulo: Roca, 3º edição,. p. 238.
Hollenbach CB, Bortolini CE, Batista JM (2010), Hollenbach EB, Schuch TL, Pachedo MH, Mello FB, Mello JR. Desenvolvimento pós-natal e potencial teratogênico da prole de ratos Wistar no estudo da toxicidade reprodutiva de duas preparações fitoterápicas contendo soja Glycine max (L.) Merr. Arq. Bras. Med. Vet. Zootec. 662(.4):845-852.
Jain NC (1993). Essentials of veterinary hematology. Philadephia: Lea & Febiger.
Lindzey J, Korach KS (1999). Estrogen action on the female reproductive tract. In: Knobil E, Neill JD (eds.). Enciclopedia of reproduction. San Diego, Academic Press. 2:79-86.
Lourenço ACS, Miguel KL, Sensiate LA, Salles MJS (2009). Óleo de copaíba (Copaifera langsdorfii Desf.) em padrões reprodutivos de camundongos e no desenvolvimento embriofetal. Rev. Bras. Plantas Med. 11(4):407-413.
Marcondes FK, Miguel KJ, Melo LL, Spadari-Bratfisch RC (2001). Estrous cycle influences the response of female rats in the elevated plus-maze. Physiol. Behav. 74:435-440.
Mello M (2007) Avaliação da toxicidade reprodutiva do pesticida trifenil hidróxido de estanho (TPTH) em camundongos. Tese (Doutorado em Vigilância Sanitária). Fundação Oswaldo Cruz. Rio de Janeiro. p.131.
Mesquita AG (1997). Contribuição ao conhecimento químico de plantas do Nordeste do Brasil: *Simarouba versicolor* (Simaroubaceae). Dissertação de Mestrado do Programa de Pós-Graduação em Química Orgânica da Universidade Federal do Ceará: Fortaleza, 119f.
Mesquita ML (2009). Potencial antitumoral de substâncias isoladas de plantas do Cerrado brasileiro: Estudos preliminares do mecanismo de ação da atividade citotóxica. Tese de doutorado. Universidade de Brasília, Brasil.
Muller JBBS, Fernandes RM, Batista MCS, Moura ER, Silva RVP, Filho ESF, Oliveira RCM, Fernandes MZLCM (2013). Studies of *Copaifera luetzelburgii* Harms in reproductive pharmacology: in vivo and in vitro approaches. Afr. J. Biotechnol. 12(24):3864-3871.
Muller JC, Giuliana GK, Botelho AC, Bufalo AC, Boareto YD, Martins ES, Cabrini DA, Otuki MF, Dalsenter PR (2009). Toxicidade reprodutiva da Morinda citrifolia Linn. J. Ethnopharmacol.12:229-233.
Pires JEP, Fernandes RM, Fernandes MZLCM, Viana GEN, Dourado JCL, Sousa SAA (2006). Determinação da concentração inibitória média (CI50) do extrato aquoso de Simarouba versicolor, St. Hill sobre a ovipostura do carrapato bovino (Boophilus microplus, Canestrine, 1887). Rev. Bras. Plantas Med. 9(4):23-26.
Ramos JG, Varayoud J, Bosquiazzo VL, Luque EH, Munoz-de- toro M (2002). Cellular turnover in the rat uterine cervix and its relationship to estrogen and progesterone receptor dynamics. Biol. Reprod. 67:735-42.
Santos KRP, Mendonça JS, Teixeira VW, Teixeira AAC (2003). Influência da ausência de luz sobre o ciclo estral de ratas. Arq. Inst. Biol. 70(1):21-23.
Shivalingappa H, Satyanarayan ND, Purohit MG, Sharanabasappa A, Patil SB (2002). Effect of extract of *Rivea hipocreteriformis* on the estrous cycle of the rat. J. Ethnopharmacol. 82(1):11-17.
Tresvenzol LM, Paula JR, Ricardo AF, Ferreira HD, Zatta DT(2006). Estudo sobre o comércio informal de plantas medicinais em Goiânia e cidades vizinhas. Revista Eletrônica de Farmácia 3(1) 22-28.
US EPA (1996). Guidelines for reproductive toxicity risk assessment. EPA/630/R-96/009, Washington.
Valente CA, Sasso WS (1992). Morphology and morphometry of the cervix uteri off emale albino rats in the estrus and diestrus phases. Rev. Bras. Biol. 52:527-32.

academicJournals

Vol. 15(8), pp. 236-251, 24 February, 2016
DOI: 10.5897/AJB2015.15111
Article Number: 535FEC657329
ISSN 1684-5315

http://www.academicjournals.org/AJB

African Journal of Biotechnology

Full Length Research Paper

Codon usage bias analysis for the coding sequences of *Camellia sinensis* and *Brassica campestris*

Prosenjit Paul and Supriyo Chakraborty*

Department of Biotechnology, Assam University, Silchar-788011, Assam, India.

Received 20 November, 2015; Accepted 1 February, 2016

Codon usage bias plays an important role in the regulation of gene expression. A couple of measures are widely used to quantify the codon usage in genes. On the other hand, no quantitative endeavour has been made to compare the pattern of codon usage diversity within and between different genes of *Camellia sinensis* and *Brassica campestris.* Nucleotide composition and its relationship with codon usage bias were analyzed. Additionally, the rare codons were identified by computing the recurrence of event of all codons in coding sequences of *C. sinensis* and *B. campestris.* The host cell, *Escherichia coli* used universally, failed to express smoothly many eukaryotic genes. For this, the authors prognosticated the codons showing the highest and the lowest expressivity of the coding sequences of *C. sinensis* and *B. campestris,* in *E. coli K12* strain to improve the expression level of the genes.

Key words: Codon usage bias, gene expressivity, codon usage pattern, residual value, synonymous codon.

INTRODUCTION

Gene expression is a fundamental cellular process by which proteins are synthesized in a cell based on the information encoded in the genes. Most amino acids can be encoded by more than one codon; such codons are depicted as being synonymous, and mostly vary by one nucleotide in the third position. Synonymous codons are not used uniformly, varies across species and within genome in the same species, the phenomenon is called codon usage bias (CUB) (Akashi, 1994; Behura and Severson, 2013). Molecular evolutionary investigations on codon bias suggest that recurrence of codon use changes between genes from the same genome and also between genomes (Hooper and Berg, 2000). Highly expressed genes are more biased in terms of their codon usage as compared to low expressed genes, and provide differential efficiency as well as accuracy in the translation of genes (Rocha, 2004; Hershberg and Petrov, 2008). The selection associated with translational efficiency/ accuracy is often termed as 'translation selection'. During the last two decades, numerous lines of evidence suggested that codon usage bias is driven by selection, particularly for species of fungi (Bennetzen and Hall, 1982; Ikemura, 1985), bacteria (Ikemura, 1981; Sharp and Li, 1987a) and insects (Akashi, 1997; Moriyama and Powell, 1997).

Soon, after the discovery of whole genome sequencing

*Corresponding author. E-mail: supriyoch2008@gmail.com. Tel: +919435700831. Fax: 03842-270802.

technology, codon usage bias was analysed for numerous organisms (Plotkin and Kudla, 2011). Numerous factors have been shown to influence codon usage bias: (i) genomic composition (Supek and Vlahovicek, 2005); (ii) selective forces (Ikemura, 1985); and (iii) horizontal gene transfer, with transferred genes retaining the codon frequencies of their former host (Lawrence and Ochman, 1998). Connections have also been demonstrated between codon usage and several factors namely: (a) gene length (Lawrence and Ochman, 1998); (b) gene translation initiation signal (Ma et al., 2002); (c) expression level (Gouy and Gautier, 1982; Sharp and Li, 1986; Sharp et al., 1986; Sharp and Li, 1987b); (d) protein amino acid composition (Lobry and Gautier, 1994); (e) protein structure (D'Onofrio et al., 2002); (f) tRNA abundance (Ikemura, 1981, 1982); (g) mutation frequency and patterns (Sueoka, 1999); and (h) GC composition (Sueoka and Kawanishi, 2000). Besides, the relative impact of each of these factors varies from genome to genome, and from gene to gene. Despite the fact that there is still no final result on the formation mechanism, codon bias has been widely used to predict the exogenous and endogenous gene expression level (Lee et al., 2007; Yu et al., 2007; Zheng et al., 2007), identify horizontally transferred genes (Goldman et al., 2007), evolutionary relationship (Ram et al., 2007), and confirm the coding sequences. Researchers proposed that in some prokaryotes, many indices exhibit a positive correlation with the gene expression level, such as codon adaptation index (CAI) (Sharp and Li, 1987b), codon bias index (CBI) (Bennetzen and Hall, 1982), and frequency of optimal codons (Kanaya et al., 2001). Then again, in a few eukaryotes there is no confirmation to bolster this, particularly for higher eukaryotes where, the correlation between codon bias and expression level is extremely weak (Murray et al., 1989; Kanaya et al., 2001).

In this study, we investigated the codon usage bias (CUB) for *Camellia sinensis* and *Brassica campestris* by analyzing the codon adaptation index (CAI), relative codon usage bias (RCBS), effective number of codons (ENc), synonymous codon usage order (SCUO), and GC/AT content at each codon position. The purpose of this study was to perform a comparative analysis of codon usage bias and codon contexts pattern among the coding sequences (cds) of *C. sinensis* and *B. campestris.*

Escherichia coli cells were, as often as possible, utilized as host cells as a part of the investigation of exogenous protein expression. Many eukaryotic genes cannot be efficiently expressed in a prokaryote like *E. coli*. One of the effective methods for improving the expression level of a eukaryotic gene in a prokaryote is to replace the usage of 'rare codons' with synonymous codons showing highest expressivity in prokaryotes. While replacing the rare codons, the stability of genes at genomic or transcriptional level should be taken into consideration. Here, a novel computational method to identify the codons of *C. sinensis* and *B. campestris* was introduced exhibiting the highest and lowest expressivity in *E. coli* k12 strain.

MATERIALS AND METHODS

The complete coding sequences of the thirty genes from *C. sinensis* and forty seven genes from *B. campestris* were retrieved from the National Centre of Biotechnology (NCBI) nucleotide database accessible from the website www.ncbi.nlm.nih.gov. Each of those cds were devoid of any unknown base (N), intercalary stop codon and possessed the start and stop codons.

Relative codon usage bias and codon adaptation index were used to study the overall codon usage variation among the genes. RCBS is the overall score of a gene indicating the influence of RCB of each codon in a gene. RCB reflects the level of gene expression. RCBS was calculated as by Roymondal et al. (2009). Gene expressivity was again measured by calculating the codon adaptation index as per Sharp and Li (1986). It essentially measures the distance from a given gene to a reference gene with respect to their amino-acid codon usages. CAI defines translational optimal codons as those that appear frequently in highly expressed genes that is:

$$CAI(L(g)) = \exp\left(\frac{1\sum_{l=1}^{L} \log w_{c(l)}}{L}\right) = \left(\prod_{l=1}^{L} w_{c(l)}\right)^{1/L}$$

Where, L is the length of gene g and w_c (l) is the relative adaptiveness of the codon c in the reference genes (not g).

Certain codons will appear multiple times in the gene. Hence we can rewrite the equation to sum up codons rather than length, and use counts rather than frequencies. This makes the dependence on the actual gene more clear. The more usual form is:

$$CAI(o(g)) = \exp\left(\frac{1}{o_{tot}} \sum_{c \in C} o_c \log w_c\right) = \left(\prod_{c \in C} o_c \log w_c\right)^{\frac{1}{o_{tot}}}$$

The effective number of codons (ENc) is the total number of different codons used in a sequence. The values of ENc for standard genetic code range from 20 (where only one codon is used per amino acid) to 61 (where all possible synonymous codons are used with equal frequency). ENc measures bias toward the use of a smaller subset of codons, away from equal use of synonymous codons. For example, as mentioned above, highly expressed genes tend to use fewer codons due to selection. The underlying idea of ENc is similar to the concept of zygosity from population genetics, which refers to the similarity for a gene from two organisms. ENc value was calculated as per Wright (1990). The measure of codon usage, synonymous codon usage orders (SCUO) of genes was computed as per Wan et al. (2004). GC3s is the frequency of (G+C) and A3s, T3s, G3s, and C3s are the distributions of A, T, G and C bases at the third codon position (Gupta and Ghosh, 2001). A series of scripts (programs) were writen in Perl language and run in Windows for analysis. These programs were used to estimate the above mentioned genetic parameters.

The correlations between all the above mentioned parameters were measured with the gene expressivity to find out the genetic factors playing major role in the genes of *C. sinensis* and *B. campestris.* All codon quantifications were performed using the Anaconda software (Moura et al. 2007). The residual values of each codon pair were also quantified from the coding sequences of each plant species by the Anaconda program. The occurrence frequency of each codon for a particular amino acid was also calculated and compared with their expressivity values to identify

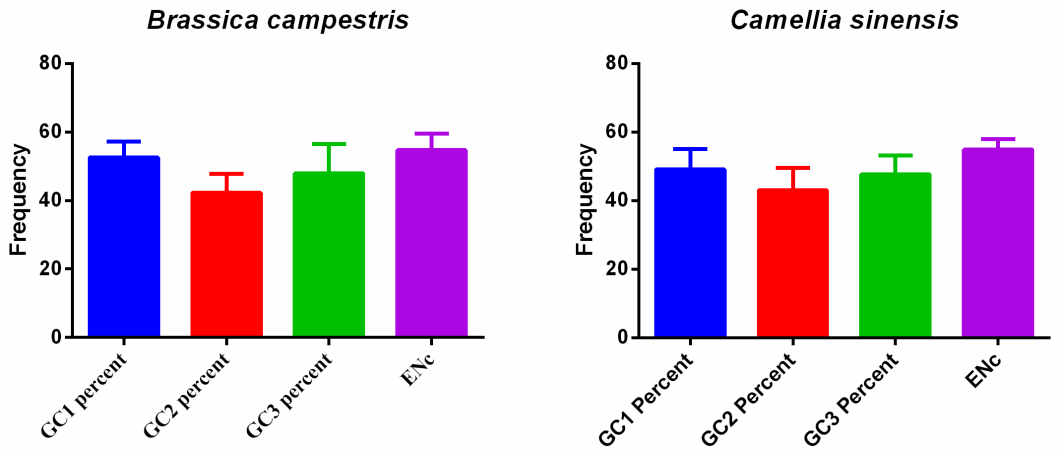

Figure 1. Effective number of codon (ENc) distribution for the genes of *B. campestris* and *C. sinensis.* GC% at third codon position for *C. sinensis* and for first codon position for *B. campestris* showed strong correlation (0.3, 0.4) respectively with the ENc among all the codon positions.

the codons playing a prominent role in determining the level of gene expression.

RESULTS AND DISCUSSION

The present study was carried out to assess the codon usage pattern and gene expressivity for the genes of *C. sinensis* and *B. campestris*. In numerous microscopic organisms, intragenomic diversity in codon usage among genes has been reported. The genes selected for the present study from the two plants with their accession numbers together with the overall AT and GC%, RCBS, CAI, ENc, SCUO, GC1, GC2 and GC3 are given in the supplementary file. It was found that the codons of *C. sinensis* and *B. campestris* are rich in A and/or T. Yet, on account of *Homo sapiens*, it has been shown that the codons ending in G and/or C are dominating in the whole coding region.

Due to the difference in mutational bias, the GC percentage among different species varies to a great extent, even for the species within the same order. To determine if GC bias among *C. sinensis* and *B. campestris* has an association with codon bias, the non-directional codon bias measure effective number of codons (ENc) was resorted to. The effective number of codons used by a gene and GC% at the three different synonymous codon positions (GC1s, GC2s and GC3s) are used to study the codon usage variation among the genes of *B. campestris* and *C. sinensis* (Figure 1). To quantify the level of diversity in the synonymous codon usage among all the selected cds within the genome of *B. campestris* and *C. sinensis*, the mean distance between the pairs of cds was estimated. The mean distance was found to be 0.07 with a median of 0.06 for *C. sinensis* and a mean distance of 0.09 with the median of 0.07 for the cds sequence of *B. campestris*. When focusing on the previously studied genomes (Lafay et al., 2000; Grocock and Sharp, 2002; Wu et al., 2005), the mean values for *Bacillus subtilis* 168 (0.60), *E. coli* K12 MG1655 (0.47), *Helicobacter pylori* 26695 (0.38), and *Haemophilus influenzae* Rd KW20 (0.37) indicated that the mean values varied widely among species. ENc is a widely accepted measure of codon usage bias that quantifies the degree of deviation from equal use of synonymous codons. It has been suggested that ENc may be dependent on the strength of the codon bias discrepancy (Fuglsang, 2004). The coefficient of determination (denoted as R^2) indicates how well the data points fit a straight line or curve. From the analysis, it is apparent that the coefficient of determination is 0.37 and 0.15 for the genes of *C. sinensis* and *B. campestris*, respectively (Figure 2). This reveals that 37% of the variation in expressivity for the cds of *C. sinensis* and 15% for the cds of *B. campestris* could be explained by the ENc. The remaining percentage of the variation in expressivity could be attributed to unknown factors, that is, genetic variation and/or other external factors.

Synonymous codon usage orders (SCUO) of genes of each species were further analyzed. SCUO is a relatively easier approach as compared to RSCU and is considered as more robust for comparative analysis of codon usage. The SCUO analysis shows that a majority of the genes selected for the present study are associated with high codon usage bias (43% cds in *C. sinensis* and 68% in *B. campestris* have SCUO≥0.5). This outcome proposes that these genes are associated with specific functions such as translational processes, ribosomes (mostly ribosomal protein genes), intracellular activities, transport, oxidation-reduction process and others (Supplementary Tables 1 and 2).

The Anaconda software was used to determine the adjusted residual values for association of each codon pair in genome-wide manner for the two plant species.

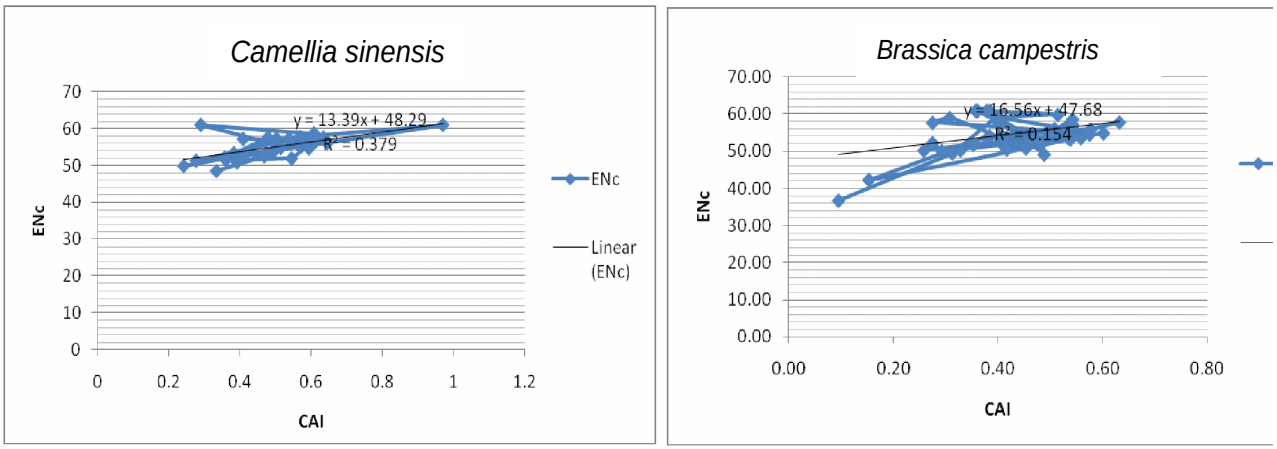

Figure 2. ENc values plotted against the CAI for the cds of *Camellia sinensis* and *Brassica campestris*. The coefficient of determination (denoted as R^2) is 0.37 and 0.15 for the genes of *Camellia sinensis* and *Brassica campestris* respectively suggesting that 37% of the variation in expressivity for the cds of *Camellia sinensis* and 15% for the cds of *Brassica campestris* could be explained by the ENc.

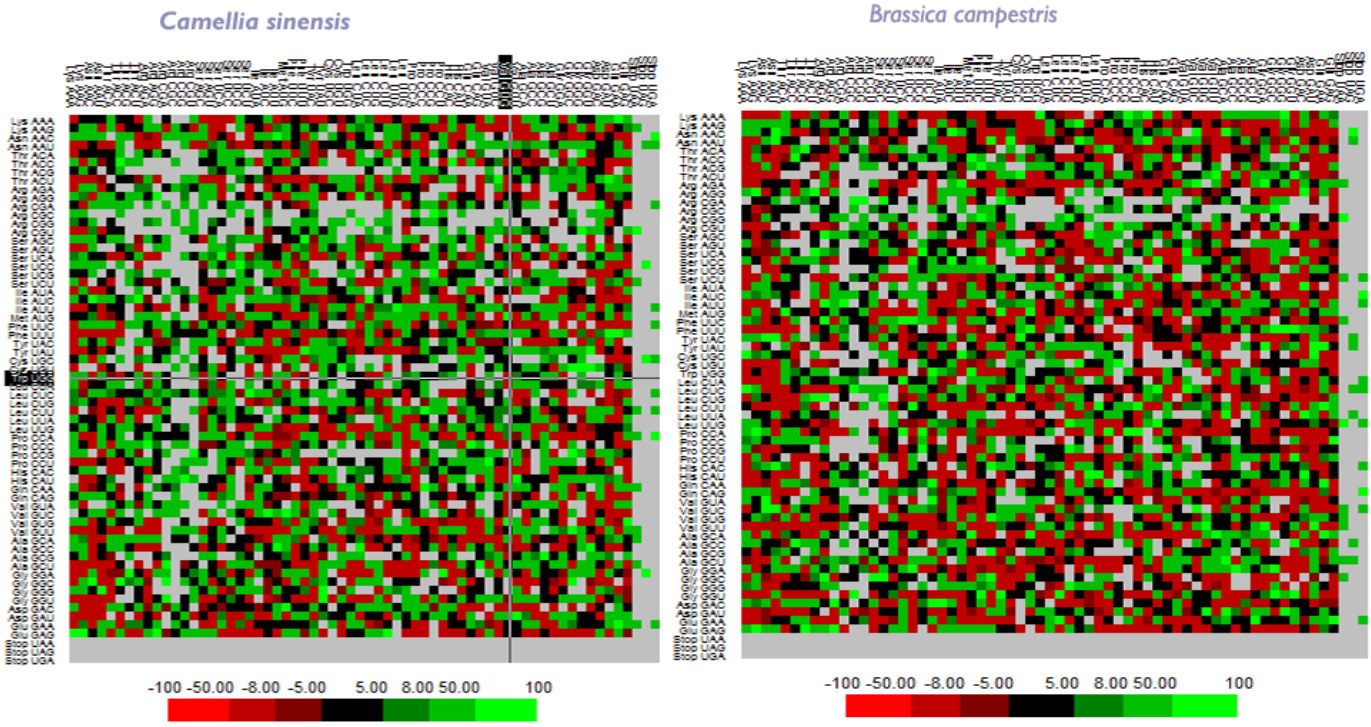

Figure 3. Patterns of codon context variation in *C. sinensis* and *B. campestris.* The green colour represents the highest number of the contexts and red colour represents the lowest number of contexts. The 59 codons are in rows and the 39 codons in columns. The colour intensity corresponds to the residual value present in each cell of the contingency table.

The residual values signify the Chi-square test association between the two codons of each context (Moura et al., 2007). Furthermore, based on the average cluster patterns of adjusted residual values of codon pair frequencies among the *C. sinensis* and *B. campestris*, it was found that specific contexts were represented more often than other contexts. The cluster patterns revealed distinctions as well as commonalities of codon context variations between *C. sinensis* and *B. campestris*. The codon contexts are localized diagonally from left top to right bottom. Being in the diagonal positions, they represent contexts of the same triplet sequences suggesting that these contexts (homogenous codon contexts) are generally frequent in these plants (Figure 3). The cluster pattern is based on the average matrix of residuals of each codon context among the species of

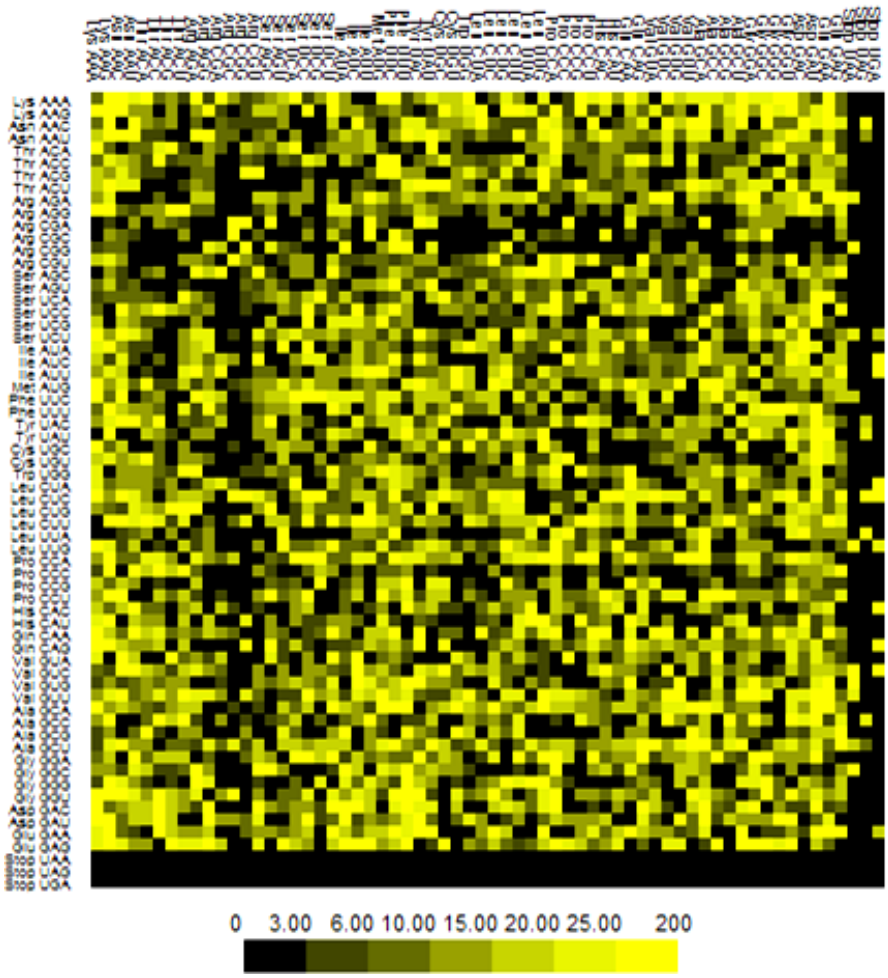

Figure 4. Figure 4: Comparison of codon context pattern between Camellia sinensis and Brassica campestris. Differential display map was obtained by calculating the module of the difference between the residuals of each map. The yellow cells indicate the highest context difference and the black cells represent pairs of codons that have similar residual values between two species.

each order. The map constructed for the two plants was, again, compared in one single display to allow detection of overall patterns of codon context. Differential Display Map (DDM) was constructed from the absolute value by subtracting both maps cell-by-cell (Figure 4).

Researchers proposed that codons which are utilized less as often as possible all through the genome are rate limiting factors of exogenous gene expression supported by experimental verification (Garcia et al., 1986; Zhang et al., 2004). In *C. sinensis* and *B. campestris*, the 'rare codon' was defined by calculating the recurrence of event of all codons (Threshold selected: 10/1000) in coding sequences (Figure 5). In the meantime, our examination demonstrated that many of these rare codon pairs contain termination codons (Table 1). Based on the hypothesis that gene expressivity and codon composition are strongly correlated, the codon adaptation index has been defined to provide an intuitively meaningful measure of the extent of the codon preference in a gene. We have estimated the CAI and RCBS for each cds as a measure of gene expressivity (supplementary material). The CAI with RCBS were compared and it was observed that both showed a similar pattern. In concurrence with different past studies (Ikemura, 1981, 1982; Moriyama and Powell, 1997), it was observed that RCBS decreased with the length of the encoded cds. Since the RCBS value depends on cds length, CAI was used as a central measure for expressivity analysis.

Gene expression studies are essential for predicting the expression potentiality of a particular gene of interest. This will help in the discovery of new coding sequences of genes for most elevated protein expression in a cell so that these man-made proteins can be synthesized and used for therapeutic drives world-wide. Along these lines, it is important to find the codons that dictate the highest and the lowest expressivity of a cds within a particular

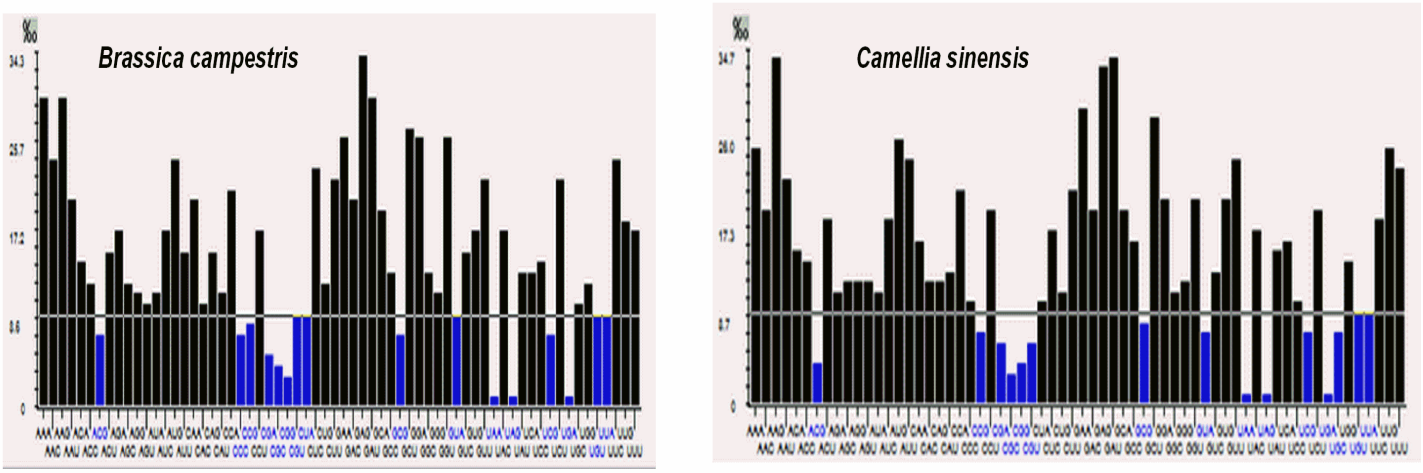

Figure 5. Rare codons for the cds of *B. Campestris* and *C. sinensis*. The 'rare codon' was defined by calculating the frequency of occurrence of all codons in coding sequences (threshold selected 10/1000).

Table 1. Rare codons for the cds of *Brassica Campestris* and *Camellia sinensis.*

	Brassica campestris	***Camellia sinensis***
Rare codons	ACG, CCG, CGA, CGG, CUA, CCC, CGC, CGU, GCG, GUA, UCG, UGU	ACG, CCG, CGA, CGG, CGC, CGU, GCG, GUA, UCG, UUA, UGU, UGC

expression system. The DDM analysis results suggested that both plants showed similar codon context pattern to some extent. For confirmation, the pattern of synonymous codons usage for both plants were compared. In support of our previous study on cereals (Chakraborty and Paul, 2015), both plants selected for the present study also maintained more or less similar pattern of synonymous codon usage (Figure 6). These result indicated that througout the evolution, both plants maintained a precise pattern of codon usage, may be due to the natural selection, mutation or any other external factors. Again, the role of each codon in terms of expressivity within the two plants were analyzed. The occurrence frequency of 59 codons (except stop codons and codons for Met & Trp) were calculated for each cds of *C. sinensis and B. campestris* and predicted their expression level in *E. coli* K12 strain. The occurrence frequency for each codon in cds was again allied with their expressivity values. Using the criterion derived from statistical analysis (positive and negative codon bias relating to the gene expression level), the codons showing the highest and lowest expressivity in *E. coli* k12 we obtained (Table 2). *E. coli* genome tRNA copy number data sets available in the genomic tRNA database (http://gtrnadb.ucsc.edu/) also support the results of highest and lowest productive codons.

To confirm the results of this analysis, we changed the original cds downloaded from the database to the highest expressive and the lowest expressive cds sequence by replacing the codons with highest and lowest expressive codons, respectively. The expressivity values for all the three sets of a cds sequence (original, highest was lowest cds) was calculated by using codonW. These results revealed that the highest as well as the lowest coding sequences significantly differed in expression level from the original cds downloaded from the NCBI database.

Conclusion

A novel method for identification of codons showing the highest and the lowest expressivity was introduced, in view of their recurrence of event. The event recurrence for every codon/cds was again allied with their expressivity values. Using the criterion derived from statistical analysis, the codons showing the highest and the lowest expressivity in *E. coli* k12 were obtained. The natural codons present in cds were replaced by the predicted codons of this study showing the lowest and the highest expressivity using a Perl program developed by the authors of this study. By comparing the expressivity values of our cds with that of original cds downloaded from NCBI, we have established that our method is a general one, not connected with the adjustments in gene length and overall nucleotide

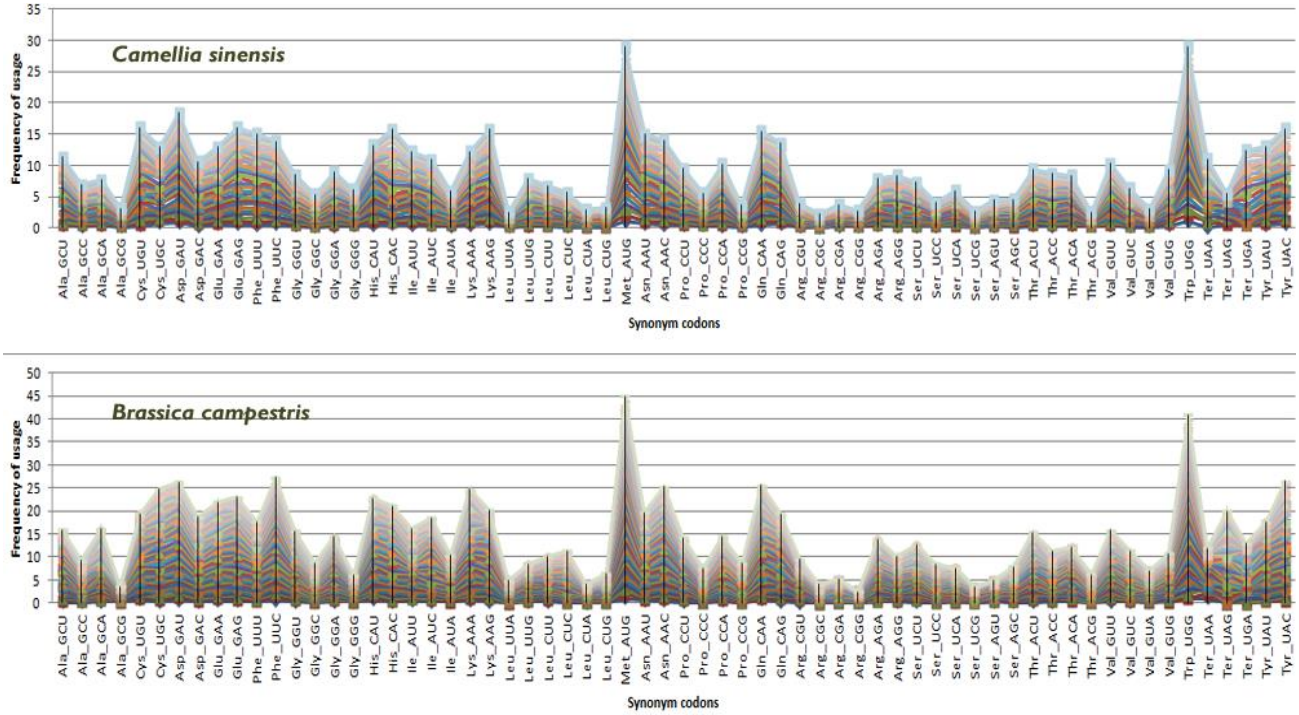

Figure 6. Comparison of the pattern of synonymous codons usage for *C. sinensis* and *B. campestris*. Synonymous codons were placed in the x-axis and their usage frequency in the y-axis. Both plants showed the almost similar pattern of synonymous codon usage with little variation in the usage frequency.

Table 2. Codons for highest and lowest expressivity for the genes of *C. sinensis* and *B. campestris*.

Amino acids	Codons showing lowest expressivity		Codons showing highest expressivity	
	Camellia sinensis	***Brassica campestris***	***Camellia sinensis***	***Brassica campestris***
Serine	TCG, TCC	TCA, TCG	TCT, AGC	AGC
Phenylalanine	TTT	TTT	TTC	TTC
Leucine	CTA, CTG	CTA	CTT, TTG	CTC, TTG
Tyrosine	TAT	TAT	TAC	TAC
Cysteine	TGC	TGT	TGT	TGC
Proline	CCA	CCA	CCC, CCT	CCC, CCT
Histidine	CAC	CAT	CAT	CAC
Glutamine	CAG	CAG	CAA	CAG
Arginine	AGG,CGA, CGT	AGA	AGA	CGT
Isoleucine	ATT, ATA	ATT, ATA	ATC	ATC
Threonine	ACG	ACG	ACA, ACC	ACC
Asparagine	AAT	AAT	AAC	AAC
Lysine	AAA	AAA	AAG	AAG
Valine	GTA, GTC	GTA	GTG	GTC
Alanine	GCG	GCG	GCT, GCC	GCC
Aspartic acid	GAC	GAC	GAT	GAT
Glutamic acid	GAA	GAA	GAG	GAG
Glycine	GGC	GGG	GGA	GGC

composition, with a little noise in measurements. To design the highest and lowest expressive cds of the genes of *C. sinensis* and *B. campestris* in *E. coli* K12 strain, the restriction sites in the bacterium were not

considered.

Availability

The coding sequences for both plants are available in the nucleotide database of NCBI. The softwares used, that is, codon W and Anaconda for the present study are freely available, downloaded from (http://codonw.sourceforge.net/) and (http://bioinformatics.ua.pt/software/anaconda/), respectively.

Conflicts of interests

The authors declare that there is no conflict of interests regarding the publication of this paper.

ACKNOWLEDGEMENTS

The authors are thankful to Assam University, Silchar, Assam, India for providing the necessary facilities in carrying out this research work.

REFERENCES

Akashi H (1994). Synonymous codon usage in Drosophila melanogaster: natural selection and translational accuracy. Genetics 136(3):927-935.

Akashi H (1997). Codon bias evolution in Drosophila. Population genetics of mutation-selection drift. Gene 205(1-2):269-278.

Behura SK, Severson DW (2013). Codon usage bias: causative factors, quantification methods and genome-wide patterns: with emphasis on insect genomes. Biol. Rev. Camb. Philos. Soc. 88(1):49-61.

Bennetzen JL, Hall BD (1982). Codon selection in yeast. J. Biol. Chem. 257(6):3026-3031.

Chakraborty S, Paul P (2015). Guanine and Cytosine at the Second Codon Position Influence Gene Expression in Cereals. Proc. Natl. Acad. Sci. India B Biol. Sci. 1-11.

D'Onofrio G, Ghosh TC, Bernardi G (2002). The base composition of the genes is correlated with the secondary structures of the encoded proteins. Gene 300(1-2):179-187.

Fuglsang A (2004). Bioinformatic analysis of the link between gene composition and expressivity in Saccharomyces cerevisiae and Schizosaccharomyces pombe. Antonie Van Leeuwenhoek 86(2):135-147.

Garcia GM, Mar PK, Mullin DA, Walker JR, Prather NE (1986). The E. coli dnaY gene encodes an arginine transfer RNA. Cell 45(3):453-459.

Goldman B, Bhat S, Shimkets LJ (2007). Genome evolution and the emergence of fruiting body development in Myxococcus xanthus. PLoS One 2(12):e1329.

Gouy M, Gautier C (1982). Codon usage in bacteria: correlation with gene expressivity. Nucleic Acids Res. 10(22):7055-7074.

Grocock RJ, Sharp PM (2002). Synonymous codon usage in Pseudomonas aeruginosa PA01. Gene 289(1-2):131-139.

Gupta SK, Ghosh TC (2001). Gene expressivity is the main factor in dictating the codon usage variation among the genes in Pseudomonas aeruginosa. Gene 273(1):63-70.

Hershberg R, Petrov DA (2008). Selection on codon bias. Annu. Rev. Genet. 42:287-299.

Hooper SD, Berg OG (2000). Gradients in nucleotide and codon usage along *Escherichia coli* genes. Nucleic Acids Res. 28(18):3517-3523.

Ikemura T (1981). "Correlation between the abundance of Escherichia coli transfer RNAs and the occurrence of the respective codons in its protein genes: a proposal for a synonymous codon choice that is optimal for the *E. coli* translational system." J. Mol. Biol. 151(3):389-409.

Ikemura T (1982). Correlation between the abundance of yeast transfer RNAs and the occurrence of the respective codons in protein genes. Differences in synonymous codon choice patterns of yeast and Escherichia coli with reference to the abundance of isoaccepting transfer RNAs. J. Mol. Biol. 158(4):573-597.

Ikemura T (1985). Codon usage and tRNA content in unicellular and multicellular organisms. Mol. Biol. Evol. 2(1):13-34.

Kanaya S, Yamada Y, Kinouchi M, Kudo Y, Ikemura T (2001). Codon usage and tRNA genes in eukaryotes: correlation of codon usage diversity with translation efficiency and with CG-dinucleotide usage as assessed by multivariate analysis. J. Mol. Evol. 53(4-5):290-298.

Lafay B, Atherton JC, Sharp PM (2000). Absence of translationally selected synonymous codon usage bias in Helicobacter pylori. Microbiology 146(4):851-860.

Lawrence JG, Ochman H (1998). Molecular archaeology of the *Escherichia coli* genome. Proc. Natl. Acad. Sci. USA 95(16):9413-9417.

Lee MH, Yang SJ, Kim JW, Lee HS, Kim JW, Park KH (2007). Characterization of a thermostable cyclodextrin glucanotransferase from Pyrococcus furiosus DSM3638. Extremophiles 11(3):537-541.

Lobry JR, Gautier C (1994).Hydrophobicity, expressivity and aromaticity are the major trends of amino-acid usage in 999 Escherichia coli chromosome-encoded genes. Nucleic Acids Res. 22(15):3174-3180.

Ma J, Campbell A, Karlin S (2002). Correlations between Shine-Dalgarno sequences and gene features such as predicted expression levels and operon structures. J. Bacteriol. 184(20):5733-5745.

Moriyama EN, Powell JR (1997). Codon usage bias and tRNA abundance in Drosophila. J. Mol. Evol. 45(5):514-523.

Moura G, Pinheiro M, Arrais J, Gomes AC, Carreto L, Freitas A, Oliveira JL, Santos MA (2007). Large scale comparative codon-pair context analysis unveils general rules that fine-tune evolution of mRNA primary structure. PLoS One 2(9):e847.

Murray EE, Lotzer J, Eberle M (1989). Codon usage in plant genes. Nucleic Acids Res. 17(2):477-498.

Plotkin JB, Kudla G (2011). Synonymous but not the same: the causes and consequences of codon bias. Nat. Rev. Genet. 12(1):32-42.

Ram MR, Beena G, Ragunathan P, Malathi R (2007). Analysis of structure, function, and evolutionary origin of the ob gene product-leptin. J. Biomol. Struct. Dyn. 25(2):183-188.

Rocha EP (2004). Codon usage bias from tRNA's point of view: redundancy, specialization, and efficient decoding for translation optimization. Genome Res. 14(11):2279-2286.

Roymondal U, Das S, Sahoo S (2009). Predicting gene expression level from relative codon usage bias: an application to Escherichia coli genome. DNA Res. 16(1):13-30.

Sharp PM, Li WH (1986). An evolutionary perspective on synonymous codon usage in unicellular organisms. J. Mol. Evol. 24(1-2):28-38.

Sharp PM, Li WH (1987b). The codon Adaptation Index-a measure of directional synonymous codon usage bias, and its potential applications. Nucleic Acids Res. 15(3):1281-1295.

Sharp PM, Li WH (1987a). The rate of synonymous substitution in enterobacterial genes is inversely related to codon usage bias. Mol. Biol. Evol. 4(3):222-230.

Sharp PM, Tuohy TM, Mosurski KR (1986). Codon usage in yeast: cluster analysis clearly differentiates highly and lowly expressed genes. Nucleic Acids Res. 14(13):5125-5143.

Sueoka N (1999). Two aspects of DNA base composition: G+C content and translation-coupled deviation from intra-strand rule of A = T and G = C. J. Mol. Evol. 49(1):49-62.

Sueoka N, Kawanishi Y (2000). DNA G+C content of the third codon position and codon usage biases of human genes. Gene 261(1):53-62.

Supek F, Vlahovicek K (2005). Comparison of codon usage measures and their applicability in prediction of microbial gene expressivity. BMC Bioinformatics 6:182.

Wan XF, Xu D, Kleinhofs A, Zhou J (2004). Quantitative relationship between synonymous codon usage bias and GC composition across

unicellular genomes. BMC Evol. Biol. 4:19.
Wright F (1990). The 'effective number of codons' used in a gene. Gene 87(1):23-29.
Wu G, Culley DE, Zhang W (2005). Predicted highly expressed genes in the genomes of Streptomyces coelicolor and Streptomyces avermitilis and the implications for their metabolism. Microbiology 151(7):2175-2187.
Yu X, Li Z, Xia X, Fang H, Zhou C, Chen H (2007). Expression and purification of ancrod, an anticoagulant drug, in Pichia pastoris. Protein Exp. Purif. 55(2):257-261.
Zhang R, Ou HY, Zhang CT (2004). DEG: a database of essential genes. Nucleic Acids Res. 32(Database issue):D271-272.
Zheng Y, Zhao WM, Wang H, Zhou YB, Luan Y, Qi M, Cheng YZ, Tang W, Liu J, Yu H, Yu XP (2007). Codon usage bias in Chlamydia trachomatis and the effect of codon modification in the MOMP gene on immune responses to vaccination. Biochem. Cell Biol. 85(2):218-226.

Supplementary Table 1. *Camellia sinensis.*

Gene Names with their Accession numbers	A	T	G	C	CDS length	AT percent	GC percent
>gi|90968983|gb|DQ366599.2| *Camellia sinensis* acetyl CoA carboxylase mRNA, complete cds	484	460	489	367	1800	52.44	47.56
>gi|224037813|gb|FJ656220.1| *Camellia sinensis* polyphenol oxidase (PPO) mRNA, complete cds	502	415	439	444	1800	50.94	49.06
>gi|89111302|dbj|AB247284.1| *Camellia sinensis* pRB mRNA for retinoblastoma related protein, complete cds	877	879	695	627	3078	57.05	42.95
>gi|89111300|dbj|AB247283.1| *Camellia sinensis* cycD3-2 mRNA for cyclin D3-2, complete cds	298	337	268	216	1119	56.75	43.25
>gi|89111298|dbj|AB247282.1| *Camellia sinensis* cycD3 mRNA for cyclin D3-1, complete cds	303	292	241	280	1116	53.32	46.69
>gi|89111294|dbj|AB247280.1| *Camellia sinensis* cycb mRNA for cyclin B, complete cds	388	334	329	272	1323	54.57	45.43
>gi|472247167|gb|KC242133.1| *Camellia sinensis* stearoyl-acyl carrier protein desaturase mRNA, complete cds	332	319	295	245	1191	54.66	45.34
>gi|529205468|gb|KC920896.1| *Camellia sinensis* cultivar Longjing43 glycerol-3-phosphate acyltransferase mRNA, complete cds	349	376	317	311	1353	53.59	46.42
>gi|523713207|gb|KC847167.1| *Camellia sinensis* omega-3 fatty acid desaturase (FAD8) mRNA, complete cds	353	372	323	311	1359	53.35	46.65
>gi|480359963|gb|KC700025.1| *Camellia sinensis* AMP deaminese mRNA, complete cds	717	718	605	531	2571	55.82	44.19
>gi|76177060|gb|DQ194356.1| *Camellia sinensis* cultivar UPASI-10 4-coumaroyl CoA ligase mRNA, complete cds	433	440	420	473	1766	49.43	50.57
>gi|449082926|dbj|AB741571.1| *Camellia sinensis* CsFT1 mRNA for flowering locus T, complete cds	116	144	148	117	525	49.52	50.48
>gi|357966792|gb|JN392472.1| *Camellia sinensis* chitinase (CHIT1) mRNA, complete cds	250	237	244	238	969	50.26	49.74
>gi|398025483|gb|JX042312.1| *Camellia sinensis* clone 111/1 ricin B lectin domain protein II mRNA, complete cds	103	83	82	68	336	55.36	44.64
>gi|339232482|gb|JN024667.1| *Camellia sinensis* anthocyanidin reductase 2 (ANR2) mRNA, complete cds	297	276	249	222	1044	54.89	45.12
>gi|161789847|gb|EU284131.1| *Camellia sinensis* glutamine synthetase mRNA, complete cds	297	265	288	221	1071	52.47	47.53
>gi|307090029|gb|HM204933.1| *Camellia sinensis* isolate yuanxiaolv caffeic acid O-methyltransferase (comt) mRNA, complete cds	272	278	280	262	1092	50.37	49.63
>gi|50841418|gb|AY574920.1| *Camellia sinensis* dihydroflavonol 4-reductase mRNA, complete cds	291	270	260	223	1044	53.74	46.26
>gi|294847479|gb|GU944768.1| *Camellia sinensis* anthocyanidin reductase (ANR) mRNA, complete cds	276	256	242	240	1014	52.47	47.54

Supplementary Table 1. Contd.

>gi|117622287|gb|EF055882.1| *Camellia sinensis* cytosolic glutamine synthetase mRNA, complete cds	295	267	288	221	1071	52.47	47.53
>gi|91992505|gb|DQ461974.1| *Camellia sinensis* ATPase mRNA, complete cds	61	87	62	48	258	57.36	42.64
>gi|76177136|gb|DQ194358.1| *Camellia sinensis* cultivar UPASI-10 flavonoid 3',5'-hydroxylase mRNA, complete cds	397	397	376	363	1533	51.79	48.21
>gi|76152008|gb|DQ120521.2| *Camellia sinensis* cultivar UPASI-10 chalcone isomerase mRNA, complete cds	181	166	176	170	693	50.07	49.93
>gi|59611828|gb|AY907710.1| *Camellia sinensis* caffeine synthase mRNA, complete cds	334	303	253	208	1098	58.02	41.99
>gi|532212606|gb|KF006992.1| *Camellia sinensis* cultivar Longjing43 S-adenosylmethionine decarboxylase mRNA, complete cds	265	333	259	223	1080	55.37	44.63
>gi|428135437|gb|JQ790527.1| *Camellia sinensis* caffeoyl-CoA-O-methyltransferase (CCoAOMT) mRNA, complete cds	198	165	189	186	738	49.19	50.81
>gi|326380569|gb|GU992402.1| *Camellia sinensis* anthocyanidin reductase 1 mRNA, complete cds	299	275	248	222	1044	54.98	45.02
>gi|308943876|gb|HM440161.1| *Camellia sinensis* lipoxygenase mRNA, complete cds	769	703	654	580	2706	54.40	45.60
>gi|62955863|gb|AY945842.1| *Camellia sinensis* flavonoid 3',5'-hydroxylase mRNA, complete cds	401	398	374	360	1533	52.12	47.88
>gi|76786310|gb|DQ198089.1| *Camellia sinensis* flavonol synthase (FLS) mRNA, complete cds	288	259	236	213	996	54.92	45.08

All the cds selected for the present study from the two plants, this file provides the gene name, accession numbers along with the overall AT and GC percentage, RCBS, CAI, ENc, SCUO, GC1, GC2 & GC3 for all the genes. These data allow for the reconstruction of all the analyses.

Supplementary Table 1. Contd.

Gene Names with their Accession numbers	CAI	ENc	RCBS	SCUO	GC1 Percent	GC2 percent	GC3 percent
>gi|90968983|gb|DQ366599.2| *Camellia sinensis* acetyl CoA carboxylase mRNA, complete cds	0.64	57.55	0.041	0.055	55	42.3	45.3
>gi|224037813|gb|FJ656220.1| *Camellia sinensis* polyphenol oxidase (PPO) mRNA, complete cds	0.61	56.63	0.041	0.050	52.3	40.5	54.3
>gi|89111302|dbj|AB247284.1| *Camellia sinensis* pRB mRNA for retinoblastoma related protein, complete cds	0.55	51.89	0.025	0.090	47.9	43.9	37.1
>gi|89111300|dbj|AB247283.1| *Camellia sinensis* cycD3-2 mRNA for cyclin D3-2, complete cds	0.36	51.48	0.064	0.111	50.4	34.3	45
>gi|89111298|dbj|AB247282.1| *Camellia sinensis* cycD3 mRNA for cyclin D3-1, complete cds	0.52	54.79	0.063	0.080	53	38.2	48.9

Supplementary Table 1. Contd.

>gi|89111294|dbj|AB247280.1| *Camellia sinensis* cycb mRNA for cyclin B, complete cds	0.47	52.52	0.054	0.115	53.7	39.5	43.1
>gi|472247167|gb|KC242133.1| *Camellia sinensis* stearoyl-acyl carrier protein desaturase mRNA, complete cds	0.33	48.51	0.060	0.164	54.2	37.8	44.1
>gi|529205468|gb|KC920896.1| *Camellia sinensis* cultivar Longjing43 glycerol-3-phosphate acyltransferase mRNA, complete cds	0.49	53.64	0.053	0.102	52.5	42.1	44.6
>gi|523713207|gb|KC847167.1| *Camellia sinensis* omega-3 fatty acid desaturase (FAD8) mRNA, complete cds	0.57	57.70	0.054	0.059	53	42.2	44.8
>gi|480359963|gb|KC700025.1| *Camellia sinensis* AMP deaminese mRNA, complete cds	0.59	54.63	0.030	0.064	52.5	37.5	42.6
>gi|76177060|gb|DQ194356.1| *Camellia sinensis* cultivar UPASI-10 4-coumaroyl CoA ligase mRNA, complete cds	0.54	57.23	0.045	0.055	39.4	54.8	57.5
>gi|449082926|dbj|AB741571.1| *Camellia sinensis* CsFT1 mRNA for flowering locus T, complete cds	0.28	51.27	0.123	0.175	55.4	48	48
>gi|357966792|gb|JN392472.1| *Camellia sinensis* chitinase (CHIT1) mRNA, complete cds	0.61	58.72	0.081	0.062	43.2	51.2	55.1
>gi|398025483|gb|JX042312.1| *Camellia sinensis* clone 111/1 ricin B lectin domain protein II mRNA, complete cds	0.29	61.00	0.194	0.060	43.8	35.7	54.5
>gi|339232482|gb|JN024667.1| *Camellia sinensis* anthocyanidin reductase 2 (ANR2) mRNA, complete cds	0.47	56.44	0.067	0.077	50.1	41.7	43.4
>gi|161789847|gb|EU284131.1| *Camellia sinensis* glutamine synthetase mRNA, complete cds	0.40	52.40	0.066	0.106	53.5	44.3	44.8
>gi|307090029|gb|HM204933.1| *Camellia sinensis* isolate yuanxiaolv caffeic acid O-methyltransferase (comt) mRNA, complete cds	0.49	53.45	0.070	0.105	38.4	58.6	51.9
>gi|50841418|gb|AY574920.1| *Camellia sinensis* dihydroflavonol 4-reductase mRNA, complete cds	0.50	57.27	0.067	0.070	46.8	38.8	53.2
>gi|294847479|gb|GU944768.1| *Camellia sinensis* anthocyanidin reductase (ANR) mRNA, complete cds	0.97	61.00	0.068	0.159	51.6	41.1	49.7
>gi|117622287|gb|EF055882.1| *Camellia sinensis* cytosolic glutamine synthetase mRNA, complete cds	0.41	52.71	0.066	0.106	53.2	44.3	45.1
>gi|91992505|gb|DQ461974.1| *Camellia sinensis* ATPase mRNA, complete cds	0.57	55.31	0.241	0.050	48.8	40.7	38.4
>gi|76177136|gb|DQ194358.1| *Camellia sinensis* cultivar UPASI-10 flavonoid 3',5'-hydroxylase mRNA, complete cds	0.61	56.57	0.049	0.072	54	40.9	49.7
>gi|76152008|gb|DQ120521.2| *Camellia sinensis* cultivar UPASI-10 chalcone isomerase mRNA, complete cds	0.24	49.87	0.095	0.147	51.5	43.3	55
>gi|59611828|gb|AY907710.1| *Camellia sinensis* caffeine synthase mRNA, complete cds	0.36	52.11	0.064	0.118	48.9	35.8	41.3
>gi|532212606|gb|KF006992.1| *Camellia sinensis* cultivar Longjing43 S-adenosylmethionine decarboxylase mRNA, complete cds	0.39	50.87	0.065	0.123	46.9	42.8	44.2

Supplementary Table 1. Contd.

>gi|428135437|gb|JQ790527.1| *Camellia sinensis* caffeoyl-CoA-O-methyltransferase (CCoAOMT) mRNA, complete cds	0.38	53.34	0.097	0.160	34.9	62.7	54.8
>gi|326380569|gb|GU992402.1| *Camellia sinensis* anthocyanidin reductase 1 mRNA, complete cds	0.48	57.58	0.067	0.076	50.3	41.4	43.4
>gi|308943876|gb|HM440161.1| *Camellia sinensis* lipoxygenase mRNA, complete cds	0.65	56.13	0.029	0.056	52.1	40.4	44.3
>gi|62955863|gb|AY945842.1| *Camellia sinensis* flavonoid 3',5'-hydroxylase mRNA, complete cds	0.59	56.85	0.049	0.067	53.4	40.3	49.9
>gi|76786310|gb|DQ198089.1| *Camellia sinensis* flavonol synthase (FLS) mRNA, complete cds	0.41	57.19	0.076	0.059	33.9	45.6	55.7

Supplementary Table 2. *Brassica campestris.*

Gene names with their accession numbers	A	T	G	C	CDS length	AT percent	GC percent
receptor protein kinase SRK12 (dbj-D38564)	758	697	617	499	2571	56.59	43.41
oleifera copper and zinc superoxide dismutase mRNA(gb-KF356248)	111	122	121	105	459	50.76	49.24
Brassica rapa cultivar Samjin Col-2-like protein mRNA (gb-AY356370)	288	235	237	206	966	54.14	45.86
Brassica rapa cultivar Samjin reduced vernalization response 1 mRNA (gb-AY356368)	288	248	238	216	990	54.14	45.86
Brassica rapa plastid-lipid associated protein PAP3 mRNA (gb-AF290565)	245	269	269	300	1083	47.46	52.54
Brassica rapa subsp. campestris glutathione reductase mRNA (gb-JN795550)	403	388	437	275	1503	52.63	47.37
Brassica rapa subsp. pekinensis cultivar Huangya 14 MF21 mRNA (gb-JF437596)	129	123	105	99	456	55.26	44.74
Brassica rapa subsp. chinensis exocyst subunit EXO70A1 mRNA (gb-JX997396)	572	488	478	379	1917	55.30	44.71
Brassica rapa subsp. chinensis male sterility 2 mRNA (gb-EF093533)	567	491	467	326	1851	57.16	42.84
Brassica rapa subsp. chinensis cultivar Aikangqing MF21 mRNA (gb-JF437595)	128	123	106	99	456	55.04	44.96
Brassica rapa var. purpuraria cultivar Zitai 1 MF21 mRNA(gb-JF437594)	129	122	105	100	456	55.04	44.96
Brassica rapa subsp. chinensis receptor-like kinase SSP mRNA(gb-KC576523)	427	399	312	260	1398	59.08	40.92
Brassica rapa subsp. chinensis MLPK mRNA(gb-KC576522)	370	324	318	245	1257	55.21	44.79
Brassica rapa subsp. chinensis kinase-associated protein phosphatase mRNA(gb-KC576521)	447	452	439	312	1650	54.49	45.52
Brassica rapa subsp. chinensis aspartic proteinase mRNA(gb-KC576520)	359	434	412	316	1521	52.14	47.86
Brassica rapa subsp. chinensis senescence-associated cysteine protease mRNA(gb-KC576519)	282	266	292	240	1080	50.74	49.26
Brassica rapa subsp. chinensis ARC1 mRNA(gb-KC576518)	522	484	484	496	1986	50.66	49.35
Brassica rapa subsp. pekinensis beta-carotene hydroxylase mRNA(gb-GQ178285)	211	242	239	229	921	49.19	50.81
Brassica rapa subsp. pekinensis cultivar Huangya14 profilin mRNA(gb-EU163278)	107	88	119	91	405	48.15	51.85
Brassica rapa subsp. rapa cultivar Wenzhoupancai profilin mRNA(gb-EU163276)	109	89	117	90	405	48.89	51.11
Brassica rapa subsp. pekinensis cultivar Huangya14 anther-specific proline rich protein mRNA(gb-EF101148)	518	402	314	512	1746	52.69	47.31
Brassica rapa subsp. pekinensis cultivar Xiaoqingko anther-specific proline rich protein mRNA(gb-EF101141)	513	398	312	508	1731	52.63	47.37

Supplementary Table 2. Contd.

Brassica rapa subsp. pekinensis flowering locus C3 mRNA(gb-DQ866876)	172	143	144	135	594	53.03	46.97
Brassica rapa subsp. pekinensis flowering locus C2 mRNA(gb-DQ866875)	177	140	138	136	591	53.64	46.36
Brassica rapa subsp. pekinensis flowering locus C1 mRNA(gb-DQ866874)	177	151	161	132	621	52.82	47.18
Brassica rapa subsp. pekinensis cold-regulated protein mRNA(gb-DQ491005)	130	80	114	78	402	52.24	47.76
Brassica rapa subsp. pekinensis MORN mRNA(gb-FJ460465)	371	382	391	365	1509	49.90	50.10
Brassica rapa subsp. pekinensis cultivar Matsushima SUR1 mRNA(gb-EF611271)	353	306	349	354	1362	48.39	51.62
Brassica rapa subsp. pekinensis cultivar Kwan-Hoo Choi ST5a mRNA(gb-EF611266)	267	236	264	253	1020	49.31	50.69
Brassica rapa subsp. pekinensis cultivar Matsushima ST5a mRNA(gb-EF611263)	268	236	263	253	1020	49.41	50.59
Brassica rapa subsp. pekinensis CYP83B1 mRNA(gb-EF611260)	404	379	343	374	1500	52.20	47.80
Brassica rapa subsp. pekinensis MYB mRNA(gb-DQ903665)	284	268	248	247	1047	52.72	47.28
Brassica rapa subsp. pekinensis acyl desaturase mRNA(gb-DQ886528)	319	300	323	288	1230	50.33	49.68
Brassica rapa subsp. pekinensis geranylgeranyl reductase mRNA(gb-DQ886527)	385	338	434	334	1491	48.49	51.51
Brassica rapa subsp. pekinensis biotin synthase mRNA(gb-DQ886525)	317	273	279	259	1128	52.31	47.70
Raphanus sativus cultivar Sakurashimadakon MF21 mRNA(gb-JF437605)	129	120	107	100	456	54.61	45.40
Brassica nigra cultivar 071-01 MF21 mRNA(gb-JF437604)	131	117	107	101	456	54.39	45.61
Brassica juncea var. rugosa cultivar Yamakada MF21 mRNA(gb-JF437603)	128	123	106	99	456	55.04	44.96
Brassica carinata cultivar 079-01 MF21 mRNA(gb-JF437602)	129	120	107	100	456	54.61	45.40
Brassica napus cultivar 071-02 MF21 mRNA(gb-JF437601)	131	120	109	102	462	54.33	45.67
Brassica napus var. napobrassica cultivar Datou1 MF21 mRNA(gb-JF437600)	120	121	105	95	441	54.65	45.35
Brassica oleracea var. capitata cultivar Jixin MF21 mRNA(gb-JF437599)	119	119	108	95	441	53.97	46.03
Brassica juncea var. multiceps cultivar Maertou MF21 mRNA(gb-JF437598)	129	123	105	99	456	55.26	44.74
Brassica rapa subsp. nipposinica cultivar Wanshengwanye MF21 mRNA(gb-JF437597)	129	123	105	99	456	55.26	44.74
Brassica rapa subsp. chinensis napin mRNA(gb-HM027884)	158	111	130	156	555	48.47	51.53
Mesostigma viride photosystem II PsbR protein mRNA(gb-DQ370085)	76	84	115	139	414	38.65	61.35
Brassica rapa BcNDK 2 mRNA for nucloside diphosphate kinase 2(dbj-AB078008)	164	190	179	160	693	51.08	48.92

All the cds selected for the present study from the two plants, this file provides the gene name, accession numbers along with the overall AT and GC percentage, RCBS, CAI, ENc, SCUO, GC1, GC2 & GC3 for all the genes. These data allow for the reconstruction of all the analyses.

Supplementary Table 2. Contd.

Gene names with their accession numbers	CAI	ENc	RCBS	SCUO	GC1 Percent	GC2 percent	GC3 percent
receptor protein kinase SRK12 (dbj-D38564)	0.60	54.90	0.03	0.051	44.8	40.1	45.3
oleifera copper and zinc superoxide dismutase mRNA(gb-KF356248)	0.15	42.28	0.14	0.093	62.7	51	34
Brassica rapa cultivar Samjin Col-2-like protein mRNA (gb-AY356370)	0.38	54.15	0.07	0.077	51.2	44.7	41.6
Brassica rapa cultivar Samjin reduced vernalization response 1 mRNA (gb-AY356368)	0.48	51.75	0.07	0.097	50	40.3	47.3
Brassica rapa plastid-lipid associated protein PAP3 mRNA (gb-AF290565)	0.51	56.13	0.06	0.127	55.4	48.2	54

Supplementary Table 2. Contd.

Brassica rapa subsp. campestris glutathione reductase mRNA (gb-JN795550)	0.53	56.00	0.05	0.126	54.9	42.7	44.5
Brassica rapa subsp. pekinensis cultivar Huangya 14 MF21 mRNA (gb-JF437596)	0.40	59.19	0.14	0.053	48	42.8	43.4
Brassica rapa subsp. chinensis exocyst subunit EXO70A1 mRNA (gb-JX997396)	0.48	52.26	0.04	0.104	53.1	36.6	44.4
Brassica rapa subsp. chinensis male sterility 2 mRNA (gb-EF093533)	0.49	49.16	0.04	0.085	48.3	37.8	42.5
Brassica rapa subsp. chinensis cultivar Aikangqing MF21 mRNA (gb-JF437595)	0.40	58.37	0.14	0.080	48	43.4	43.4
Brassica rapa var. purpuraria cultivar Zitai 1 MF21 mRNA(gb-JF437594)	0.40	59.19	0.14	0.072	48	42.8	44.1
Brassica rapa subsp. chinensis receptor-like kinase SSP mRNA(gb-KC576523)	0.41	52.12	0.05	0.104	40.9	35.6	37.8
Brassica rapa subsp. chinensis MLPK mRNA(gb-KC576522)	0.42	50.53	0.06	0.086	51.6	43.7	39.1
Brassica rapa subsp. chinensis kinase-associated protein phosphatase mRNA(gb-KC576521)	0.63	57.87	0.04	0.124	54.4	39.6	42.5
Brassica rapa subsp. chinensis aspartic proteinase mRNA(gb-KC576520)	0.45	50.83	0.05	0.087	55.2	41.4	46.9
Brassica rapa subsp. chinensis senescence-associated cysteine protease mRNA(gb-KC576519)	0.54	58.69	0.07	0.086	53.6	42.2	51.9
Brassica rapa subsp. chinensis ARC1 mRNA(gb-KC576518)	0.56	53.59	0.04	0.077	52.9	40	55.1
Brassica rapa subsp. pekinensis beta-carotene hydroxylase mRNA(gb-GQ178285)	0.40	53.54	0.08	0.073	54.7	43.6	54.1
Brassica rapa subsp. pekinensis cultivar Huangya14 profilin mRNA(gb-EU163278)	0.31	59.09	0.16	0.088	60.7	40	54.8
Brassica rapa subsp. rapa cultivar Wenzhoupancai profilin mRNA(gb-EU163276)	0.27	57.77	0.16	0.103	60	40	53.3
Brassica rapa subsp. pekinensis cultivar Huangya14 anther-specific proline rich protein mRNA(gb-EF101148)	0.57	54.61	0.04	0.109	54.5	54.1	33.3
Brassica rapa subsp. pekinensis cultivar Xiaoqingko anther-specific proline rich protein mRNA(gb-EF101141)	0.58	54.70	0.04	0.117	54.6	54.1	33.4
Brassica rapa subsp. pekinensis flowering locus C3 mRNA(gb-DQ866876)	0.35	51.77	0.11	0.091	59.1	33.3	48.5
Brassica rapa subsp. pekinensis flowering locus C2 mRNA(gb-DQ866875)	0.26	50.23	0.11	0.119	59.4	32	47.7
Brassica rapa subsp. pekinensis flowering locus C1 mRNA(gb-DQ866874)	0.27	52.26	0.10	0.157	60.4	30.4	50.7
Brassica rapa subsp. pekinensis cold-regulated protein mRNA(gb-DQ491005)	0.29	50.10	0.15	0.133	55.2	36.6	51.5
Brassica rapa subsp. pekinensis MORN mRNA(gb-FJ460465)	0.53	53.53	0.05	0.167	53.9	47.5	48.9
Brassica rapa subsp. pekinensis cultivar Matsushima SUR1 mRNA(gb-EF611271)	0.54	57.12	0.05	0.163	56.4	38.5	59.9
Brassica rapa subsp. pekinensis cultivar Kwan-Hoo Choi ST5a mRNA(gb-EF611266)	0.38	53.50	0.07	0.153	52.6	36.5	62.9
Brassica rapa subsp. pekinensis cultivar Matsushima ST5a mRNA(gb-EF611263)	0.41	53.89	0.07	0.280	52.6	36.5	62.6
Brassica rapa subsp. pekinensis CYP83B1 mRNA(gb-EF611260)	0.58	55.99	0.05	0.127	54.4	35.8	53.2
Brassica rapa subsp. pekinensis MYB mRNA(gb-DQ903665)	0.53	54.51	0.07	0.118	52.4	50.1	39.3
Brassica rapa subsp. pekinensis acyl desaturase mRNA(gb-DQ886528)	0.50	55.46	0.06	0.127	53.7	38.8	56.6
Brassica rapa subsp. pekinensis geranylgeranyl reductase mRNA(gb-DQ886527)	0.54	53.35	0.05	0.127	51.5	51.5	62
Brassica rapa subsp. pekinensis biotin synthase mRNA(gb-DQ886525)	0.46	53.28	0.06	0.144	52.9	44.7	45.5
Raphanus sativus cultivar Sakurashimadakon MF21 mRNA(gb-JF437605)	0.36	61.00	0.14	0.118	48	44.7	43.4
Brassica nigra cultivar 071-01 MF21 mRNA(gb-JF437604)	0.51	59.90	0.14	0.117	48	46.1	42.8
Brassica juncea var. rugosa cultivar Yamakada MF21 mRNA(gb-JF437603)	0.40	59.22	0.14	0.127	48.7	42.8	43.4
Brassica carinata cultivar 079-01 MF21 mRNA(gb-JF437602)	0.36	61.00	0.14	0.118	48	44.7	43.4
Brassica napus cultivar 071-02 MF21 mRNA(gb-JF437601)	0.38	61.00	0.14	0.118	48.7	44.2	44.2
Brassica napus var. napobrassica cultivar Datou1 MF21 mRNA(gb-JF437600)	0.38	61.00	0.15	0.133	48.3	42.9	44.9
Brassica oleracea var. capitata cultivar Jixin MF21 mRNA(gb-JF437599)	0.36	61.00	0.15	0.111	48.3	44.9	44.9

Supplementary Table 2. Contd.

Brassica juncea var. multiceps cultivar Maertou MF21 mRNA(gb-JF437598)	0.40	59.19	0.14	0.474	48	42.8	43.4
Brassica rapa subsp. nipposinica cultivar Wanshengwanye MF21 mRNA(gb-JF437597)	0.40	59.19	0.14	0.163	48	42.8	43.4
Brassica rapa subsp. chinensis napin mRNA(gb-HM027884)	0.31	49.50	0.12	0.192	59.5	37.8	57.3
Mesostigma viride photosystem II PsbR protein mRNA(gb-DQ370085)	0.09	36.65	0.16	0.116	54.3	50	79.7
Brassica rapa BcNDK 2 mRNA for nucloside diphosphate kinase 2(dbj-AB078008)	0.33	50.33	0.10	0.116	54.5	48.5	43.7

academicJournals

Vol. 15(8), pp. 252-263, 24 February, 2016
DOI: 10.5897/AJB2015.14818
Article Number: 7A1E93B57331
ISSN 1684-5315

http://www.academicjournals.org/AJB

African Journal of Biotechnology

Full Length Research Paper

Identification of accelerated evolution in the metalloproteinase domain of snake venom metalloproteinase sequences (SVMPs) through comparative analysis

Md. Mahmudul Islam[1]*, Zahida Yesmin Roly[1], Md. Mirza Ruhullah[1], Zohorul Islam[1], Md. Alsan Sharia[1], Rafsan Zani Tanvir[2] and Md. Khaja Foyasal[2]

[1]Department of Genetic Engineering and Biotechnology, Faculty of Life and Earth Sciences, University of Rajshahi, Rajshahi-6205, Bangladesh.
[2]Department of Biotechnology and Genetic Engineering, Islamic University, kushtia-7003, Bangladesh.

Received 25 June, 2015, Accepted 31 August, 2015

Computational protein sequence analysis is one of the most important tools used for understanding the evolution of closely related proteins sequences including snake venom metalloproteinase sequences (SVMPs) which give valuable information regarding genetic variations. The fundamental objective of the present study is to screen the evolution distributed in metalloproteinase domain regions of protein sequences among different SVMPs in snake species which are involved in a range of pathological disorders such as arthritis, atherosclerosis, liver fibrosis, cardiovascular, cancer, liver and neurodegenerative disorders. In fact, SVMPS are responsible for hemorrhage and may also interfere with the hemostatic system. A comparative characterization of the metalloproteinase sequences has been carried out to analyze their multiple sequence alignment, phylogenic tree, homology, physico-chemical, secondary structural and functional properties. DNAMAN software was used for multiple sequence alignment, phylogenic tree and homology and Expasy's Prot-param server was used for amino acid composition, physico-chemical and functional characterization of these SVMPs sequences. Studies of secondary structure of these SVMPs were carried out by computational program. Based on the observed patterns of occurrence of atypical features, we hypothesize that amino acids of metalloproteinase domain region (66.63% identity) of protein sequences are highly changeable; whereas, signal peptide region (93.98% identity) is the lowest changeable protein sequence and the remaining other three domains such as propeptide region (87.36% identity), desintegrin domain region (78.63% identity) and cysteine-rich domain region (75.70% identity) show moderate changeable protein sequence. SVMPs might be an accelerated evolution, which is a key player in causing diseases. From the data, it can be suggested that over -changed metalloproteinase domain regions in snake venom metalloproteinase might be responsible for the generation of functional variation of proteins expressed, which in turn may lead to different disorders in humans after snake bite. The results of this study would be an effective tool for the study of mutation, drugs resistance mechanisms and development of new drugs for different diseases.

Key words: SVMPs, evolution, multiple sequence alignment, phylogenic tree, secondary structure, homology.

INTRODUCTION

Metalloproteinase is a ubiquitous enzyme that exists in nearly all organisms from animal to plants. However, apart from its different expression sites in different plants and animals for performing distinct physiological roles, metalloproteinase also exists in the toxin/venom of several venomous creatures (snake, caterpillar, scorpion etc.) to cause agony, suffering and even death of the prey/victim. Among them, snake venom is a very rich source of metalloproteinase and they are termed as snake venom metalloproteinases (SVMPs). Several diseases are shown to be associated with metalloproteinase. For example, genetic polymorphisms in matrix metalloproteinase genes MMP1, MMP9 and MMP12 are shown to be important in the development of chronic obstructive pulmonary disease (COPD) (Wallace and Sandford, 2002). Metalloproteinases also play role in the development of renal cyst (Obermüller et al., 2001), uterine cervical carcinoma (Libra et al., 2009), angiogenesis (Pepper, 2001) and various inflammatory diseases of the central nervous system such as bacterial meningitis.

SVMPs are more abundantly found in viper snake venom; however, they are also from few elapid families (Birrell et al., 2007; Fry et al., 2003). They are synthesized as zymogens in the venom gland and contain a pro-peptide which is cleaved off during maturation. They have a common zinc-binding motif with a consensus sequence of HEXXHXXGXXH (Bode et al., 1993). They are classified into different types (PI to P-IV) on the basis of the other domains that are present in these complexes (Hite et al., 1994). These families of enzymes are responsible for haemorrhagic, local myonecrotic, antiplatelet, edema-inducing and other inflammatory effects. Recently, it has been shown that SVMPs are potential tools in the development of drugs for the prevention and treatment of several illnesses. These enzymes are extensively used in the treatment and prevention of thrombotic disorders, since they serve as defibrinogenating agents (Costa et al., 2010; Bjarnason and Fox, 1994). Animal models of septic shock have also delivered proof-of-concept that MMPs can be of therapeutic interest (Vanlaere and Libert, 2009).

Evolution and diversification of snake venom is a very interesting phenomenon. Snake venom glands are believed to have evolved by the modification of the salivary glands, and various body proteins have been recruited in the venom gland and adapted to attack and damage various physiological system of the prey (Reza et al., 2006). Therefore, study of the expressed venom protein among and within a particular family enables us to understand the mode and direction of evolution of that gene family. A lot of variation is evident in the SVMPs among the species even within the same species with indication of accelerated evolution of this particular venom component. Therefore, this study was undertaken to perform a detailed bioinformatics analysis of the different domains of snake venom metalloproteinase sequences in order to understand their pattern of accelerated evolution.

MATERIALS AND METHODS

Sequence retrieval

Twelve (12) SVMPs sequences from different venomous snake species including *Agkistrodon contortrix laticinctus, Agistrodon piscivorus leucostoma, Deinagkistrodon acutus, Gloydius halys, Sistrurus catenatus edwardsi, Naja naja atra, Bothrops jararaca, Bothrops insularis, Protobothrops flavoviridis, Bungarus multicinctus, Crotalus viridis* and *Crotalus atrox* were obtained from National Center for Biotechnology Information (NCBI) with the following accession numbers: O42138, C9E1S0, Q9W6M5, Q8AWI5, ABG26979, A8QL59, O93523, Q8QG88, Q90ZI3, ABN72537, C9E1R8 and Q9DGB9, respectively.

Multiple sequence alignment

Twelve (12) SVMPs sequences from different venomous snake species were used for multiple sequence alignment of the species, with the aid of DNAMAN software. After multiple sequence alignment of SVMPs sequences of the different snake species, black color indicates positions with fully conserved residue; pink color indicates that one of the following high scoring groups is fully conserved; cyan color indicates that one of the following moderate scoring groups is fully conserved; white color indicates that one of the following 'weaker' scoring groups is fully conserved.

Classification of SVMPs sequences

SVMPs sequences were divided into five domains: signal peptide, propeptide, metalloprotease, disintegrin and cysteine-rich domain based on their domain organization after multiple sequence alignment. Signal peptide sequence (about 18 residues long), propeptide (about 176 residues long), metalloproteinase (about 205 residues long), desintegrin (about 95 residues long) and cyestine-rich (about 194 residues long) domains are aligned separately. Cys-switch sites (PKMCGV) and Zn^{2+} binding motifs (HEXXHXXGXXH) are marked in the box of black color.

Phylogenetic tree and homology construction

Phylogenetic tree of 12 SVMPs sequences was done using

*Corresponding author. E-mail: mahmudulgebru@gmail.com.

Table 1. The name of twelve SVMPs sequences of different venomous snake species with number of accession and amino acids

Snake species	Accession number	Number of amino acids
Agkistrodon contortrix laticinctus	O42138	620
Agkistrodon piscivorus leucostoma	C9E1S0	613
Deinagkistrodon acutus	Q9W6M5	610
Gloydius halys	Q8AWI5	610
Sistrurus catenatus edwardsi	ABG26979	612
Naja atra	A8QL59	621
Bothrops jararaca	O93523	610
Bothrops insularis	Q8QG88	610
Protobothrops flavoviridis	Q90ZI3	612
Bungarus multicinctus	ABN72537	614
Crotalus viridis viridis	C9E1R8	609
Crotalus atrox	Q9DGB9	610

molecular evolutionary genetic analysis (MEGA) software (version 4.0.02) (Tamura et al., 2007), with UPGMA method. Each node was tested using the bootstrap approach by taking 1,000 replicates; the bootstrap analysis indicates strong support. Homology of 12 SVMPs sequences was done using DNAMAN software.

Analysis of physico-chemical properties

The SVMPs sequences were utilized as the input data type to compute the percentage of amino acid composition (%) (Islam et al., 2013), molecular weight, theoretical isoelectric point (pI), number of positively and negatively charged residues, extinction coefficient, instability and aliphatic index, Grand Average of Hydropathy (GRAVY), using Expasy Protparam tool (http://web.expasy.org/protparam).

Analysis of secondary structure

SOPMA tool (Self-Optimized Prediction Method with Alignment) of NPS@ (Network Protein Sequence Analysis) server was used to characterize the secondary structural features of the proteins such as, alpha helix, 310 helix, Pi helix, beta bridge, extended strand, beta turn, bend region, random coil, ambiguous and other states (Geourjon and Deleage, 1995; Roly et al., 2014a, Islam et al., 2015).

Analysis of functional properties

The analysis of the selected 12 SVMPs sequences was done with the help of Motif scan (http://myhits.isb-sib.ch/cgibin/motif_scan) tool (Roly et al., 2014b). The input data type was in FASTA format and scanned against 'PROSITE Patterns' which is a selected protein profile.

RESULTS AND DISCUSSION

In our present investigation, the NCBI database was used as source to collect SVMPs sequences from different venomous snake species with accession number (Table 1). A total of 12 SVMPs sequences (after removing the duplicates and partial sequences) were obtained from different venomous snake species. SVMPs sequences were reckoned into five domains: signal peptide, propeptide, metalloproteinase, desintegrin and cyestine-rich domains based on their domain organization. Some researchers reported same result (Brust et al., 2013; Casewell, 2012; Ryan et al., 2003). Signal peptides of all the sequences are highly conserved and they are nearly identical. There are 18 residues in signal peptide which show 93.98% identity (Figure 1). However, the 13th residues in five sequences (*A. c. laticinctus, D. acutus, B. jararaca, B. insularis, C. v. viridis*) are Alanine while the remaining two (*A. p. leucostoma, G. halys, S. c. edwardsi, N. n. atra, P. flavoviridis, B. multicinctus, C. atrox*) is valin. However, as the properties of these two amino acid residues are almost the same we do not expect any change in signaling the secretion of the protein or in the removal of the signal peptide after secretion of the protein. Propeptide sequences of all the sequences are highly conserved and they are nearly identical. They are about 176 residues long showing 87.36% (Figure 2). The Cys-switch site (PKMCGV) within the propeptide is in the position of 165th residues (Figure 2). Cys-switch site (PKMCGV) is a short peptide of prodomain and is blocking the active site of metalloproteinase. When this peptide is removed, metalloproteinase is active. Metalloproteinase domains are 205 residues long and they have 66.63% identity (Figure 3). Desintegrin domains are approximately 95 residues long and have 78.63% identity. Same sort of grouping like metalloproteinase is also evident in the Desintegrin domain. The cystine-rich domains are 194 residues long and show 75.70% identity. In this study we showed that amino acids of metalloproteinase domain

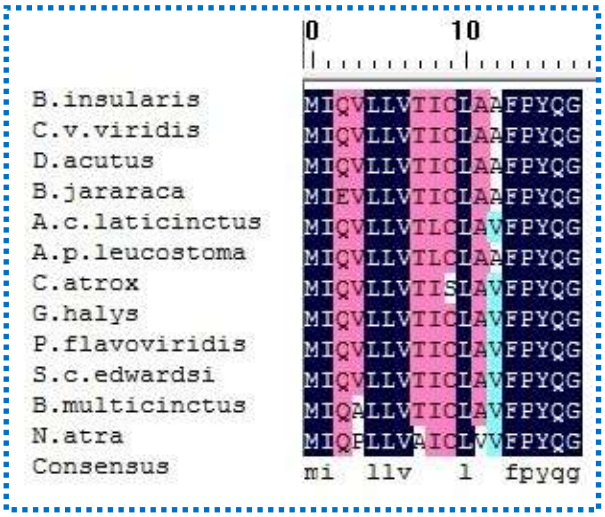

Figure 1. Multiple sequence alignment of signal peptide (93.98% identity) of SVMPs sequences: black color indicates positions with fully conserved residue; pink color indicates that one of the following high scoring groups is fully conserved; cyan color indicates that one of the following moderate scoring groups is fully conserved; white color indicates that one of the following 'weaker' scoring groups is fully conserved.

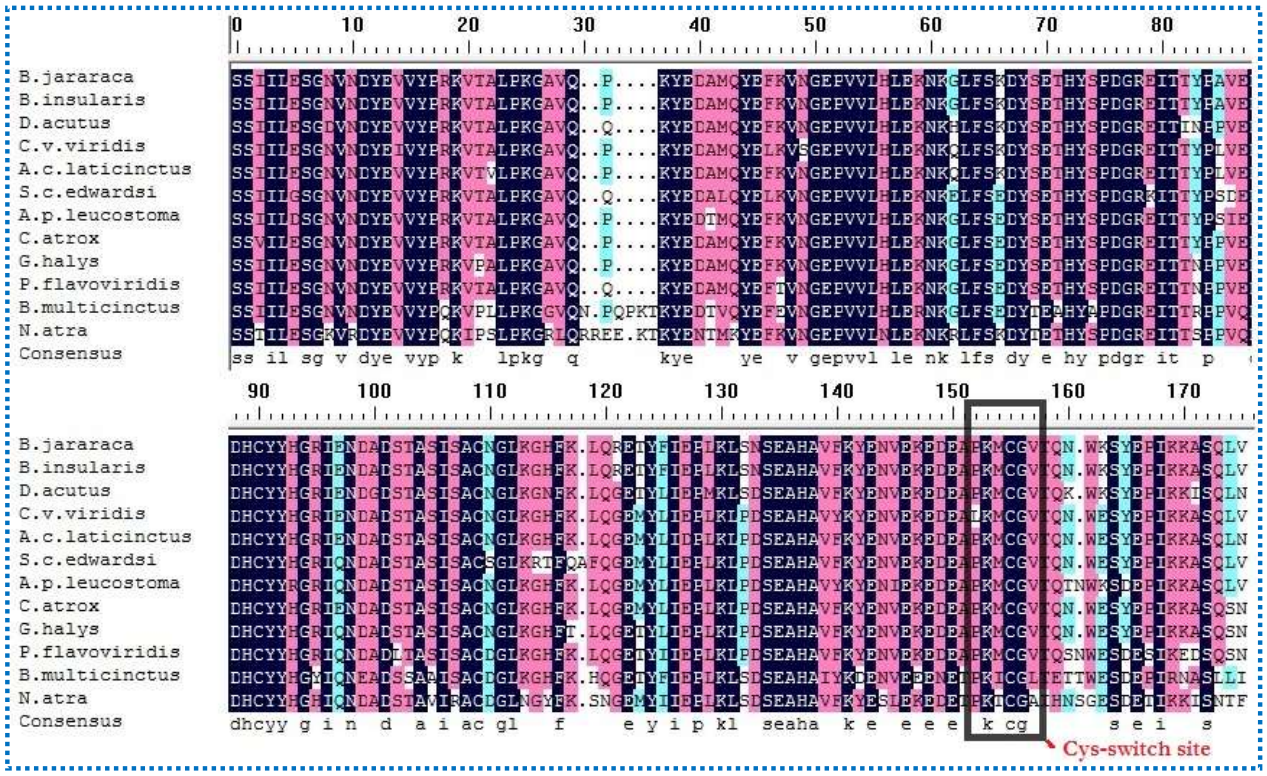

Figure 2. Multiple sequence alignment of propeptide (87.36% identity) of SVMPs sequences: black color indicates positions with fully conserved residue; pink color indicates that one of the following high scoring groups is fully conserved; cyan color indicates that one of the following moderate scoring groups is fully conserved; white color indicates that one of the following 'weaker' scoring groups is fully conserved.

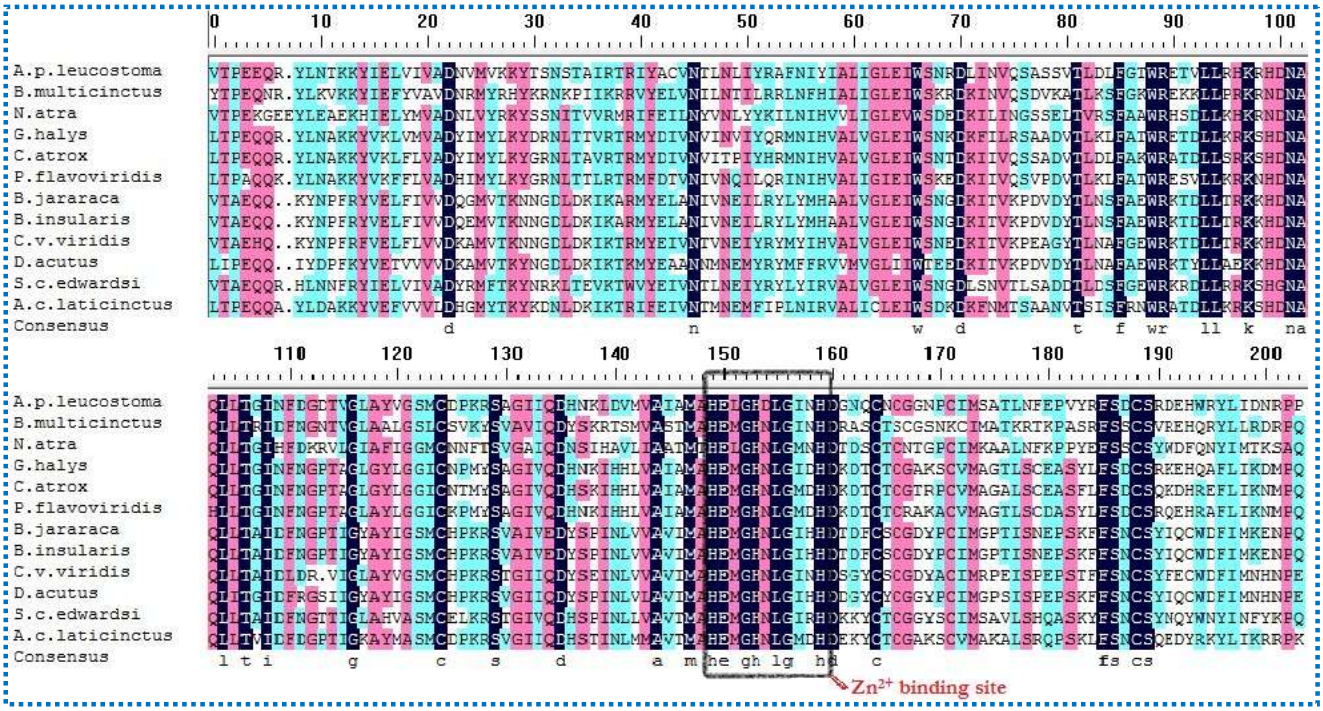

Figure 3. Multiple sequence alignment of metalloproteinase domain (66.63% identity) of SVMPs sequences: black color indicates positions with fully conserved residue; pink color indicates that one of the following high scoring groups is fully conserved; cyan color indicates that one of the following moderate scoring groups is fully conserved; white color indicates that one of the following 'weaker' scoring groups is fully conserved.

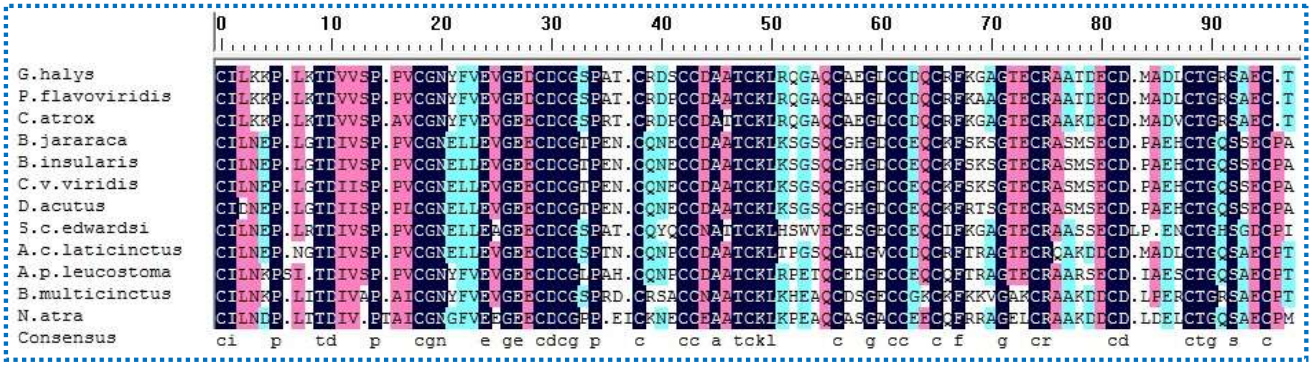

Figure 4. Multiple sequence alignment of desintegrin domain (78.63% identity) of SVMPs sequences: black color indicates positions with fully conserved residue; pink color indicates that one of the following high scoring groups is fully conserved; cyan color indicates that one of the following moderate scoring groups is fully conserved; white color indicates that one of the following 'weaker' scoring groups is fully conserved.

region were more changeable due to synonymous and non-synonymous mutation (Figure 3) and have very low identity; whereas signal peptide domain region was very less changeable and has the highest percentage similarity among different SVMPs sequences. The remaining other three domains: propeptide (Figure 2), desintegrin (Figure 4) and cyestine-rich domains (Figure 5) were moderately changeable and showed moderate percentage identity.

Phylogenetic tree and homology indicate that metalloproteinase domain has very high distance relationship (Figure 8A and B) among twelve SVMPs; on

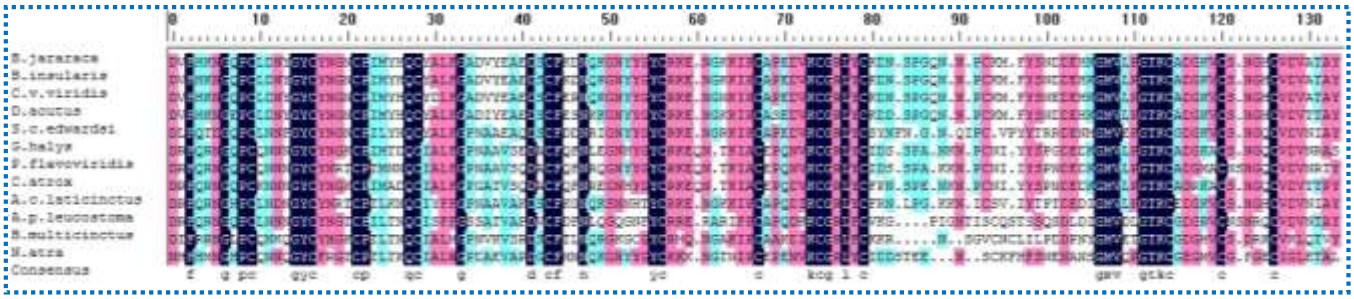

Figure 5. Multiple sequence alignment of cyestine-rich domain (75.70% identity) of SVMPs sequences: black color indicates positions with fully conserved residue; orange color indicates that one of the following high scoring groups is fully conserved; blue color indicates that one of the following moderate scoring groups is fully conserved; white color indicates that one of the following 'weaker' scoring groups is fully conserved.

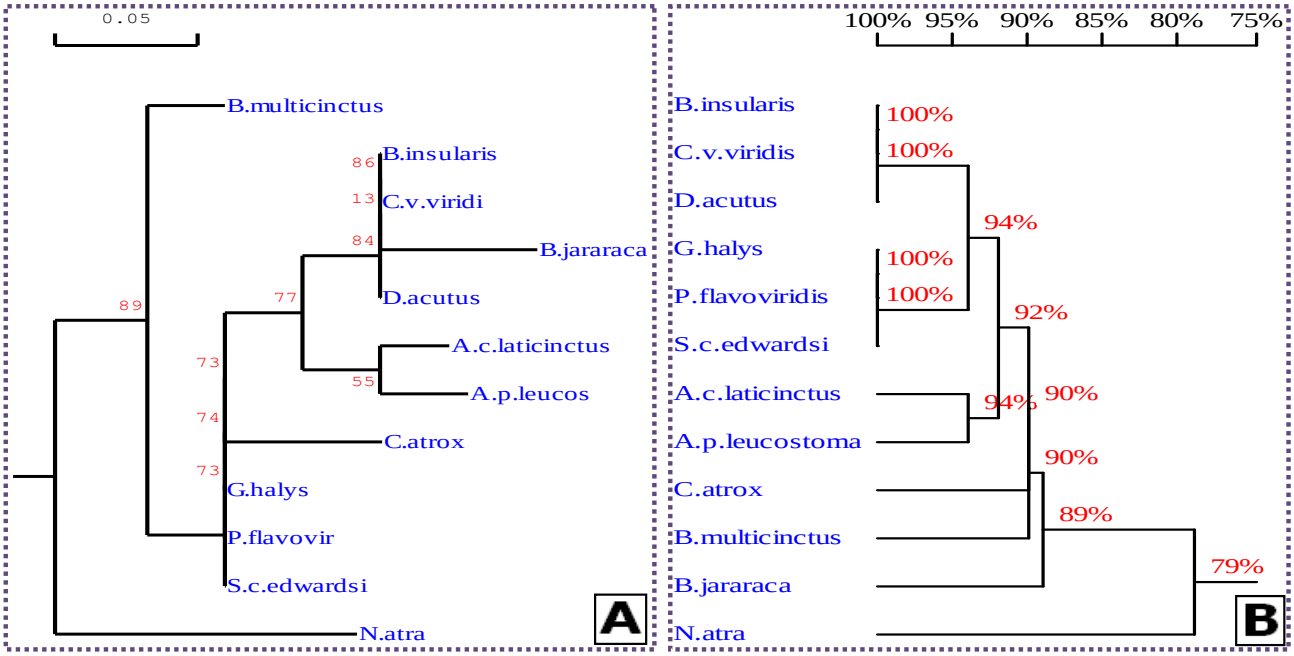

Figure 6. (A) Phylogenetic tree construction using by DNAMAN software of signal peptide of 12 SVMPS sequences from different venomous snake species using the bootstrap approach by taking 1,000 replicates and the bootstrap analysis indicates strong support **(B)** Homology construction of signal peptide using by DNAMAN software of 12 SVMPS sequences from different venomous snake species.

the other hand, signal peptide has very close distance relationship (Figure 6A and B) while the other remaining three domains (Propetide, Desintegrin domain and Cyestine rich domain) show moderate distance relationship (Figures 7A, 7B, 9A, 9B, 10A and 10B respectively)

In the analysis of amino acid composition, the percentage of cysteine residues in majority of the SVMPs sequences lies in the range of 6.1-6.7%; SVMPs sequences of *B. multicinctus*, *C. v. viridis* and *A. p. leucostoma* show a significant increase with values of 6.7, 6.6 and 6.5 percent, respectively (Table 2). The highest quantity of cysteine residues in *B. multicinctus* and *C. v. viridis* SVMPs sequences might be correlated with presence of cysteine switch motif and role of these SVMPs s in pathological conditions. These gelatinases have been early associated with several disorders such as carcinomas, cardio-vascular and so on. Highly significant presence of cysteine suggests its role as a critical residue for SVMPs activity and thus these SVMPs may be investigated for possible role in diseased

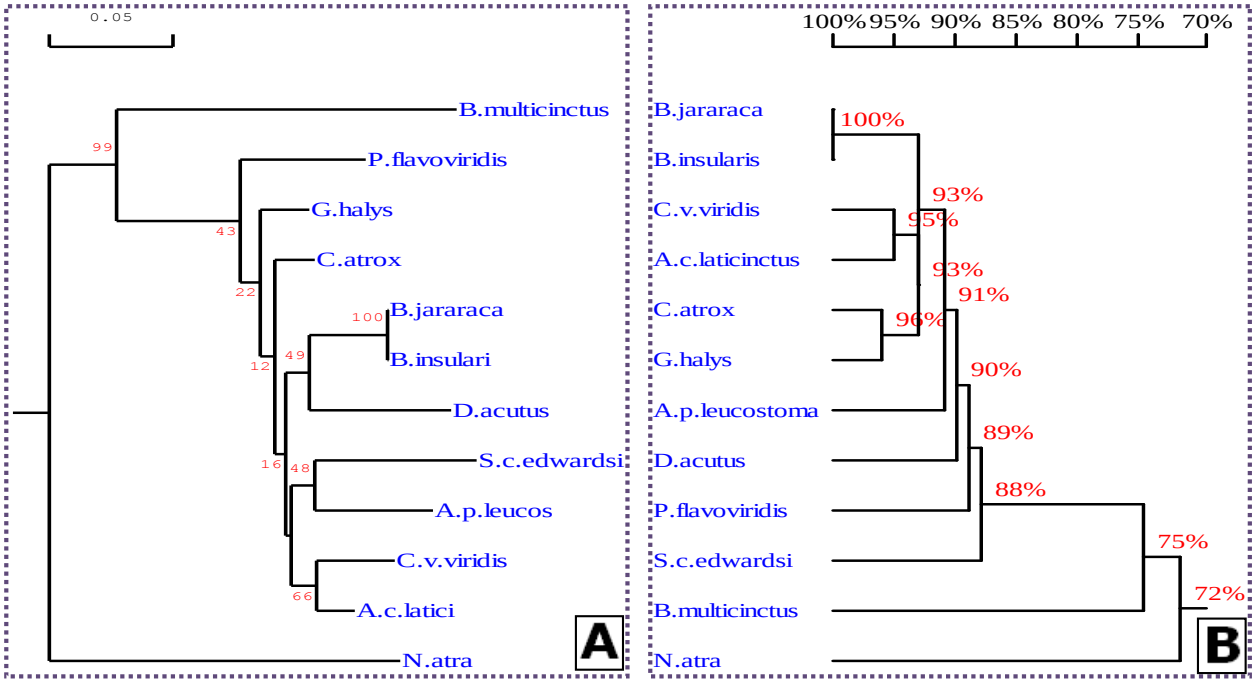

Figure 7. (A) Phylogenetic tree construction using by DNAMAN software of propeptide of 12 SVMPS sequences from different venomous snake species using the bootstrap approach by taking 1,000 replicates and the bootstrap analysis indicates strong support **(B)** Homology construction of signal peptide using by DNAMAN software of 12 SVMPS sequences from different venomous snake species.

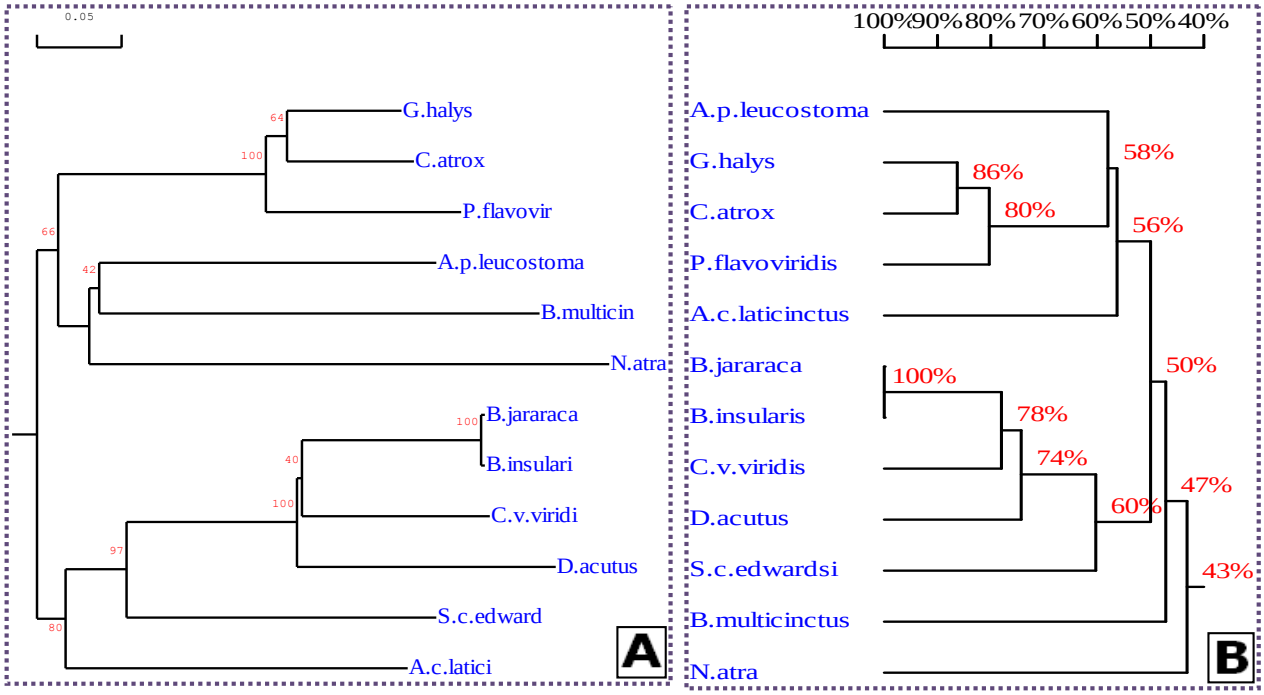

Figure 8. (A) Phylogenetic tree construction using by DNAMAN software of metalloproteinase domain of 12 SVMPS sequences from different venomous snake species using the bootstrap approach by taking 1,000 replicates and the bootstrap analysis indicates strong support **(B)** Homology construction of signal peptide using by DNAMAN software of 12 SVMPS sequences from different venomous snake species.

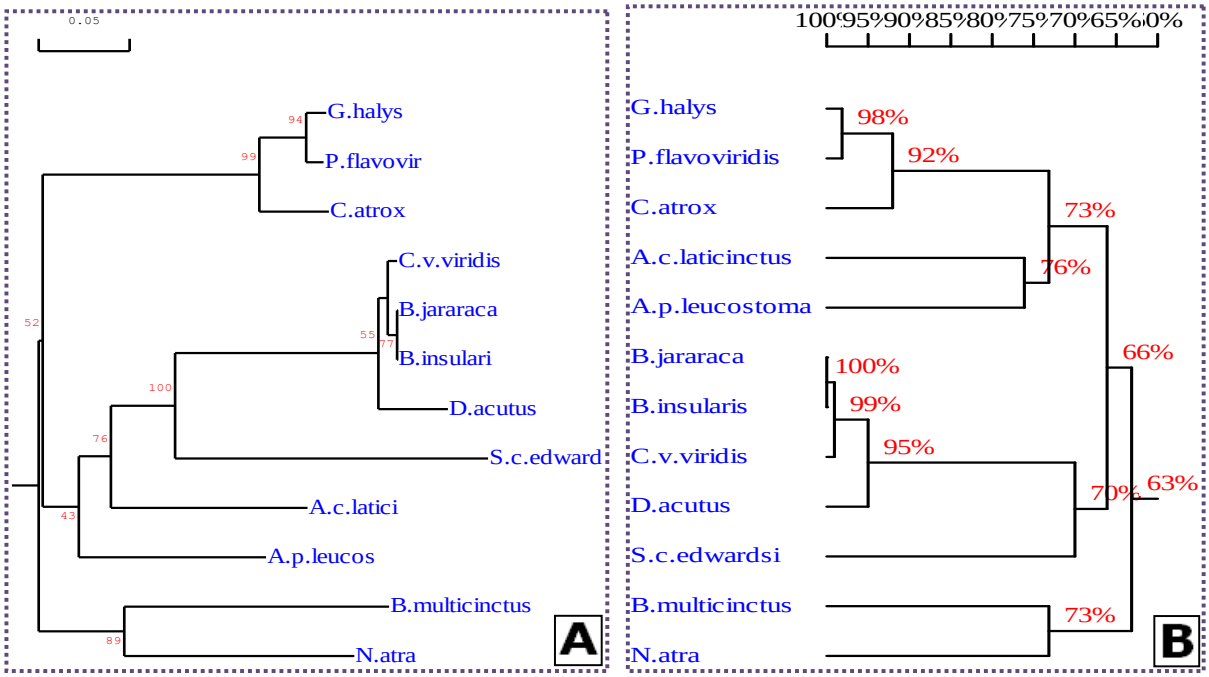

Figure 9. (A) Phylogenetic tree construction using by DNAMAN software of desingtegrin domain of 12 SVMPS sequences from different venomous snake species using the bootstrap approach by taking 1,000 replicates and the bootstrap analysis indicates strong support **(B)** Homology construction of signal peptide using by DNAMAN software of 12 SVMPS sequences from different venomous snake species.

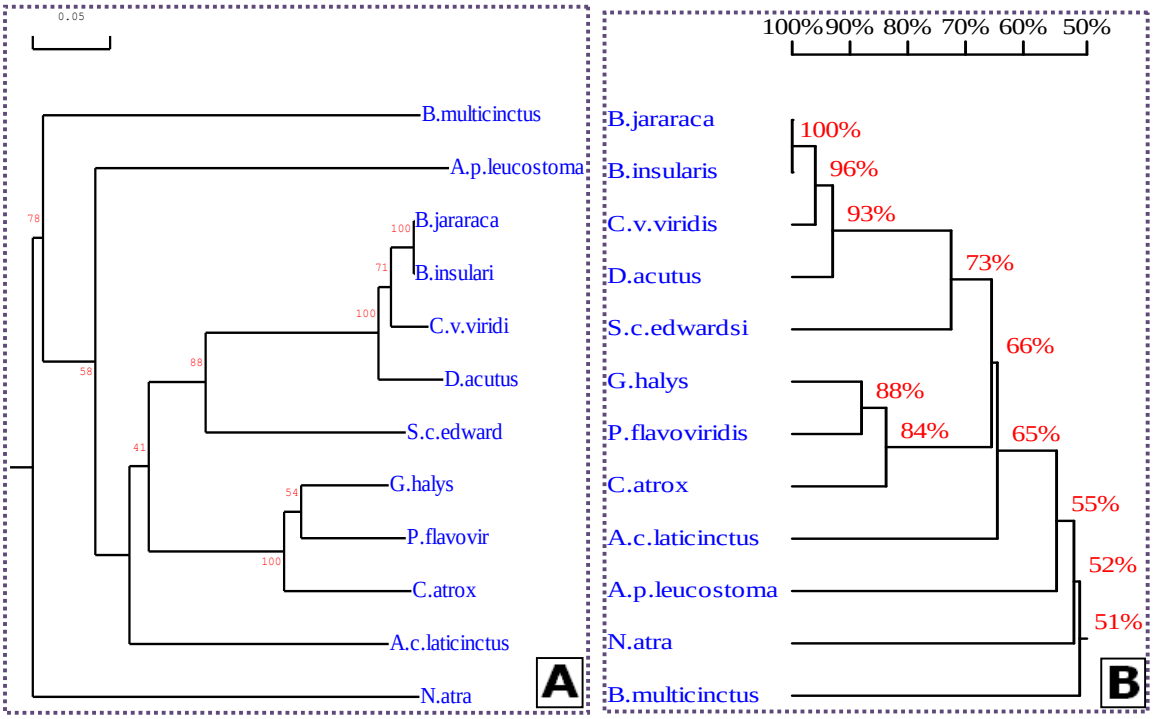

Figure 10. (A) Phylogenetic tree construction using by DNAMAN software of cyestine-rich domain of 12 SVMPS sequences from different venomous snake species using the bootstrap approach by taking 1,000 replicates and the bootstrap analysis indicates strong support **(B)** Homology construction of signal peptide using by DNAMAN software of 12 SVMPS sequences from different venomous snake species.

Table 2. Amino acid compositions of twelve SVMPs sequences of different venomous snake species (in %).

Species	Ala	Arg	Asn	Asp	Cys	Gln	Glu	His	Gly	Ile	Leu	Lys	Met	Phe	Pro	Ser	Thr	Trp	Tyr	Val
A. c. laticinctus	5.8	3.5	6.3	6.8	6.3	3.9	5.8	6.0	2.4	5.2	6.8	7.9	2.9	3.1	5.2	5.6	5.6	0.5	4.5	6.0
A. p. leucostoma	6.0	4.7	6.5	6.5	6.5	4.4	6.0	6.8	2.1	6.0	7.0	4.6	1.6	3.1	4.9	6.2	5.7	0.7	4.4	6.2
D. acutus	5.1	2.0	5.7	6.6	6.4	3.1	7.9	7.5	3.1	6.1	5.2	7.4	3.1	3.0	5.2	5.9	3.9	0.7	6.4	5.7
G. halys	7.5	3.6	6.2	6.4	6.4	4.3	5.9	7.0	2.6	4.8	7.0	6.6	2.5	2.6	4.8	5.2	4.9	0.5	4.9	6.2
S. c. edwardsi	5.9	3.9	6.5	5.2	6.2	4.2	7.2	7.0	2.6	5.1	7.5	5.1	1.6	2.8	4.2	6.2	4.9	1.0	6.5	6.2
N. atra	5.6	3.1	6.9	5.0	6.1	3.1	8.5	7.4	3.1	6.1	6.9	6.4	2.4	3.5	4.5	5.6	5.6	0.6	4.3	5.0
B. jararaca	6.1	2.1	6.4	6.2	6.4	3.3	7.5	7.0	3.1	4.9	5.9	7.2	2.5	3.1	5.2	5.9	4.1	0.7	5.9	6.4
B. insularis	6.1	2.1	6.4	6.2	6.4	3.4	7.5	6.9	3.1	4.9	5.9	7.2	2.5	3.1	5.2	5.9	4.1	0.7	5.9	6.4
C. atrox	7.0	3.9	5.7	6.2	6.2	4.1	6.1	7.0	2.8	4.4	6.7	6.6	2.6	3.0	5.1	5.2	5.2	0.5	5.1	6.4
C. v. viridis	5.6	2.5	6.2	5.9	6.6	3.1	8.3	7.1	3.3	5.1	6.6	6.6	2.6	2.6	4.9	5.9	4.1	0.7	6.1	6.2
P. flavoviridis	7.5	3.9	6.5	6.4	6.4	4.9	5.6	6.4	2.8	5.2	6.9	6.4	2.5	2.9	4.6	4.9	5.4	0.5	4.4	6.0
B. multicinctus	6.0	6.0	5.9	5.2	6.7	3.4	6.0	6.7	2.3	5.5	7.3	8.3	1.6	2.4	4.7	5.7	5.0	0.5	4.6	6.0

conditions. Further analysis of the amino acid composition can help to place amino acid presence at remarkable level and be correlated with precise pathological conditions (Shckorbatov et al., 2008).

Other physico-chemical parameters also signify the behavior of SVMPs in different conditions (Table 3). pH values for majority of the SVMPs (*A. c. laticinctus, D. acutus, B. jararaca, B. insularis, C. v. viridis*, *A. p. leucostoma, G. halys, S. c. edwardsi, N. n. atra, P. flavoviridis & C. atrox*) lie in the acidic range (pH<7); while for the only one SVMPs sequence (*B. multicinctus*), it increases in the alkaline range (pH>7). In addition, the instability index SVMPs sequences of different snake species of *A. c. laticinctus, D. acutus, B. jararaca, B. insularis, C. v. viridis*, *G. halys, S. c. edwardsi, N. n. atra & C. atrox* were stable (Instability index <40), but the remaining were unstable metalloproteinases (Instability index <40) (Table 3). Secondary structural analysis indicates a pre-dominance of random coils, followed by α-helices, extended strands and β-turns in 12 SVMPs sequences while the extended strands exceed α-helices in *A. c. laticinctus, A. p. leucostoma, D. acutus, N. n. atra, B. jararaca, B. insularis, B. multicinctus* and *C. v. viridis* (Table 4). This is very useful to predict three dimensional structures of proteins and can also help in approximation of some aspects of protein function and their classification into families (Rost, 2001).

Furthermore, the Motif Scan tool predicts the presence of a cysteine switch, a zinc protease and desintegrin motif in SVMPs sequences which have been the subject of discussion in various literatures (Table 5). The cysteine switch regulates activity of SVMPs sequences via complex formation between cysteine residue of prodomain and zinc atom of catalytic domain (Van Wart et al., 1990). Cys-switch site (PKMCGV) motif is present in the propeptide (Figure 2) and blocks the active site of metalloproteinase domain; and when this peptide is removed metalloproteinase is active. The primary sequence motif HExxH is present in the catalytic domain of zinc-dependant SVMPs sequences. The two conserved histidine residues coordinate the zinc atom and the glutamic acid residue is a member of the active site of enzyme (Devault et al., 1988). The zinc binding region signature has been characterized as (uncharged)-(uncharged)-H-E-(uncharged) -(uncharged)-H-(uncharged)-(hydro phobic) (Jongeneel et al., 1989). Zinc protease motif is present within the catalytic domain (metalloproteinase domain) of SVMPs sequences (Table), playing a pivotal role in the collagen binding region of these enzymes.

Conclusion

Intensive characterization and comparative analysis of the SVMPs sequence of proteins with the help of numerous bio-computational tools yielded new insights and perspectives which can

Table 3. Physico-chemical parameters of twelve SVMPs sequences of different venomous snake species.

Species	No. of A.A.	M.W (Da)	pI	"-" charged residues	"+" charged residues	Extinction coefficient	Instability index	Aliphatic index	GRAVY
A. c. laticinctus	620	69512.2	6.14	78	71	60595	34.26	69.66	-0.452
A. p. leucostoma	613	68212.0	5.17	77	57	64605	41.15	74.91	-0.355
D. acutus	610	68542.4	5.03	88	57	82485	37.11	65.84	-0.462
G. halys	610	67651.7	5.71	75	62	63575	39.28	71.64	-0.389
S. c. edwardsi	612	68930.7	5.27	76	55	94975	34.61	72.96	-0.399
N. atra	621	69402.5	5.25	84	59	64605	39.88	70.98	-0.411
B. jararaca	610	68213.0	5.15	84	57	78015	35.29	66.80	-0.451
B. insularis	610	68284.0	5.15	84	57	78015	34.76	66.80	-0.456
C. atrox	610	67960.1	5.90	75	64	65065	36.86	69.07	-0.417
C. v. viridis	609	68364.1	5.01	88	55	79505	40.85	69.15	-0.449
P. flavoviridis	612	68191.4	5.97	73	63	59105	42.25	72.21	-0.396
B. multicinctus	614	68988.1	8.73	69	88	60720	42.57	73.68	-0.487

Table 4. Secondary structural features of twelve SVMPs sequences of different venomous snake species (in %).

Snake species	A helix	310 Helix	Pi Helix	β Bridge	Extended strand	β Turn	Bend region	Random coil	Ambiguous states	Other states
A. c. laticinctus	22.42%	0.00%	0.00%	0.00%	24.68%	11.13%	0.00%	41.77%	0.00%	0.00%
A. p. leucostoma	16.48%	0.00%	0.00%	0.00%	29.53%	9.95%	0.00%	44.05%	0.00%	0.00%
D. acutus	23.28%	0.00%	0.00%	0.00%	27.21%	10.00%	0.00%	39.51%	0.00%	0.00%
G. halys	26.23%	0.00%	0.00%	0.00%	23.61%	9.67%	0.00%	40.49%	0.00%	0.00%
S. c. edwardsi	29.90%	0.00%	0.00%	0.00%	24.18%	8.82%	0.00%	37.09%	0.00%	0.00%
N. atra	23.67%	0.00%	0.00%	0.00%	24.96%	10.79%	0.00%	40.58%	0.00%	0.00%
B. jararaca	21.97%	0.00%	0.00%	0.00%	25.41%	10.82%	0.00%	41.80%	0.00%	0.00%
B. insularis	22.62%	0.00%	0.00%	0.00%	25.08%	10.49%	0.00%	41.80%	0.00%	0.00%
P. flavoviridis	25.65%	0.00%	0.00%	0.00%	25.33%	10.78%	0.00%	38.24%	0.00%	0.00%
B. multicinctus	21.82%	0.00%	0.00%	0.00%	25.57%	10.59%	0.00%	42.02%	0.00%	0.00%
C. v. viridis	23.81%	0.00%	0.00%	0.00%	25.62%	11.82%	0.00%	38.75%	0.00%	0.00%
C. atrox	26.89%	0.00%	0.00%	0.00%	22.62%	22.62%	0.00%	40.82%	0.00%	0.00%

be used to identify accelerated evolution of SVMPs sequence of proteins of different venomous snake species that play a crucial role in pathological conditions. In this study, multiple sequence alignment, phylogenetic tree, homology, physico-chemical, secondary structural and functional analysis of SVMPs sequence of proteins of different venomous snake species was carried out. The findings through this study may be used by researchers working on metalloproteinase of SVMPs in the context of any experimental system. So, from the identity comparison we can say that metalloproteinase domain is more diverse and under the evolutionary pressure. The amino acid composition shows a considerably high percentage of cysteine residues in *B. multicinctus* and *C. v. viridis* of SVMPs sequences, which might be a key player in pathological conditions. Future studies with the help of experimental research and test need to be carried out to validate this proposal. This study may be taken as a prototype for similar *in silico* investigational studies with regard to other large proteins families, where such comparative analysis might aid in giving a direction and help to rationalize the conduct of experimentation; it will also be very helpful to develop new drugs.

Conflicts of interest

The authors have not declared any conflict of interests.

ABBREVIATIONS

SVMP, Snake venom metalloproteinase sequences;

Table 5. Motifs found in of twelve SVMPs sequences of different venomous snake species.

Snake species	Motif found	Motif ID	Description	Start	End
A. c. laticinctus	ZINC_PROTEASE	PS00142	*Neutral zinc metallopeptidases, zinc-binding region signature.*	**332**	**341**
	DISINTEGRIN_1	PS00427	*Disintegrins signature*	**443**	**462**
A. p. leucostoma	ZINC_PROTEASE	PS00142	*Neutral zinc metallopeptidases, zinc-binding region signature.*	**333**	**342**
	DISINTEGRIN_1	PS00427	*Disintegrins signature*	**444**	**463**
D. acutus	ZINC_PROTEASE	PS00142	*Neutral zinc metallopeptidases, zinc-binding region signature.*	**331**	340
	DISINTEGRIN_1	PS00427	*Disintegrins signature*	**442**	461
G. halys	ZINC_PROTEASE	PS00142	*Neutral zinc metallopeptidases, zinc-binding region signature.*	**332**	341
	DISINTEGRIN_1	PS00427	*Disintegrins signature*	**443**	462
S. c. edwardsi	ZINC_PROTEASE	PS00142	*Neutral zinc metallopeptidases, zinc-binding region signature.*	**333**	342
	DISINTEGRIN_1	PS00427	*Disintegrins signature*	**444**	463
N. atra	ZINC_PROTEASE	PS00142	*Neutral zinc metallopeptidases, zinc-binding region signature.*	**339**	348
	DISINTEGRIN_1	PS00427	*Disintegrins signature*	**450**	469
B. jararaca	ZINC_PROTEASE	PS00142	*Neutral zinc metallopeptidases, zinc-binding region signature.*	**331**	340
	DISINTEGRIN_1	PS00427	*Disintegrins signature*	**442**	461
B. insularis	ZINC_PROTEASE	PS00142	*Neutral zinc metallopeptidases, zinc-binding region signature.*	**331**	340
	DISINTEGRIN_1	PS00427	*Disintegrins signature*	**442**	461
P. flavoviridis	ZINC_PROTEASE	PS00142	*Neutral zinc metallopeptidases, zinc-binding region signature.*	**333**	342
	DISINTEGRIN_1	PS00427	*Disintegrins signature*	**444**	463
B. multicinctus	ZINC_PROTEASE	PS00142	*Neutral zinc metallopeptidases, zinc-binding region signature.*	**338**	347
	DISINTEGRIN_1	PS00427	*Disintegrins signature*	**449**	468
C. v. viridis	ZINC_PROTEASE	PS00142	*Neutral zinc metallopeptidases, zinc-binding region signature.*	**330**	339
	DISINTEGRIN_1	PS00427	*Disintegrins signature*	**441**	460
C. atrox	ZINC_PROTEASE	PS00142	*Neutral zinc metallopeptidases, zinc-binding region signature.*	**332**	341
	DISINTEGRIN_1	PS00427	*Disintegrins signature*	**443**	462

NCBI, National Center for Biotechnology Information; **MEGA**, molecular evolutionary genetic analysis.

ACKNOWLEDGEMENTS

We are thankful to Md. Zohorul Islam (Student of Genetic Engineering and Biotechnology Department, University of Rajshahi, Rajshahi-6205, Bangladesh) for their valuable support and discussions related to this research and we are also grateful to Protein Science Laboratory for instrument facility.

REFERENCES

Birrell GW, Earl S, Wallis TP, Masci PP, de Jersey J, Gorman JJ, Lavin MF (2007). The diversity of bioactive proteins in Australian snake venoms. Mol. Cell. Proteomics 6:973-986.

Bjarnason JB, Fox JW (1994). Hemorrhagic metalloproteinase from snake venom. Pharmacol. Theor. 62:325-372.

Bode W, Gomis-Rüth FX, Stockler W (1993). Astacins, serralysins, snake venom and matrix metalloproteinases exhibit identical zinc-binding environments (HEXX-HXXGXXH and Met-turn) and topologies and should be grouped into a common family, the 'metzincins'. Febs Lett. 331:134-140.

Brust A, Sunagar K, Undheim EA, Vetter I, Yang DC, Casewell NR, Jackson TNW, Koludarov I, Alewood PF, Hodgson WC, Lewis RJ, King GF, Antunes A, Hendrikx I, Fry BG (2013). Differential evolution

and neofunctionalization of snake venom metalloprotease domains. Mol. Cell Proteomics. 12(3):651-663.
Casewell NR (2012). On the ancestral recruitment of metalloproteinases into the venom of snakes. Toxicon, 60(4):449-454.
Costa Jde O, Fonseca KC, Garrote-Filho MS, Cunha CC, de Freitas MV, Silva HS, Araújo RB, Penha-Silva N, de Oliveira F (2010). Structural and functional comparison of proteolytic enzymes from plant latex and snake venoms. Biochimie. 92(12):1760-1765.
Devault A, Sales V, Nault C, Beaumont A, Roques B, Crine P, Boileau G (1988). Exploration of the catalytic site of endopeptidase 24.11 by site-directed mutagenesis Histidine residues 583 and 587 are essential for catalysis. FEBS Lett. 231(1):54-58.
Fry BG, Wüster W, Kini RM, Brusic V, Khan A, Venkataraman D, Rooney AP (2003). Molecular evolution and phylogeny of elapid snake venom three-finger toxins. J. Mol. Evol. 57(1):110-129.
Geourjon C, Deleage G (1995). SOPMA: significant improvements in protein secondary structure prediction by consensus prediction from multiple alignments. Comput. Appl. Biosci. 11(6):681-684.
Hite LA, Jia LG, Bjarnason JB, Fox JW (1994). cDNA sequences for four snake venom metalloproteinases: structure, classification, and their relationship to mammalian reproductive proteins. Arch. Biochem Biophys. 308(1):182-191.
Islam MM, Haque ME, Dutta AK, Islam MA, Khalekuzzaman M, Sikdar B (2013). A Computational Study on Metalloproteinase in the Snake Venomous of Different Rattle Snake Species in Comparison with the Asian Snake Species. Int. J. Pharm. Bio. Sci. 4(4):741-748.
Islam Z, Islam MM, Saha S, Jahangir CA, Basak B, Islam MN, Islam MS, Paul S, Khalekuzzaman M (2015). Identification and Computational Analysis of Chicken Alpha-1 Collagen Sequences. Int. J. Sci. Eng. Res. 6(1):217-221.
Jongeneel CV, Bouvier J, Bairoch A (1989). A unique signature identifies a family of zinc-dependent metallopeptidases. FEBS let. 242(2):211-214.
Libra M, Scalisi A, Vella N, Clementi S, Sorio R, Stivala S, Demetrios A, Spandidos, Mazzarino C (2009). Uterine cervical carcinoma: Role of matrix metalloproteinases. Int. J. Oncol. 34:897-903.
Obermüller N, Morente N, Kränzlin N, Gretz N, Witzgall R (2001). A possible role for metalloproteinases in renal cyst development. Renal. Physiol. 280(3):540-550.
Pepper MS (2001). Role of the matrix metalloproteinase and plasminogen activator–plasmin systems in angiogenesis. Arterioscler Thromb. Vasc. Biol. 21(7):1104-1117.
Reza MA, Swarup S, Kini RM (2006). Molecular Evolution Caught In Action: Gene Duplication and Evolution of Molecular Isoforms of Prothrombin Activators in *Pseudonaja textilis* (Brown Snake). J. Thromb. Haemost. 4:1346-1353.
Roly ZY, Hasan SN, Ferdaus KMKB, Reza MA (2014). Predicted structure model of Bungarotoxin from Bungarus fasciatus snake. Bioinformation 10(10):617.
Roly ZY, Islam MM, Reza MA.(2014). A comparative in silico characterization of functional and physicochemical properties of 3FTx (three finger toxin) proteins from four venomous snakes. Bioinformation 10(5):281-287.
Rost B (2001). Review: protein secondary structure prediction continues to rise. J. Struct. Biol. 134(2):204-218.
Ryan CA, Pearce G (2003). Systemins: a functionally defined family of peptide signals that regulate defensive genes in Solanaceae species. Proc Natl Acad Sci. 100(2):14577-14580.
Shckorbatov YG, Zhuravleva LA, Navrotskaya VV, Miroshnichenko EV, Montvid PY, Shakhbazov VG, Sutushev TA (2008). Chromatin structure and the state of human organism. Cell Biol. Internat. 2005(29):77-81.
Tamura K, Dudley J, Nei M, Kumar S (2007). MEGA4: molecular evolutionary genetics analysis (MEGA) software version 4.0. Mol. Biol. Evol. 24(8):1596-1599.
Vanlaere I, Libert C (2009). Matrix metalloproteinases as drug targets in infections caused by gram-negative bacteria and in septic shock. Clin. Microbiol. Rev. 22(2):224-239.
Van Wart HE, Birkedal-Hansen H (1990). The cysteine switch: a principle of regulation of metalloproteinase activity with potential applicability to the entire matrix metalloproteinase gene family. Proc. Natl. Acad. Sci. 87(14):5578-5582.
Wallace AM, Sandford AJ (2002). Genetic polymorphisms of matrix metalloproteinases: functional importance in the development of chronic obstructive pulmonary disease? Am. J. Pharmacogenomics 2(3):167-175.

academicJournals

Vol. 15(8), pp. 264-271, 24 February, 2016
DOI: 10.5897/AJB2015.14680
Article Number: ADD7DD757334
ISSN 1684-5315

http://www.academicjournals.org/AJB

African Journal of Biotechnology

Full Length Research Paper

Genetic variability of sorghum landraces from lower Eastern Kenya based on simple sequence repeats (SSRs) markers

Catherine W. Muui[1]*, Reuben M. Muasya[2], Duncan T. Kirubi[1], Steven M. Runo[3] and Arthur Karugu[4]

[1]School of Agriculture and Enterprise Development, Department of Agricultural Science and Technology, Kenyatta University, P.O. Box 43844-00100, Nairobi, Kenya
[2]School of Agriculture and Veterinary Sciences, Department of Dry Land Agriculture, South Eastern Kenya University, P.O. Box 170-90200, Kitui, Kenya.
[3]Department of Biotechnology and Biochemistry, Kenyatta University, P.O. Box 43844-00100, Nairobi, Kenya.
[4]International Maize and Wheat Improvement Centre CIMMYT Kenya, P.O. Box 1041-00621, Nairobi, Kenya.

Received 27 April, 2015; Accepted 2 December, 2015

The aim of this study was to estimate the genetic variability of sorghum landraces grown in lower eastern Kenya based on simple sequence repeats (SSRs) markers. A total of 44 landraces obtained from the farmers and four improved varieties were analyzed using 20 SSR markers. All markers were polymorphic with polymorphism information content (PIC) value ranging from 0.04 to 0.81 with a mean of 0.49. Heterozygosity ranged from 0.00 to 0.04 suggesting that each detected a single genetic locus and that each of the sorghum accession used was stable. The alleles ranged between 2 and 10 and an average of 5.05 alleles per primer pair. The gene diversity ranged from 0.04 to 0.83 with a mean value of 0.53. All possible allele combinations ranged from 2 to 10, while major allele frequency ranged from 0.32 to 0.98. Genetic distances varied from 0.15 to 0.90 with two genotypes Karuge 1 and Karuge 2 obtained from Kiritiri in Mbeere having the minimum (0.15) and indication of very close relatedness. The diversity of the landraces was structured more on geographical locations and on seed colorations than agro-ecological conditions. Such intraregional genetic proximity in sorghum landraces would arise through seed exchanges among farmers. Analysis of molecular variation indicated higher variation within populations than among the groups. The genetic diversity can be exploited in hybridization programs to improve sorghum varieties grown by farmers in semi arid areas.

Key words: Genetic variability, landraces, simple sequence repeats, sorghum.

INTRODUCTION

Sorghum (*Sorghum bicolor* (L.) Moench) is one of the important staple crops for the world's poorest and food insecure people in the semi-arid regions of the world (Timu et al., 2012; Rohrbach et al., 2002; Doggett, 1988). In Kenya, sorghum is an important food crop and dietary staple in the country's arid and semi-arid lands which account for over 80% of the total land area. Sorghum is uniquely cultivated due to its tolerance to drought, water logging, saline-alkali infertile soils and high temperature (Taylor, 2003). It has for a long time been considered as

a crop of the resource-poor small-scale farmers and is grown predominately in arid and semi-arid lands (ASALs) (USAID, 2010).

All subspecies of *S. bicolor* are inter-fertile under sympatric conditions, leading to a continuum of wild-domesticate complex forms that have been documented to occur in many sorghum growing parts of Africa (Mutegi et al., 2010; Tesso et al., 2008; Dogget, 1988; Dogget and Majisu, 1968). Therefore, a wide genetic diversity is expected in the landraces of cultivated sorghum in Africa.

In lower Eastern Kenya, a wide diversity of sorghum landraces is cultivated under diverse agro-climatic conditions and practices by subsistence farmers (Muui et al., 2013; Mutegi et al., 2010). Farmers maintain sorghum landraces unique in their adaptation, grain yield, quality of harvested products, biotic stress resistance and in postharvest processing (Muui et al., 2013).

Sorghum with diverse morpho-types have been reported in many of the sorghum growing regions of Africa, often as indistinct races of *S. bicolor* that form a crop-wild-weed complex (Ejeta and Grenier, 2005; de Wet, 1978). Lower Eastern Kenya has a diverse of sorghum seed colorations, an indication of a possibility of early existence of crop-wild-weed complex of sorghum (Muui et al., 2013). Seed exchange among resource-poor small-scale farmers is a contributing factor to high variation among sorghum landraces (Tulole et al., 2009).

Farmers grow a mixture of several sorghum landraces per field (Muui et al., 2013; Barnaud et al., 2007). Over time, outcrossing occurs in sorghum though variable among different landraces (Barnaud et al., 2008). Also, selection exerted by farmers is a key parameter for determining the fate of new genetic combinations from the outcrossing events and thus in the patterns of genetic differentiation among landraces. Landraces perform well under sub-optimal conditions as they are well adapted to local stresses and possesses farmers' preferable traits (Bantilan et al., 2004; Setimela et al., 2004). It is, therefore, necessary to study the genetic relationships of these landraces and identify traits to be incorporated in the released varieties. Estimation of genetic diversity to identify groups with similar genotypes is important for conserving, evaluating and utilising genetic resources, for studying the diversity of different germplasm as possible sources of genes that can improve the performance of cultivars, and for determining the uniqueness and distinctness of the genetic constitution of genotypes (Subudhi et al., 2002).

Levels and patterns of diversity within and between cultivated and wild sorghum gene pools have been reported (Cui et al., 1995; Deu et al., 1995; Casa et al., 2005). In Kenya, studies were done to establish the extent and direction of introgression between cultivated and wild sorghum relatives (Mutegi et al., 2010). However, the extent of genetic diversity within and between landraces grown by farmers in different agro-ecological zones of lower Eastern Kenya has not been established. Our study therefore applied microsatellite markers to analyze cultivated sorghum sampled from different growing regions in lower Eastern Kenya, in order to elucidate patterns of diversity. The objective of the study was to determine the genetic relationships and thus establish the potential for landraces as sources of breeding material for future sorghum improvement.

MATERIALS AND METHODS

This research was conducted at the lower Eastern Kenya which extends between 38° 15 E and 39° 30 E as well as 1° N and 3° S. The study covered four regions of lower eastern varying in agro-climatology, namely Mbeere, Makueni, Kitui, and Mutomo, which are major sorghum growing areas in Kenya. The regions range from zone IV (semi humid to semi arid) to zone V (semi arid) (Jaetzold and Schmidt, 1983). The Mbeere and Kitui sites are classified as Lower Midland (LM) with some regions in transitional zone towards Upper Midland (UM). Makueni and Mutomo sites are classified as LM (Jaetzold et al., 2006).

Mbeere region where sorghum is grown receives an annual rainfall ranging from 800 to 1000 mm and an altitude of 840 to 1189 m above the sea level (Jaetzold et al., 2006). Makueni area receives an average annual rainfall ranging from 600 to 800 mm and an altitude of 914 to 1600 m above the sea level. Kitui receives an annual rainfall ranging from 600 to 1181 mm and an altitude of 1036 to 1115 m above the sea level, while Mutomo receives 500 to 700 mm annual rainfall and is at an altitude of 914 m above the sea level (Jaetzold et al., 2006). Collection of landraces was done in 2010 to 2011 (Muui et al., 2013) in the major sorghum growing agro ecological zones as follows; Mbeere in Kiritiri (LM_4), Ishiara (LM_4) Siakago (LM_3); Makueni in Kibwezi (LM_5), Kiboko (LM_5; LM_6), Makindu (LM_5); Kitui in Kitui central (LM_3), Kitui west (LM_3) and Mutomo in zone 1 and 2 (LM_4; LM_5) (Jaetzold et al., 2006) (Figure 1).

Forty four sorghum landraces collected from farmers in the study region and four commercially released cultivars were used to assess the genetic diversity (Table 1). Seeds for each accession were sown in trays containing soil and seedlings raised under standard glasshouse conditions at International Crops Research Institute for Semi-Arid Tropics (ICRISAT), World Agroforestry campus, Nairobi between July and September, 2012. Leaves were taken from two weeks old individual plants, from each accession.

DNA extraction was done using cetyl trimethyl ammonium bromide (CTAB) according to Mace et al. (2003). The quality of genomic DNA was assessed using agarose (0.8%) gel and quantification was done using a spectrophotometer nanodrop according to Mace et al. (2003). Polymerase chain reaction (PCR) amplifications were performed in 60 µl reaction mixture. Twenty primers of known sequence were used in amplification of the 48 samples (Billot et al., 2012). The amplification was carried out using the profile developed by Folkertsma et al. (2005). The PCR product was then loaded on 2% agarose gel and DNA fragments were visualized by illumination device with UV light. The success of amplification was indicated by the presence of one or two sharp

*Corresponding author. E-mail: catherinemuui@gmail.com

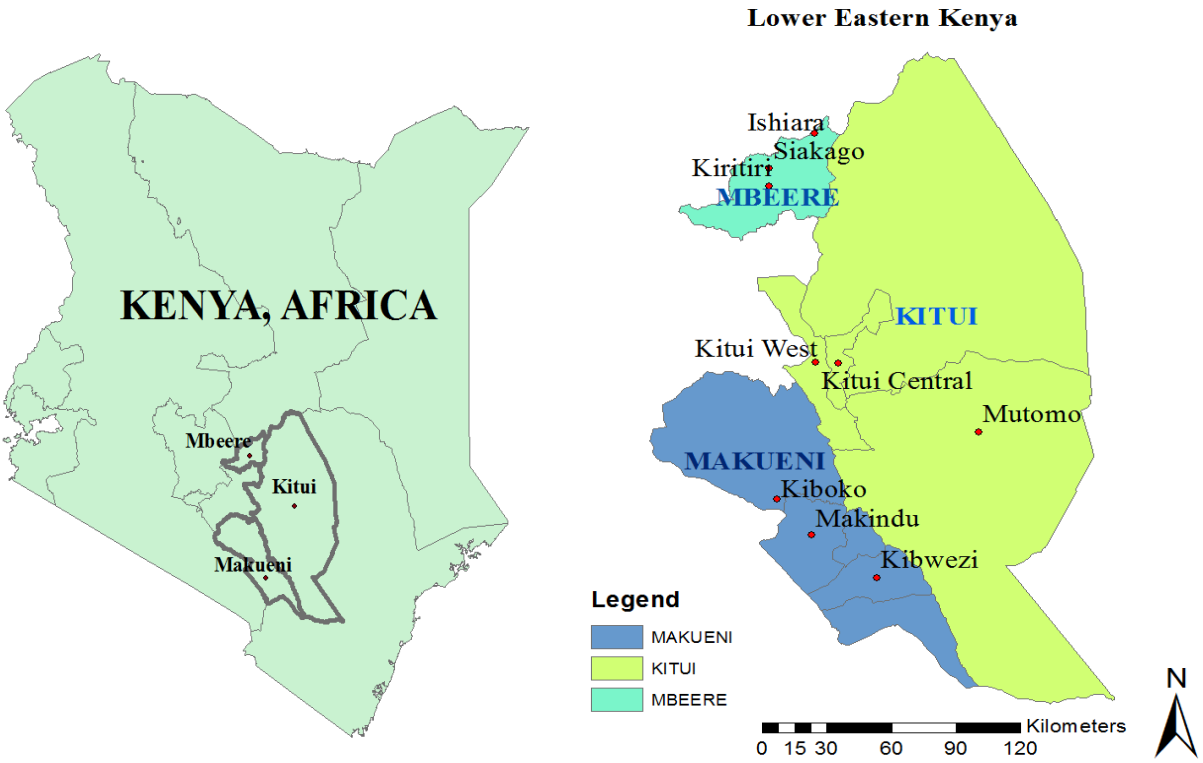

Figure 1. Map showing the study area in lower Eastern Kenya.

Table 1. Reference numbers for 44 landraces and 4 improved sorghum seed accessions used in diversity experiment.

Number	Accession identity	Number	Accession identity	Number	Accession identity
1	Kitui West white	17	Mbeere Kiritiri local A	33	Mbeere Kiritiri mubaku
2	Mbeere Kiritiri Gatengu	18	Kitui West white brown	34	Kitui Central brown white 2
3	Serena commercial	19	Mutomo black red	35	Mbeere Ishiara red
4	Mbeere Siakago white	20	Makueni Kiboko dirty white	36	Makueni Kibwezi brownwhite
5	Kitui Central brown	21	Makueni Makindu brown	37	Kitui West brown 1
6	Mbeere Kiritiri purple	22	Kitui Central white	38	Kitui West brown 2
7	Mbeere Kiritiri mwitia	23	Mutomo brown white	39	Mbeere Kiritiri thiriku 2
8	Mbeere Kiritiri ciakiondo	24	Kitui Central brown white 1	40	Mbeere Siakago red Seredo
9	Makueni Makindu white	25	Makueni Kiboko brown white	41	Gaddam commercial
10	Makueni Kibwezi brown	26	Mbeere Kiritiri thiriku 1	42	Kitui West brown 3
11	Mbeere Kiritiri karuge 2	27	Mbeere Siakago thiriku	43	Mutomo white
12	KARI Mtama 1commercial	28	Mutomo brown	44	Kitui Central brown red
13	Mbeere Kiritiri karuge 1	29	Seredo commercial	45	Kitui West white mweruba
14	Mbeere Kiritiri local B	30	Makueni Kiboko red	46	Makueni Kibwezi red
15	Makueni Makindu red	31	Makueni Kiboko brown	47	Mbeere Kiritiri muthiriku
16	Kitui Central red 1	32	Mbeere Siakago Serena	48	Kitui Central red 2

bands within the size range of up to 100 bp. Simple sequence repeats (SSR) was done by loading the PCR products for DNA fragments denaturation and size fractioning using capillary electrophoresis. Fragment size fractioning was done using ABI 3730 automatic DNA sequencer (Perkin Elmer-Applied Biosystems). Genemapper software Version 4.0 (Perkin Elmer-Applied Biosystems) was applied to size peak patterns, using the internal ROX 400 HD size standard and for allele calling.

Statistical analysis

Using the binned dataset, PowerMarker v.3.25 (Liu and Muse, 2005) was used to calculate the total numbers of alleles, the numbers

Table 2. Characteristics of 20 SSR markers across 44 sorghum landraces and 4 commercial varieties.

Marker	Repeat motif	Major allele frequency	Genotype number	Allele number	Availability	Gene diversity	Heterozygosity	PIC
gpsb067	(GT)10	0.55	4	4	0.98	0.57	0.00	0.50
mSbCIR238	(AC)26	0.54	4	4	0.96	0.61	0.00	0.54
mSbCIR248	(GT)7.5	0.36	4	4	0.98	0.72	0.00	0.67
mSbCIR276	(AC)9	0.83	5	5	0.98	0.30	0.00	0.29
mSbCIR283	(CT)8 (GT)8.5	0.58	4	4	1.00	0.58	0.00	0.52
mSbCIR329	(AC)8.5	0.63	2	2	0.90	0.47	0.00	0.36
Xcup02	(GCA)6	0.59	6	6	0.96	0.58	0.00	0.53
Xcup53	(TTTA)5	0.79	3	3	1.00	0.34	0.00	0.31
Xcup61	(CAG)7	0.72	6	4	0.98	0.44	0.04	0.41
Xcup63	(GGATGC)4	0.71	6	6	1.00	0.47	0.00	0.43
Xtxp010	(CT)14	0.32	10	10	0.92	0.83	0.00	0.81
Xtxp012	(CT)22	0.52	4	4	0.96	0.61	0.00	0.54
Xtxp015	(TC)16	0.38	7	7	0.98	0.76	0.00	0.73
Xtxp021	(AG)18	0.39	10	9	0.98	0.78	0.02	0.76
Xtxp040	(GGA)7	0.96	3	3	1.00	0.08	0.00	0.08
Xtxp057	(GT)21	0.38	8	8	1.00	0.77	0.00	0.73
Xtxp141	(GA)23	0.25	9	8	1.00	0.83	0.02	0.81
Xtxp145	(AG)22	0.95	3	2	1.00	0.10	0.02	0.09
Xtxp146	(GAA)19	0.98	2	2	1.00	0.04	0.00	0.04
Xtxp320	(AAG)20	0.47	6	6	0.98	0.69	0.00	0.65
Mean	-	0.60	5	5	0.98	0.53	0.01	0.49

numbers of common alleles with frequencies of at least 5%, the observed allele size ranges (bp), as the polymorphic information content (PIC) values (Botstein et al., 1980; Smith et al., 2000) and gene diversity. DARwin v.5.0 (Perrier et al., 2003; Perrier and Jacquemoud-Collet, 2006) was used to calculate pair-wise genetic dissimilarities of accessions using simple matching. The dissimilarity coefficients were used to perform principal coordinates analyses (PCoA) and construct weighted neighbour-joining trees (Saitou and Nei, 1987). Variation between and within accessions was assessed using analysis of molecular variance (AMOVA) using Arlequin v.3.1 (Excoffier et al., 2006).

RESULTS

SSR Polymorphism

Polymorphism among the 48 sorghum genotypes was assessed with 20 SSR markers. All the 20 SSR markers used were polymorphic across the 48 sorghum genotypes with PIC value ranging from 0.04 to 0.81 with a mean of 0.49. Of the 20 markers, 65% were highly polymorphic with a value greater than 0.5 indicating their usefulness in discriminating the genotypes (Table 2). Heterozygosity values of the 20 SSR markers ranged from 0.00 to 0.04, with a mean of 0.01 suggesting that each detected a single genetic locus and that each of the sorghum accession used was stable. The markers revealed a total of 98 alleles with a range between 2 (gpsb067, mSbCIR24 and Xcup53) and 10 (Xtxp320) alleles and an average of 5.05 alleles per primer pair. The gene diversity ranged from 0.04 to 0.83 with a mean value of 0.53. All possible allele combinations found in the 48 accessions ranged from 2 to 10, while the major allele frequency ranged from 0.32 to 0.98 (Table 2).

The weighted neighbour-joining clustering-based dendrogram generated using dissimilarity indices clustered the sorghum accessions into four major groups (Figure 2). Cluster 1 comprised of genotypes from Kitui (west and central), Mbeere (Siakago and Kiritiri), Makueni (Kibwezi, Makindu and Kiboko) and Seredo (commercial variety). The genotypes varied in color from white, brown white, brown, red, black red and purple, but distributed across the four regions. The cluster had three subgroups with genotype black red from mutomo very distinct from other genotypes. Cluster 2 had genotypes from Mbeere (Kiritiri, Siakago), Makueni (Kibwezi), KARI Mtama 1 and Serena commercially released varieties. The cluster had four subgroups with genotypes 7 and 8 from Mbeere Kiritiri grouped together distinctly. Cluster 3 had genotypes from Makueni (Makindu, Kibwezi), Mbeere (Kiritiri, Ishiara, Siakago), Kitui (west and central) and Mutomo; and the commercial variety Gaddam. The cluster had five sub groups with seed color varying greatly. Cluster 4 consists of three genotypes from Mbeere (Kiritiri), Makueni (Kiboko) and Kitui central. Genotype 26 from Mbeere (Kiritiri) and 24 from Kitui central had a closer relationship than with 25, though

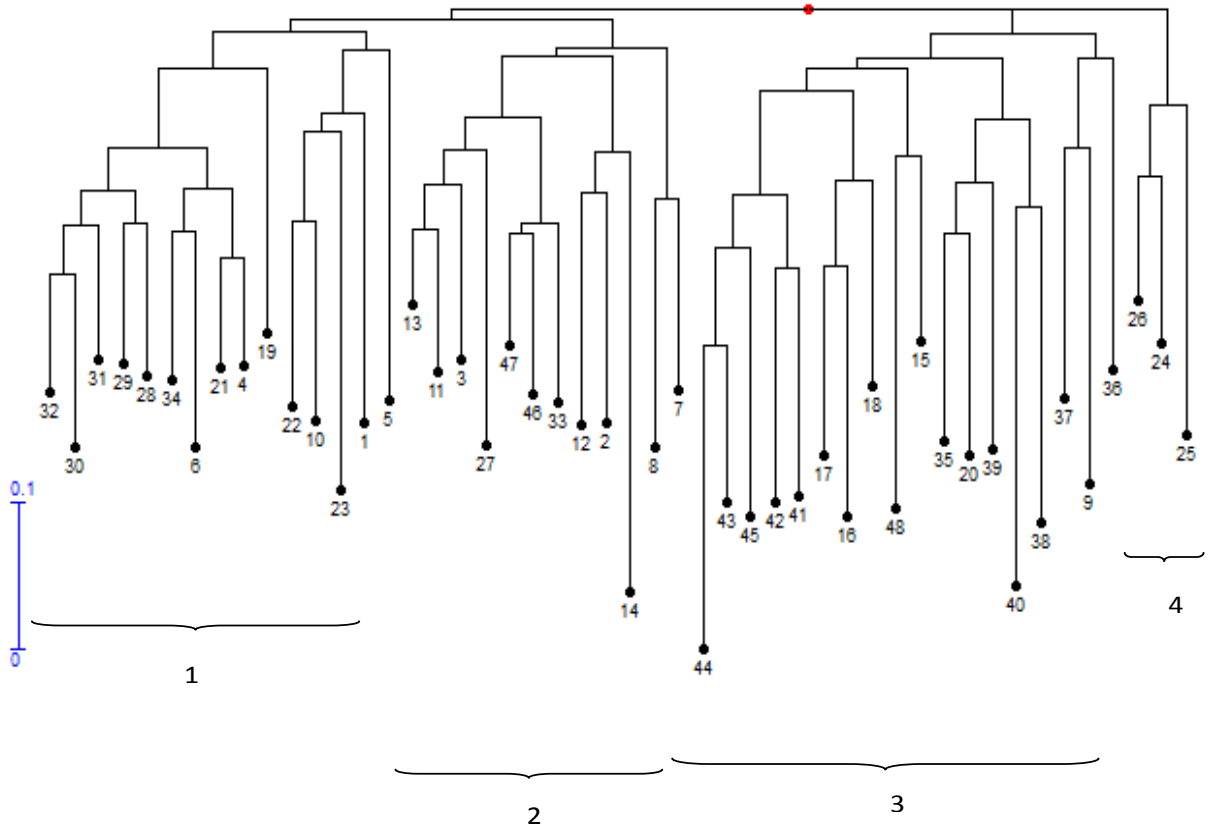

Figure 2. Tree constructed based on 20 polymorphic sorghum SSR markers using the simple matching dissimilarity index and weighted neighbor joining clustering for the 48 sorghum accessions.

in the same cluster (Figure 2).

Genetic diversity among accessions was also confirmed by scatter plot derived through PCoA (Figure 3). Forty percent of the accessions were clustered in the right portions of the plot, while 60% accessions were clustered in the left portion of the plot (axes1/2). Groupings were similar to those detected by cluster analysis where the genotypes were clearly separated across the region except for the genotype 9 from Makueni (Makindu) and genotype 11 from Mbeere (Kiritiri) which had an overlap. Genotypes 20 from Makueni (Kiboko) and 33 from Mbeere (Kiritiri) followed by genotypes 27 from Mbeere (Siakago) and 44 from Kitui central were far much apart from other genotypes; an indication of maximum dissimilarity. Genotypes 11, 13 and 3 formed a solidarity group implying high relatedness in the genetic makeup. This was also observed in genotypes 10 from Makueni (Kibwezi), 22 from Kitui central, 28 from Mutomo, 3 (commercial), 30 from Kiboko and 4 from Mbeere Siakago (Figure 3).

AMOVA showed significant (P = 0.05) differences among the various genotypes evaluated (Table 3). There was a greater variance (91.61%) represented by individuals within populations, while the variance between the groups was less (2.75%) with least variance (1.14%) expressed by the individuals.

Fixation indices between the commercial varieties and genotypes from Mbeere Ishiara was the highest (F_{ST} = 0.24249; P = 0.001), followed by between Ishiara and Kitui central (F_{ST} = 0.19055; P = 0.001). Population pair wise fixation indices was the lowest between Makindu and Kitui west (F_{ST} = 0.03523; P = 0.001) and between Mutomo and Kitui west (F_{ST} = 0.03653; P = 0.001) and Kiritiri Siakago regions (F_{ST} = 0.016; P = 0.001) (Table 4).

DISCUSSION

The genetic diversity among the sorghum accessions used in this study was high as indicated by PIC and gene diversity values. The PIC of a SSR marker gives an idea about the discriminatory power of that marker by taking into account the number of alleles detected and their relative frequencies (Smith et al., 2000). Markers with PIC more than 0.5 are efficient in discriminating genotypes and extremely useful in detecting the polymorphism rate at a particular locus (DeWoody et al., 1995).

Sorghum is primarily an inbreeding species resulting in a low level of observed heterozygosity, but the gene pool as a whole maintains a high level of allelic variation. The

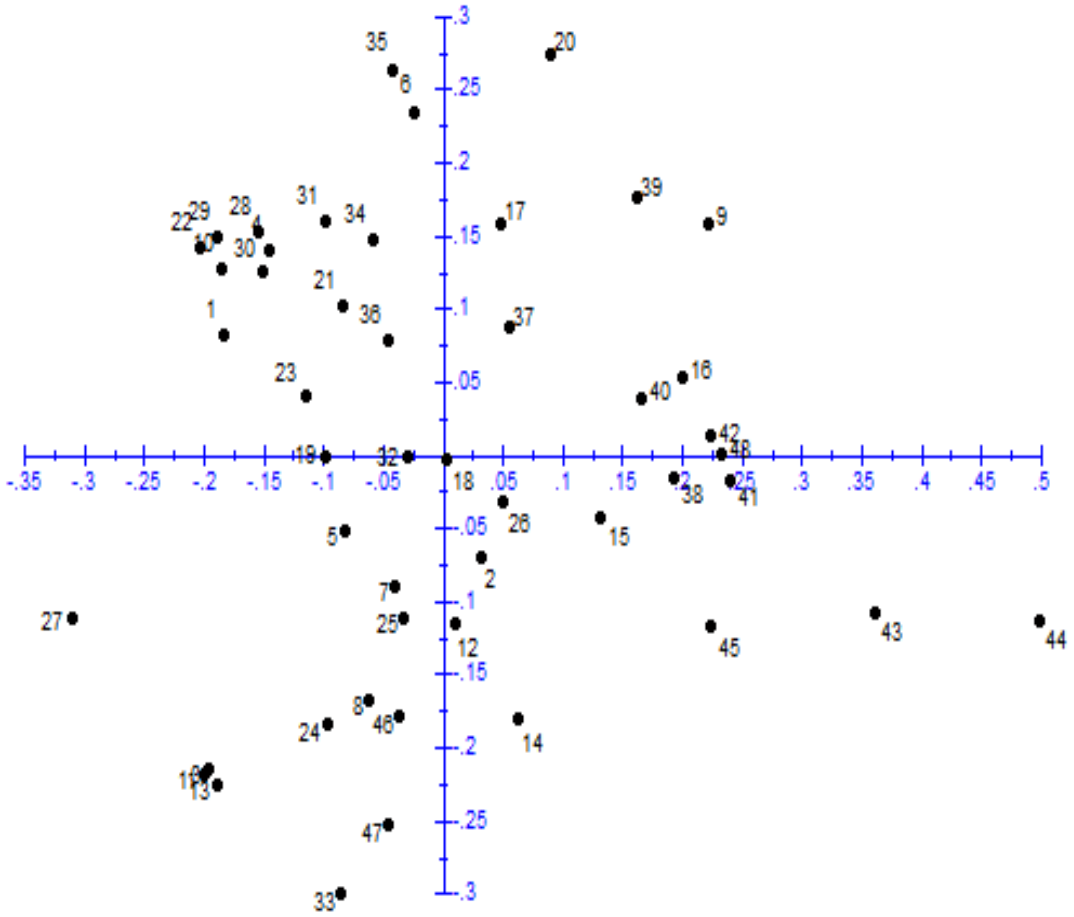

Figure 3. Plot of the axes 1 and 2 of the principal coordinate analysis based on the dissimilarity of 20 SSR markers for 44 sorghum accessions obtained from farmers in lower eastern Kenya and 4 improved varieties.

Table 3. Analysis of molecular variation (AMOVA) of 4 sorghum improved varieties and 44 landraces from farmers in different locations of Mbeere, Mutomo, Kitui and Makueni based on 20 SSR markers.

Source of variation	d.f.	Sum of squares	Variance components	Percentage of variation
Among populations	9	73.42	0.13	2.75
Among individuals	-	-	-	-
within populations	38	354.10	4.63	91.61
Within individuals	47	2.50	0.05	1.14
Total	94	430.02	4.81	-

high level of allelic variability but low level of heterozygosity observed in this study agrees with findings on diversity analysis of Eritrean sorghum landraces with SSR markers (Ghebru et al., 2002). The low heterozygosity was a clear indication the genotypes were homozygous and thus a high level of stability in the population.

Genetic distances among the 48 genotypes varied greatly indicating a wide diversity. Genotype Karuge 2 and Karuge 1 both from Mbeere (Kiritiri) had a low genetic distance (0.15). Though, the seed color and geographical location of the two accessions was identical, the two are totally different genetically. The results in this study suggest that diversity of the landraces were structured more on geographical locations and on seed colorations than agro-ecological conditions. Reports of other studies in sorghum accessions have shown grouping primarily on the basis of origin, and clustering within groups as driven by racial classification (Sharma

Table 4. Pairwise FST estimates among 4 improved varieties and 44 landraces from different locations in Mbeere, Mutomo, Kitui and Makueni; and 4 improved varieties.

Location	1	2	3	4	5	6	7	8	9	10
Kitui central	-	-	-	-	-	-	-	-	-	-
Kitui west	0.04947	-	-	-	-	-	-	-	-	-
Kiritiri	0.06672	0.07287	-	-	-	-	-	-	-	-
Siakago	0.08234	0.09518	0.07393	-	-	-	-	-	-	-
Ishiara	0.19055	0.06897	0.18737	0.09030	-	-	-	-	-	-
Makindu	0.07124	0.03523	0.05419	0.12299	0.14758	-	-	-	-	-
Kiboko	0.09667	0.11713	0.12840	0.01661	0.14327	0.12209	-	-	-	-
Kibwezi	0.08037	0.07879	0.09231	0.10533	0.18943	0.17455	0.14180	-	-	-
Mutomo	0.05847	0.03653	0.07289	0.07958	0.13146	0.06009	0.07036	0.10138	-	-
Commercial	0.16788	0.16196	0.10243	0.09135	0.24249	0.17748	0.18301	0.15586	0.10933	-

1, Kitui central landrace; 2, Kitui west_landrace; 3, Mbeerekiritiri_landrace; 4, Mbeeresiakago_landrace; 5, Mbeereishiara_landrace; 6, Makindu_landrace; 7, Kiboko_landrace; 8, Kibwezi_landrace; 9, Mutomo_landrace; 10, AS_improved.

et al., 2010; Hash et al., 2007). The main evolutionary forces responsible for producing genetic structure in plant populations are gene flow, selection associated with environmental heterogeneity and/or farmer preferences and random genetic drift (Neal, 2004).

The high genetic diversity could potentially be exploited in broadening the genetic base of germplasm used in sorghum breeding. The unique diversity implies that sorghum landraces are potential source of novel genes, such as pests and disease resistance, low moisture and soil fertility tolerance. The genetic variability and differentiation of the landraces obtained from lower eastern Kenya could be incorporated in breeding programs by developing populations with a broad genetic base. This will help to create new genetic recombinations that can be exploited in response to new breeding challenges.

The clustering of the landraces based on geographical locations was distinct with some overlaps where genotypes cut across the locations. Such intraregional genetic proximity in sorghum landraces would arise through seed exchanges among farmers. This was reported in the baseline survey conducted in sorghum seed systems in Eastern Kenya which were found to be largely traditional, with farmers playing a major role in the selection and exchange of seeds (Muui et al., 2013). A study conducted on sorghum production systems in Bomet, Kenya, indicated that farmers played a great role in seed selection, exchange and movement (Ochieng et al., 2011).

The similarity in genotypes could be attributed to proximity of the regions, though Mbeere appeared to be unique in the color of the seeds. Other studies showed that similarities in genotypes was as a result of region proximity in Africa for cultivated sorghum (Deu et al., 2008; Nkongolo and Nsapato, 2003; Ayana et al., 2000b) and its wild relatives (Ayana et al., 2000a). Results in this study showed that Mbeere had unique cluster. A study in Turkana and North-Eastern Kenya showed that cultivated sorghum was clustered into a distinct and unique genetic group (Mutegi et al., 2010). This is attributed to the fact that Mbeere is relatively geographically remote from other sorghum growing regions. The gene pools from sorghum landraces tested in this study appear to be genetically distinct. A study conducted in Turkana and North Eastern regions of Kenya on cultivated sorghum showed unique genetic clusters based on regions (Mutegi et al., 2010).

AMOVA indicated higher variation within populations than among the groups. Estimates of fixation indices revealed a strong genetic structure between commercial and Mbeere-Ishiara genotypes and between Mbeere-Ishiara and Kitui central genotypes. The presence of strong genetic structure indicates that these two groups are reproductively and genetically isolated from each other.

Conflict of interests

The author(s) did not declare any conflict of interest.

ACKNOWLEDGEMENTS

The authors acknowledge farmers from lower Eastern Kenya region for willingness to share the germplasm and information; and the Ministry of Agriculture Office in Embu for allowing us access to the region. This study was funded by the National Commission for Science, Technology and Innovation (NACOSTI), Kenya.

REFERENCES

Ayana A, Bekele E, Bryngelsson T (2000a). Genetic variation in wild sorghum (*Sorghum bicolor* ssp *verticilliflorum* (L.) Moench) germplasm from Ethiopia assessed by random amplified polymorphic DNA (RAPD). Heredity 132:249-254.

Ayana A, Bryngelsson T, Bekele E (2000b). Genetic variation of Ethiopian and Eritrean sorghum (*Sorghum bicolor* (L.) Moench) germplasm assessed by random amplified polymorphic DNA (RAPD). Genet. Resour. Crop Evol. 47:471-482.

Bantilan MCS, Deb UK, Gowda CLL, Reddy BVS, Obilana AB, Evenson RE (2004). Sorghum Genetic Enhancement: Research Process, Dissemination and Impacts. International Crops Research Institute for the Semi-Arid Tropics, Andhra Pradesh, India.

Barnaud A, Deu M, Garine E, Mckey D, Joly HI (2007). Local genetic diversity of sorghum in a village in northern Cameroon: structure and dynamics of landraces. Theor. Appl. Genet. 14:237-248.

Barnaud A, Trigueros G, Mckey D, Joly HI (2008). High outcrossing rates in fields with mixed sorghum landraces: how are landraces maintained? Heredity 101:445-452.

Billot C, Rivallan R, Sall MN, Fonceka D, Deu M, Glaszmann JC, Noyer JL, Rami JF, Risterucci AM, Wanker P, Ramu P, Hash CT (2012). A reference microsatellite kit to assess for genetic diversity of sorghum bicolor *(poaceae).* Am. J. Bot. 6:e245-e260.

Botstein D, White RL, Skolnick M, Davis RW (1980). Construction of a genetic linkage map in man using restriction fragment length polymorphisms. Am. J. Hum. Genet. 32:314-331.

Casa AM, Mitchell SE, Hamblin MT, Sun H, Bowers JE, Paterson AH, Aquadro CF, Kresovich S (2005). Diversity and selection in Sorghum: simultaneous analyses using simple sequence repeats. Theor. Appl. Genet. 111:23-30.

Cui YX, Xu GW, Magill CW, Schertz KF, Hart GE (1995). RFLP-based assay of *Sorghum bicolor* (L) Moench genetic diversity. Theor. Appl. Genet. 90:787-796.

De Wet JMJ (1978). Systematics and evolution of *Sorghum* Sect. sorghum (Graminae). Am. J. Bot. 65:477.

Deu M, Hamon P, Chantereau J, Dufour P, D'Hont A, Lanaud C (1995). Mitochondrial DNA diversity in wild and cultivated sorghum. Genome 38:635-645.

Deu M, Sagnard F, Chantereau J, Calatayud C, Hérault D, Mariac C, Pham JL, Vigouroux Y, Kapran I, Traoré PS, Mamadou A, Gérard B, Ndjeunga J, Bezançon G (2008). Niger-wide assessment of *in situ* sorghum genetic diversity with microsatellite markers. Theor. Appl. Genet. 116:903-913.

DeWoody JA, Honeycutt RL, Skow LC (1995). Microsatellite markers in white-tailed deer. J. Hered. 86:317-319.

Dogget H (1988). Sorghum. Longman Scientific and Technical, Essex.

Dogget H, Majisu BN (1968). Disruptive selection in crop development. Heredity 23:1-23.

Ejeta J, Grenier C (2005). Sorghum and its weedy hybrids. In: Gressel J. (Ed.) Crop ferality and volunteerisim. CRC Press, Boca Raton, FL. pp. 123-135.

Excoffier L, Laval G, Schneider S (2006). Arlequin ver 3.1, An Integrated Software Package for Population Genetics Data Analysis. Computational and Molecular Population Genetics Lab (CMPG). Institute of Zoology, University of Berne, Baltzerstrasse 6, 3012 Bern Switzerland.

Folkertsma RT, Rattunde HFW, Chandra S, Raju GS, Hash CT (2005). The pattern of genetic diversity of guinea-race *Sorghum bicolor* (L.) Moench land races as revealed with SSR markers. Theor. Appl. Genet. 111:399-409.

Ghebru B, Schmidt RJ, Bennetzen JL (2002). Genetic diversity of Eritrean sorghum landraces assessed with simple sequence repeat (SSR) markers. Theor. Appl. Genet. 105:229-236.

Hash CT, Billot C, Ramu P, Rami J, Gardes L, Folkertsma RT, Rivallan R, Upadhyaya HD, Deu M, Li Y, Wang T, Lu P (2007). Diversity analysis of 3365 sorghums in the GCP composite germplasm set based on allelic variation at 41 SSR loci. In: 'GCP Annual Research Meeting', Benoni, South Africa.

Jaetzold R, Schmidt H (1983). Farm Management Handbook of Kenya, Ministry of Agriculture, Kenya and German Agricultural Team (GAT) of the German Technical Cooperation.

Jaetzold R, Schmidt H, Hornetz B, Shisanya C (2006). Farm Management Handbook of Kenya, Vol. II/C1. Ministry of Agriculture, Kenya and German Agency Technical Cooperation team (CTZ).

Liu K, Muse SV (2005). PowerMarker: an integrated analysis environment for genetic marker analysis. Bioinformatics Research Center, North Carolina State University, Raleigh.

Mace ES, Buhariwalla HK, Crouch JH (2003). A high-throughput DNA extraction protocol for tropical molecular breeding programs. Plant Mol. Biol. Rep. 21:459a-459h.

Mutegi E, Sagnard F, Semagn K, Deu M, Muraya M, Kanyenji B, de Villiers S, Kiambi D, Herselman L, Labuschagne M (2010). Genetic structure and relationships within and between cultivated and wild sorghum (*Sorghum bicolor* (L.) Moench) in Kenya as revealed by microsatellite markers. Theor. Appl. Genet. 122:989-1004.

Muui CW, Muasya RM, Kirubi DT (2013). Participatory Identification and Evaluation of Sorghum (*Sorghum bicolor* (L.) Moench) Landraces from Lower Eastern Kenya. Int. Res. J. Agric. Sci. 3(8):283-290.

Neal D (2004). Introduction to population biology. Cambridge University Press Cambridge, New York.

Nkongolo KK, Nsapato L (2003). Genetic diversity in *Sorghum bicolor* (L.) Moench accessions from different ecogeographical regions in Malawi assessed with RAPDs. Genet. Res. Crop Evol. 50:149-156.

Ochieng LA, Mathenge PW, Muasya RM (2011). A survey of on-farm seed production practices of sorghum (*Sorghum bicolor* L. Moench) in Bomet district of Kenya, Africa. J. Food Agric. Nutr. Dev. 11(5): 5232-5253.

Perrier X, Flori A, Bonnot F (2003). Methods for data analysis. In: Hamon P, Seguin M, Perrier X, Glazmann JC. (Eds). Genetic diversity of cultivated tropical plants. Science Publishers, Inc and Cirad, Montpellier. pp.31-63.

Perrier X, Jacquemoud-Collet JP (2006). DARwin software.

Saitou N, Nei M (1987). The Neighbor-Joining method: a new method for reconstructing phylogenetic trees. Mol. Biol. Evol. 4:406-425.

Setimela PS, Monyo E, Bänziger M (2004). Successful Community-Based Seed Production Strategies. CIMMYT, Mexico.

Sharma R, Deshpande SP, Senthilvel S, Rao VP, Rajaram V, Hash CT, Thakura RP (2010). SSR allelic diversity in relation to morphological traits and resistance to grain mould in sorghum. Crop Pasture Sci. 61:230-240.

Smith JSC, Kresovich S, Hopkins MS, Mitchell SE, Dean RE, Woodman WL, Lee M, Porter K (2000). Genetic diversity among elite sorghum inbred lines assessed with simple sequence repeats. Crop J. Sci. 40:226-232.

Subudhi PK, Nguyen H, Gilbert ML, Rosenow DT (2002). Sorghum improvement: past achievements and future prospects. In: Kang MS. (Ed.), Crop improvement: Challenges in the twenty first century. The Haworth Press, Binghamtom, N. Y. pp.109-159.

Tesso T, Kapran I, Grenier C, Snow A, Sweeney P, Pedersen J, Marx D, Bothma G, Ejeta G (2008). The potential for crop-to-wild gene flow in sorghum in Ethiopia and Niger: A geographic survey. Crop Sci. 48:1425-1431.

Timu AG, Mulwa MR, Okello J, Kamau M (2012). The role of varietal attributes on adoption of improved seed varieties. The case of sorghum in Kenya. Tegemeo institute of agricultural policy development, Nairobi,Kenya.

Tulole LB, Gwanama C, Mgonja M, Chisi M, Folkertsma R, Mutegi R (2009). Genetic variability characterization of Tanzania sorghum landraces based on simple sequence repeats (SSRs) molecular and morphological markers. Afr. J. Crop Sci. 17:71-86.

USAID (2010). State of food value chain analysis. Country report, Kenya.

academicJournals

Vol. 15(8), pp. 272-277, 24 February, 2016
DOI: 10.5897/AJB2015.14662
Article Number: D4EC58C57336
ISSN 1684-5315

http://www.academicjournals.org/AJB

African Journal of Biotechnology

Full Length Research Paper

Effect of LED light quality on *in vitro* shoot proliferation and growth of vanilla (*Vanilla planifolia* Andrews)

Jericó Jabín Bello-Bello[1], Eduardo Martínez-Estrada[1], José Humberto Caamal-Velázquez[2] and Victorino Morales-Ramos[1]*

[1]Campus Córdoba, Colegio de Postgraduados, km 348 Carretera Federal Córdoba-Veracruz, Congregación Manuel León, Amatlán de los Reyes, Veracruz. CP 94946, México.
[2]Campus Campeche, Colegio de Postgraduados, km 17.5 Carretera Federal Haltunchen-Edzna, Sihochac, Champotón Campeche, CP 24450, México.

Received 22 April, 2015; Accepted 22 October, 2015

As an alternative to conventional lighting systems, light emitting diode (LED) has been demonstrated to be an artificial flexible lighting source for commercial micropropagation. The objective of this study was to determine the effects of different LED light quality on *in vitro* shoot proliferation and growth of *Vanilla planifolia*. To evaluate shoot proliferation, axillary bud cuttings (3 to 5 mm in diameter) of *V. planifolia* were used as explants and cultivated on Murashige and Skoog basal medium supplemented with 9.55 µM of 6-benzylaminopurine. To evaluate *in vitro* growth, unrooted shoots (2 cm in length) were used as explants cultivated on Murashige and Skoog basal medium without plant growth regulators. All explants were exposed to a 16 h photoperiod for 60 days under five different lights: fluorescent lamp, white LED, blue LED, red LED and blue plus red LED mixtures (Blue + Red = 1:1). The results indicated a clear increase in the number of shoots per explant under Fluorescent Lamp, White LED and Blue+Red LED light; these treatments produced more than 10 shoots. Shoot length was more than 3 cm in cultures under Blue, Red and Blue+Red (1:1) LEDs, and less than 3 cm in Fluorescent Lamp and White LEDs. Our results also showed that fresh weight, dry weight and dry matter were greatest in shoots under Blue+Red LED light. For shoot growth, plant height, number of leaves, number and length of roots, fresh weight, dry weight, dry matter and chlorophyll content were greater under Fluorescent Lamp and White LED. In conclusion, White or Blue+Red LED light may be used as an alternative light source for shoot proliferation, while White LED may be used for growth *in vitro*. These results demonstrate the effectiveness of light qualities using LEDs for micropropagation of *V. planifolia*.

Key words: Light quality, micropropagation, orchid, chlorophyll.

INTRODUCTION

In commercial micropropagation laboratories, light source is one of the most important factors controlling plant development. Light quality (spectral quality), quantity (photon flux) and photoperiod have a profound influence

*Corresponding author. E-mail: vicmor@colpos.mx.

on the morphogenesis and growth of plant cell, tissue and organ cultures (Reuveni and Evenor, 2007). Fluorescent lamps (FLs) are generally used to increase photosynthetic photon flux (PPF) level for *in vitro* culture. However, FLs contains unnecessary wavelengths (350 to 750 nm) that are of low quality for promoting growth and morphogenesis (Gupta and Jatothu, 2013). Recently, the use of light-emitting diodes (LEDs) as a radiation source for plants has attracted considerable interest for commercial micropropagation. The most attractive features of LEDs are their small mass, volume, wavelength specificity, long life, minimum heating and photon output that is linear with electrical input current (Brown et al., 1995; Massa et al., 2008; Gupta and Jatothu, 2013). The flexibility of matching wavelengths of LEDs to plant photoreceptors may provide more optimal production, influencing plant morphology and metabolism (Kim et al., 2004; Massa et al., 2008; Morrow, 2008). Although, previous reports have confirmed physiological and morphological effects of LED light quality on morphogenesis and growth of several plantlets *in vitro* (Hahn et al., 2000; Jao et al., 2005; Shin et al., 2008; Lin et al., 2011; Li et al., 2012; 2013), these study results showed that LED light is more suitable for plant morphogenesis and growth than FL (fluorescent lamp). However, the responses vary according to plant species.

Vanilla (*Vanilla planifolia*) is an economically important orchid that has been cultivated for its flavoring pods (Tan et al., 2011). In Mexico, *V. planifolia* is a species subject to special protection and its production is still incipient. It is propagated through clonal propagation techniques using stem cuttings. This conventional propagation method is slow, laborious, and economically unviable (Kalimuthu et al., 2006; Mengesha et al., 2012). Therefore, there is a need to search for an alternative way to mass produce this plant species. Recently, several studies have reported on the micropropagation of *V. planifolia* (Tan et al., 2011; 2013; Mengesha et al., 2012; Zuraida et al., 2013; De Oliveira et al., 2013). Prior to the present study, the effect of FL on *in vitro* propagation of vanilla has been reported but no research had been reported using LEDs. The objective of this study was to determine the effects of different LED light quality on *in vitro* shoot proliferation and growth of *V. planifoli*a.

MATERIALS AND METHODS

Plant materials and culture media

For *in vitro* establishment and disinfection of axillary buds, the method described by Lee-Espinosa et al. (2008) was followed. Axillary buds of vanilla (*V. planifolia* Mansa morphotype), between 3 to 5 mm in diameter, were collected in Papantla, Veracruz, Mexico. To evaluate the effect of LEDs on *in vitro* shoot proliferation, twenty explants were used per treatment, distributed at a rate of three explants per culture vessel. The explants were placed in Magenta boxes (Sigma Chemical Company, MO, USA) containing 40 mL of MS (Murashige and Skoog, 1962) semisolid medium supplemented with 9.55 µM BAP (6-benzylaminopurine). The pH was adjusted to 5.8 before adding 0.22% (w/v) Gelrite® (Sigma Chemical Company, MO, USA) and autoclaving (20 min at 121°C). Number of shoots per explant, shoot length, fresh weight and dry weight were recorded after 60 days of culture. Moreover, dry matter content was calculated using dry weight/fresh weight x 100. To evaluate the effect of LED on *in vitro* grown plantlets, twenty unrooted shoots previously established *in vitro* that were 2 cm in length were used as explants per treatment. Shoots were distributed at a rate of five explants per culture vessel. The explants were placed in 1 L vessels containing 50 mL of hormone-free MS semisolid medium. Plant height, number of leaves, number and length of roots, fresh weight, dry weight, dry matter and chlorophyll content were evaluated after 60 days of culture.

Light treatments and culture conditions

The cultures of *in vitro* shoots and plantlets were illuminated using 100% fluorescent light (peak wavelengths from 545 to 610 nm), 100% white LED (460 and 560 nm), 100% red LED (660 nm), 100% blue LED (460 nm) and 50% red plus 50% blue LED (660 and 460 nm, respectively). The LED light source was aligned in a rectangle (40 cm × 120 cm). The LED system consisted of LED sticks (Model 5050-1M), a main controller (L63 × W35 × H22 mm) and a DC-12V adapter power supply (Shendk Model SDK-0605). All the cultures were incubated in a controlled environment at 24 ± 2°C, 50 ± 5% relative humidity and a 16 h photoperiod. In all treatments, the photosynthetic photon flux density (PPFD) was maintained to 25 µmol m^{-2} s^{-1}. PPFD was measured using a FieldScout Quantum Light Meter® (Field Scout Spectrum Technologies, Inc., IL, USA).

Chlorophyll content

Chlorophyll content in the third leaf of the plantlets, counting from the top downwards, was measured using a Field Scout CM 1000 Chlorophyll Meter® (FieldScout Spectrum Technologies, Inc., IL, USA).

Acclimatization

After 60 days of culture under *in vitro* conditions, rooted plantlets from different light treatments that were 5 to 10 cm high were transplanted into 50 × 30 × 7 cm trays with 1:1 mixture of peat-moss (Premier, Rivière-du-Loup, Canada) and Agrolita® (Agrolita, Tlalnepantla de Baz, Mexico) as substrate and then transferred to a greenhouse for acclimatization. Plantlets were watered three times a week and foliar fertilizer (Nitrofoska® foliar PS, COMPO, Zapopan, Mexico) was applied weekly. Once the plants had grown to a height greater than 20 cm, they were transplanted to their natural habitats (shady forest floor).

Experimental design and data analysis

A completely randomized design was used for all experiments and the experiments were replicated three times. Data were subjected to a one-way analysis of variance (ANOVA) using the SPSS program (Version 11.5 for Windows Inc., Chicago, IL, USA). Means were compared using Tukey's test ($p \leq 0.05$).

Table 1. Effect of light quality on shoot proliferation of Vanilla (*V. planifolia*) after 60 days of *in vitro* culture.

Light treatment	No. of shoots/ explants	Shoot length (cm)	Fresh weight (mg)	Dry weight (mg)	Dry matter (%)
FL	10.2±0.52^{a}	2.6±0.14^{bc}	2418.7±135.59^{b}	221.8±13.15^{b}	9.1±0.10^{bc}
W	10.3±0.49^{a}	2.2±0.14^{c}	2236.2±189.99^{b}	211.2±19.24^{b}	9.4±0.10^{b}
B	5.6±0.37^{b}	3.5±0.11^{a}	1431.2±47.18^{c}	125.6±6.77^{c}	8.7±0.20^{c}
R	5.2±0.31^{b}	3.1±0.19^{ab}	1531.2±71.30^{c}	134.3±7.52^{c}	8.7±0.13^{c}
B+R (1:1)	10.8±0.59^{a}	3.4±0.09^{a}	2764.2±165.72^{a}	275.8±18.27^{a}	10.2±0.08^{a}

Abbreviations: FL = Fluorescent Lamp; W = White LED; B = Blue LED; R = Red LED and B+R = Blue and Red LEDs. Values followed by different letters denote statistically significant differences (Tukey, $p \leq 0.05$). Data represent mean ± SE.

RESULTS AND DISCUSSION

Effect of light quality on shoot proliferation

The shoot proliferation and growth of *V. planifolia* were significantly affected by different light treatments *in vitro*. The results indicated a significant increase in the number of shoots per explant under FL, W LED and B+R LED (1:1) light; these treatments produced more than 10 shoots. Explants under B and R LED conditions produced less than six shoots (Table 1). Shoot length was more than 3 cm in cultures under B, R and B+R (1:1) LEDs, and less than 3 cm in FL and W LEDs. Our results also showed that fresh weight, dry weight and dry matter were greatest in shoots under B+R (1:1) LED light, followed by FL, W, B and R LEDs (Figure 1).

Effect of light quality on the growth of plantlets

Different light qualities had variable effects on the growth of *V. planifolia* (Figure 2). Plant height, number of leaves, number and length of roots, fresh weight, dry weight, dry matter and chlorophyll content were greater under FL and W LED than under B LED, R LED and B+R LED (1:1) (Table 2). The growth variables were not significantly affected by FL and W LED light treatments. These treatments were beneficial for plantlet growth. Other studies appear to confirm that R LED retards development of plants *in* vitro (Lin et al., 2011; Edesi et al., 2014; Waman et al., 2015). Similarly, our results confirm that R LED affects the growth of *V. planifolia* plantlets *in vitro*. The present study showed that W LED light may be used as an alternative to FL for *in vitro* growth of *V. planifolia* in culture systems. After 60 days of *in vitro* culture, plantlets in all treatments were transferred to the greenhouse for acclimatization. Plant survival was 95% after 30 d growth under greenhouse conditions. The acclimatized *in vitro* plantlets were vigorous in aspect (Figure 3a) and developed normally when transplanted to soil (Figure 3b). Effect of LEDs on the micropropagation of orchid species has been studied. Fukai et al. (1997) reported in *Calanthe Satsuma* that the most vigorous protocorm development was obtained in the dark rather than by the irradiation of R, B, mixed light of R+B, and FL. In *Oncidium*, R LEDs significantly promoted the growth of PLBs, while B LEDs had the opposite effect (Xu et al., 2009). In *Dendrobium officinale,* R+B (1:2) LEDs are an effective light source for shoot growth (Lin et al., 2011). Godo et al. (2011) reported rhizoid formation in orange LED (590 nm) and R LED (625 nm) light in *Bletilla ochracea*. Our results do not coincide with those of Xu et al. (2009), Lin et al. (2011) and Godo et al. (2011). According to Kim et al. (2004), stem elongation could be promoted or inhibited by different synergistic interactions between blue or red light receptors and phytochrome depending on the species. Light quality also plays an important role in photosynthesis, influencing the way in which light is absorbed by chlorophyll (Tripathy and Brown, 1995; Topchiy et al., 2005). In our results, chlorophyll concentrations were greater in plantlets grown under FL and W LED light treatments, which is inconsistent with the idea that B light plays an important role in the synthesis of chlorophyll (Kurilcik et al., 2008; Li et al., 2010; 2012). According to Li et al. (2013), the chlorophyll content of *in vitro* plantlets grown under different light qualities may be correlated with the plant species or cultivar. In its natural habitat, *V. planifolia* grows on a shady forest floor, while other members of the Orquidacea family grow on open grassy or stony slopes.

Our results clearly demonstrate that the spectral quality of light has an influence on the morphogenesis and growth responses of *V. planifolia.* According to Chung et al. (2010), light induces plant morphogenesis. Light is a signal that is received by a photoreceptor that then regulates the differentiation and growth of plants (Wang et al., 2001; Muleo and Morini, 2006). The light source generally used for *in vitro* culture is fluorescent lamps. However, LEDs have a long life and changing the light source is therefore less frequent, resulting in reduced labor costs. Also, LEDs generate very little heat, thereby minimizing the need for an extensive cooling system in plant growth facilities. This is the first report on measuring the effects of LED light on *V. planifolia in vitro*; LED light is a novel illumination system for micropropagation of this important species.

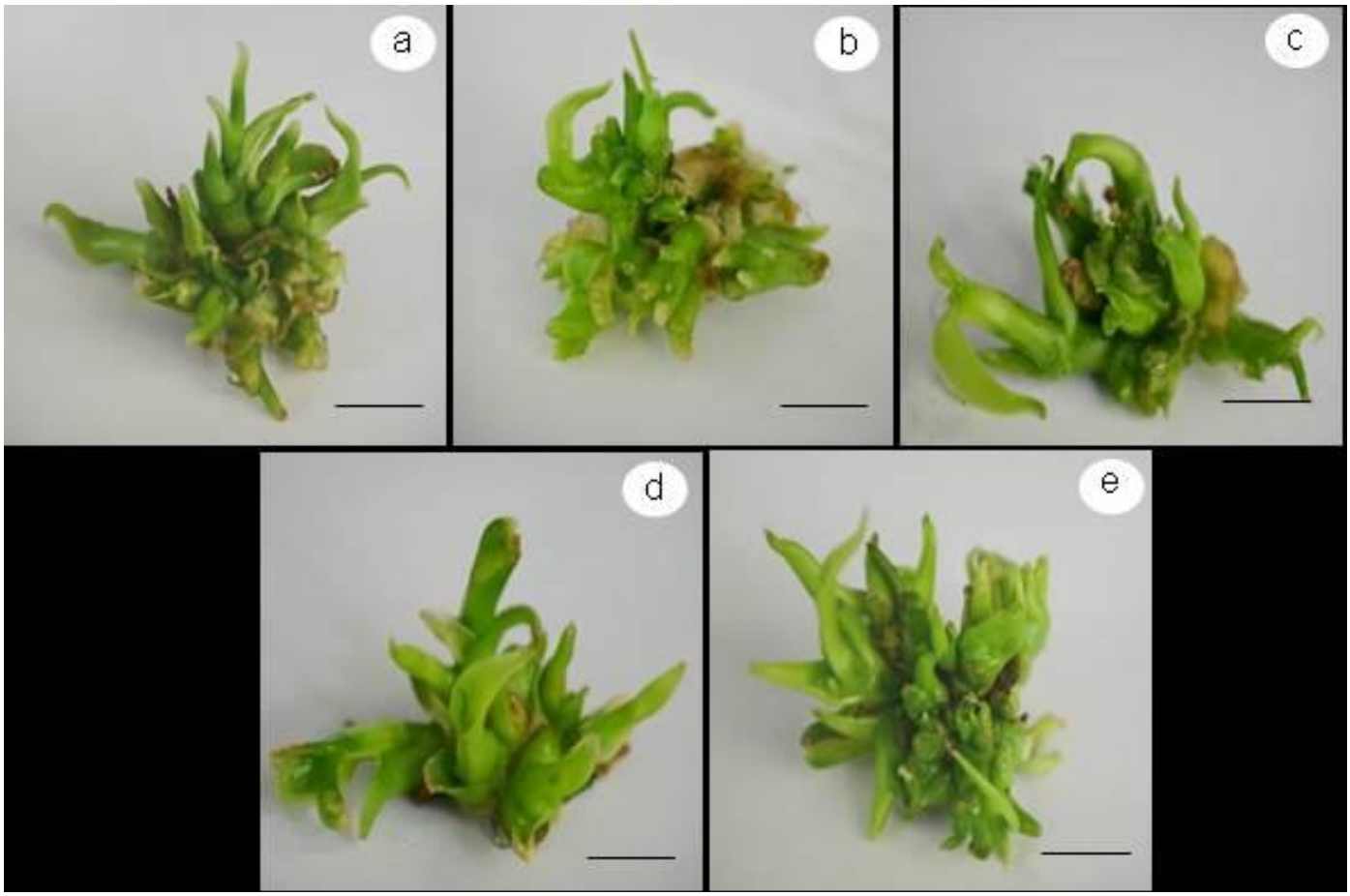

Figure 1. Effect of light quality on shoot proliferation of Vanilla (*V. planifolia*) after 60 days of *in vitro* culture. a) Fluorescent Lamp, b) White, c) Blue, d) Red and e) Blue+Red LEDs (*bar* 2.0 cm).

Figure 2. Effect of light quality on *in vitro* growth of plantlets of Vanilla (*V. planifolia*) after 60 days of *in vitro* culture. **a)** Fluorescent Lamp, **b)** White, **c)** Blue, **d)** Red and **e)** Blue+Red LEDs (*bar* = 2.0 cm).

In conclusion, the use of a LED light source was good at promoting the shoot proliferation and growth of vanilla plantlets. W or B+R LED (1:1) light may be used as an alternative light source for shoot proliferation, while W LED may be used for *in vitro* growth. These results demonstrated the effectiveness of a radiation system using

Table 2. Effect of light quality on the growth of plantlets of Vanilla (*V. planifolia*) after 60 days of *in vitro* culture.

Light treatment	Plant height(cm)	Number of Leaves	Number of roots	Root length(cm)	Fresh weight (mg)	Dry weight (mg)	Dry matter (%)	Chlorophyll content
FL	5.7±0.40^{a}	3.6±0.18^{a}	2.5±0.18^{a}	4.8±0.18^{a}	1197.5±54.30^{a}	74.2±5.65^{a}	6.6±0.50^{a}	107.6±0.37^{a}
W	5.9±0.27^{a}	3.5±0.18^{a}	2.6±0.18^{a}	4.5±0.23^{a}	1016.2±65.49^{ab}	70.5±4.96^{a}	6.2±0.44^{a}	108.7±0.64a
B	4.4±0.15^{b}	2.5±0.18^{b}	1.6±0.18^{bc}	3.5±0.13^{b}	868.7±30.43^{b}	50.1±1.85^{b}	4.4±0.16^{b}	90.0±1.18b
R	3.2±0.16^{c}	2.5±0.18^{b}	1.8±0.18^{b}	2.1±0.19^{c}	438.7±35.82^{cd}	32±2.09^{c}	2.8±0.18^{c}	82.7±0.70c
B+R (1:1)	4.1±0.23^{bc}	2.5±0.20^{b}	1.4±0.20^{c}	3.1±0.21^{b}	681.4±15.02^{c}	44.1±2.05^{bc}	3.9±0.18^{bc}	92.4±0.89b

Abbreviations: FL = Fluorescent Lamp; W = White LED; B = Blue LED; R = Red LED and B+R = Blue and Red LEDs. Values followed by different letters denote statistically significant differences (Tukey, $p \leq 0.05$). Data represent mean ± SE.

Figure 3. Plantlets of *V. planifolia* transferred from *in vitro* condition. **a)** plantlets in the process of acclimatization in the greenhouse after 30 days and **b)** plantlets growing in shady forest floor (natural habitat) after 60 days.

using LEDs for micropropagation of *V. planifolia* and subsequent acclimatization in *ex vitro* conditions.

Conflict of interests

The author(s) did not declare any conflict of interest.

ACKNOWLEDGEMENTS

The authors wish to thank the Colegio de Postgraduados for funding this research through Priority Research Line 5, Microbial, Plant and Animal Biotechnology.

REFERENCES

Brown CS, Schuerger AC, Sager JC (1995). Growth and photomorphogenesis of pepper plants grown under red light-emitting diodes supplemented with blue or far-red illumination. J. Am. Soc. Hortic. Sci. 120(5):808-813.

Chung JP, Huang CY, Dai TE (2010). Spectral effects on embryogenesis and plantlet growth of *Oncidium* 'Gower Ramsey'. Sci. Hortic. 124(4):511-516.

De Oliveira SOD, Sayd RM, Balzon TA, Scherwinski-Pereira JE (2013). A new procedure for *in vitro* propagation of vanilla (*Vanilla planifolia*) using a double-phase culture system. Sci. Hortic. 161:204-209.

Edesi J, Kotkas K, Pirttilä AM, Häggman H (2014). Does light spectral quality affect survival and regeneration of potato (*Solanum tuberosum* L.) shoot tips after cryopreservation?. Plant Cell Tissue Organ Cult. 119(3):599-607.

Fukai S, Fujikawa K, Okamoto K, Hasegawa A, Goi M (1997). Effects of red and blue light on germination and protocorm growth of *Calanthe Satsuma*. Lindleyana 12:169-171.

Godo T, Fujiwara K, Guan K, Miyoshi K (2011). Effect of wavelength of LED-light on *in vitro* asymbiotic germination and seedling growth of *Bletilla ochraceaschltr* (Orchidaceae). Plant Biotechnol. 28(4):397-400.

Gupta SD, Jatothu B (2013). Fundamentals and applications of light-emitting diodes (LEDs) in *in vitro* plant growth and morphogenesis. Plant Biotechnol. Rep. 7(3):211-220.

Hahn EJ, Kozai T, Paek KY (2000). Blue and red light-emitting diodes with or without sucrose and ventilation affects *in vitro* growth of

Rehmannia glutinose plant lets. J. Plant Biol. 43(4):247-250.
Jao RC, Lai CC, Fang W, Chang SF (2005). Effects of red light on the growth of *Zantedeschia* plantlets *in vitro* and tuber formation using light-emitting diodes. HortScience 40(2):436-438.
Kalimuthu K, Senthilkumar R, Murugalatha N (2006). Regeneration and mass multiplication of *Vanilla planifolia* Andr. a tropical orchid. Curr. Sci. 91:1401-1403.
Kim SJ, Hahn EJ, Heo JW, Paek KY (2004). Effects of LEDs on net photosynthetic rate, growth and leaf stomata of *Chrysanthemum* plantlets *in vitro*. Sci. Hortic. 101(1):143-151.
Kurilcik A, Miklusyte-Canova R, Dapkuniene S, Zilinskaite S, Kurilcik G, Tamulaitis G, Duchovskis P, Zukauskas A (2008). *In vitro* culture of *chrysanthemum* plantlets using light-emitting diodes. Cent. Eur. J. Biol. 3(2):161–167.
Lee-Espinosa H, Murguía-González J, García-Rosas B, Córdova-Contreras A, Laguna-Cerda A, Mijangos-Cortés J, Barahona-Pérez L, Iglesias-Andreu L, Santa na-Buzzy N (2008). *In vitro* clonal propagation of vanilla (*Vanilla planifolia* 'Andrews'). HortScience 43(2):454-458.
Li HM, Tang C, Xu Z (2013). The effects of different light qualities on rapeseed (*Brassi ca napus* L.) plantlet growth and morphogenesis *in vitro*. Sci. Hortic. 150:117-124.
Li HM, Tang CM, Xu ZG, Liu XY, Han XL (2012). Effects of different light sources on the growth of non-heading Chinese cabbage (*Brassica campestris* L.). J. Agric. Sci. 4(4):262-273.
Li HM, Xu ZG, Tang CM (2010). Effect of light-emitting diodes on growth and morphogenesis of upland cotton (*Gossypium hirsutum* L.) plantlets *in vitro*. Plant Cell Tissue Organ Cult. 103(2):155-163.
Lin Y, Li J, Li B, He T, Chun Z (2011). Effects of light quality on growth and development of protocorm-like bodies of *Dendrobium officinale in vitro*. Plant Cell Tissue Organ Cult. 105(3):329-335.
Massa GD, Kim HH, Wheeler RM, Mitchell CA (2008). Plant productivity in response to LED lighting. HortScience 43(7):1951-1956.
Mengesha A, Ayenew B, Gebremariam E, Tadesse T (2012). Micropropagation of *Vanilla planifolia* using Enset (Ensete ventricosum (Welw, cheesman)) starch as a gelling agent. Curr. Res. J. Biol. Sci. 4(4):519-525.
Morrow RC (2008). LED lighting in horticulture. HortScience 43(7):1947-1950.
Muleo R, Morini S (2006). Light quality regulates shoot cluster growth and development of MM106 apple genotype in *in vitro* culture. Sci. Hortic. 108(4):364-370.
Murashige T, Skoog F (1962). A revised medium for rapid growth and bioassays with tobacco tissue culture. Physiol. Plant. 15(3):473-497.
Reuveni M, Evenor D (2007). On the effect of light on shoot regeneration in petunia. Plant Cell Tissue Organ Cult. 89(1):49-54.
Shin SK, Murthy NH, Heo WJ, Hahn JE, Paek YK (2008). The effect of light quality on the growth and development of *in vitro* cultured *Doritaenopsis* plants. Acta Physiol. Plant. 30(3):339-343.
Tan BC, Chin CF, Alderson P (2011). An improved plant regeneration of *Vanilla planifolia* Andrews. Plant Tissue Cult. Biotechnol. 21(1):27-33.
Tan BC, Chin CF, Alderson P (2013). Effects of sodium nitroprusside on shoot multiplication and regeneration of *Vanilla planifolia* Andrews. *In Vitro* Cell Dev. Biol. Plant. 49(5):626-630.
Topchiy NM, Sytnik SK, Syvash OO, Zolotareva OK (2005). The effect of additional red irradiation on the photosynthetic apparatus of *Pisum sativum*. Photosynthetica 43(3):451-456.
Tripathy BC, Brown CS (1995). Root-shoot interaction in greening of wheat seedlings grown under red light. Plant Physiol.107(2):407-511.
Waman AA, Bohra P, Sathyanarayana BN, Umesha K, Gowda B, Ashok TH (2015). *In vitro* shoot multiplication and root induction in Silk banana variety Nanjana gud Rasabale as influenced by monochromatic light spectra. Proc. Natl. Acad. Sci. India Sect. B Biol. Sci. 1-8.
Wang YC, Zhang HX, Zhao B, Yuan XF (2001). Improved growth of *Artemisia annua* L. hairy roots and artemisinin production under red light conditions. Biotechnol. Lett. 23(23):1971-1973.
Xu ZG, Cui J, Di XR (2009). Effects of different spectral energy distribution on tissue culture of *Oncidium in vitro*. J. Beijing For. Univ. 31(4):45-50.
Zuraida A, Izzati KFL, Nazreena O, Zaliha WW, Radziah CC, Zamri Z, Sreeramanan S (2013). A simple and efficient protocol for the mass propagation of *Vanilla planifolia*. Am. J. Plant Sci. 4(9):1685-1692.

academicJournals

Vol. 15(8), pp. 278-283, 24 February, 2016
DOI: 10.5897/AJB2015.14822
Article Number: 4281D5B57342
ISSN 1684-5315

http://www.academicjournals.org/AJB

African Journal of Biotechnology

Full Length Research Paper

Detection of metallo-beta-lactamase producing *Pseudomonas aeruginosa* using a modified IMP-lysate assay

Olfa Sioud[1]*, Mariem Nasri[1], Mahjoub Aouni[1] and Maha Mastouri[1,2]

[1]Laboratoire des maladies transmissibles et des substances biologiquement actives Faculté de Pharmacie-5000-Monastir-Tunisie.
[2]Laboratoire de Microbiologie C H U Fattouma Bouguiba -5000- Monastir-Tunisie.

Received 27 June, 2015; Accepted 10 December, 2015

Since the increasing prevalence of carbapenem-resistant *Pseudomonas aeruginosa* spp., accurate detection of metallo-β-lactamase (MBL) such as bla_{VIM} type enzyme producing isolates became very important. However, phenotypic MBL detection methods previously reported are not highly sensitive or highly specific. This study aimed to evaluate the performance of a modified IMP-lysate test, the double-disk-synergy-test (DDST) and the combined-disk-test (CDT) for detecting MBL bla_{VIM} gene in *P. aeruginosa.* The reference technique was PCR molecular test. The study used 12 bla_{VIM2} producer isolates, 13 MBL-negative controls which included 4 imipenem-susceptible strains and 9 imipenem-resistant strains harbouring bla_{SHV-2a} genes collected from two Tunisian hospitals and *P. aeruginosa* ATCC27853 and *P. aeruginosa* COL-1 as negative and positive controls respectively. CDT showed 100% of sensitivity. The highest level of specificity was shown by IMP-lysate test (76.92%). To evaluate efficiencies of methods, the study noted that the highest Youden Index (YI) was shown by IMP-lysate method (0.7), followed by DDST (0.6) than CDT (0.2). Since MBL-Etest and PCR were expensive and not adaptable for extension use in clinical microbiology laboratories, a modified IMP-lysate MBL hydrolytic activity can be chosen by laboratories with limited resources as an inexpensive, simple, and accurate test to detect . *P. aeruginosa* producing bla_{VIM} enzyme.

Key words: Metallo-beta-lactamase, VIM, phenotypic detection, *pseudomonas aeruginosa*.

INTRODUCTION

The infections caused by multidrug-resistant *Pseudomonas aeruginosa* strains are becoming increasingly prevalent and now constitute a serious threat to public health worldwide (Oliver et al., 2015; Kaye and Pogue, 2015). Due to their stability against most β-lactamases, carbapenems such as imipenem have been

*Corresponding author. E-mail: olfasioud@yahoo.fr. Tel: +216 21 557 394. Fax: +216 73 460 678.

the drug of choice for treatment of infections caused by multidrug resistant *P. aeruginosa*. Nevertheless, the first isolate of *P. aeruginosa* with transferable imipenem resistance due to metallo-β-lactamase (MBL) production was reported in Japan in 1991 (Watanabe et al., 1991). Since then, it has been described from various parts of the world (Aubron et al., 2005; Mazzariol et al., 2011; Viedma et al., 2012;Sardelic et al., 2012) including Africa (Pitout et al., 2008; Jacobson et al., 2012; Touati et al., 2013) and Tunisia (Mansour et al., 2009; Hammami et al., 2010; Hammami et al., 2011; Ktari et al., 2011).

Treatment of infectious diseases caused by the carbapenem-resistant *P. aeruginosa* is becoming more challenging with each passing year. It have been associated with increased mortality and costs due to prolonged hospitalization and prolonged treatment with antibiotics (Liu et al., 2015). MBL producing isolates have an ability to spread and to hydrolyse virtually all β-lactam agents except monobactam (Maltezou, 2009). Detection of this resistance-phenotype by routine laboratories is essential to initiate adequate therapy and to implement proper infection control practices. However, no standardized phenotypic method is available, and previously reported phenotypic combined disk tests, are not highly sensitive or highly specific for the detection of MBL in *P. aeruginosa* (Peter et al., 2014). The most used phenotypic screening methods in clinical microbiology laboratories are double-disk-synergy-test (DDST), combined-disk-test (CDT) (Lee et al., 2001; Yong et al., 2002; Lee et al., 2003) and the current most widely accepted technique; the MBL E-test (AB Biodisk, Solna, Sweeden) (Tan et al., 2008). All of these phenotypic tests are based upon the ability of chelating agents, EDTA and thiol-based compounds, to inhibit the MBL activity (Andrade et al., 2007).

A big concern with using these methods is the direct bactericidal effect of EDTA on the test strain (Conejo et al., 2003; Tan et al., 2008) . To circumvent this problem, Tan et al. (2008) proposed an IMP-lysate assay that provides a simple, inexpensive and reproducible functional screen for MBL-producing *P. aeruginosa* (Tan et al., 2008). The IMP-lysate assay allows EDTA to interact with the carbapenamase *in vitro*, effectively reducing the concentration of EDTA that interacts with the growth of the indicator strain. However, the IMP-lysate test requires specific equipment, such as microcon concentration device (Millipore Bedford, MA) to concentrate the lysate which is not available in most laboratories. So, the study propose a modification in the technique (the study removed the lysate-concentration step with the microcon device, and the study incubated lysate solution with imipenem and EDTA before depositing it on the plate.) without reducing confidence of the assay. The aim of this study was to compare the performance of this modified IMP-lysate test, the DDST and the CDT for detecting MBL bla_{VIM} gene in *P. aeruginosa* by referring to the molecular test; the PCR.

MATERIALS AND METHODS

Clinical isolates

The *P. aeruginosa* strains used in this study were isolated from clinical specimens collected from separate patients hospitalized in different medical and surgical wards at Fattouma Bourguiba Hospital in Monastir, Tunisia and Tahar Sfar Hospital in Mahdia, Tunisia on variable periods of times (Table 1). Identification of the isolates to the species level was performed by Api 20 NE (Biomerieux, France) and by using matrix-assisted laser desorption/ionisation time-of-flight mass spectrometry (MALDI-TOF MS) (AutoflexTM; Bruker Daltonics, Bremen, Germany) with the Flex control software (Bruker Daltonics) (Seng et al., 2009). A total of 12 bla_{VIM2} producer isolates were screened. MBL-negative controls included 4 imipenem-susceptible strains and 9 imipenem-resistant strains harbouring bla_{SHV-2a} genes. Bla_{VIM2} and bla_{SHV-2a} genes were detected by PCR. Susceptibilities of stains of antimicrobials were performed by the disk diffusion method in Mueller Hinton agar (Bio-Rad, Marnes-la-Coquette, France) according to the guidelines of the Clinical and Laboratory Standards Institute (CLSI, 2014). Two control strains were used; *P. aeruginosa* ATCC27853 as negative control (NC) and *P. aeruginosa* COL-1 carrying the bla VIM2 gene as positive control.

Combined disk tests (CDT) (method A)

Test organisms were inoculated onto plates of Mueller Hinton according to the guidelines of the CLSI. Two IMP (10 µg) disks (Bio-Rad, Marnes-la-Coquette, France) were placed in an agar plate, and 10 µl of a 0.5 M EDTA solution (pH8) was added to one of the IMP disks. After incubation overnight at 37°C, the inhibition zones of the IMP disks with and without EDTA were compared. A ≥ 7 mm increase in the zone diameter for IMP in the presence of EDTA was interpreted as a positive test result.

Double disk synergy tests (DDST) (method B)

Tests organisms were inoculated onto plates of Mueller-Hinton agar as described for the standard disk diffusion test (CLSI). An IMP (10 µg) disk was placed 20 mm (center to center) from a blank disk containing 5 µl of 0.5 M EDTA (pH 8). Enhancement of the zone of inhibition in the area between the two disks was considered positive for a MBL.

PCR amplification

DNA template preparation was performed as followed. The organisms were cultured on blood agar plate (90 mm diameter) and incubated for 24 h at 37°C. Half of the overnight culture was inoculated into 600 µl of distilled water and vortexed. The cells were lysed by heating them at 100°C for 10 min and cellular debris was removed by centrifugation at 13000 r/min for 10 min. The superntent was used as a source of template for amplification. Standard PCR analysis was used for detection of VIM MBL and SHV Extended-spectrum β-lactamases (ESBL) genes. The specific primers used were: VIM-F: 5'-TGGTCTACATGACCGCGTCT3-3', VIM-R: 5'CGACTGAGCGATTTGTGTG-3', SHV-F: 5'-TTTATGGCGTTACCTTTGACC-3'and SHV-R: 5'-ATTTGTCGCTTCTTTACTCGC-3' (Yagi et al., 2000). Total bacterial DNA was purified with QUIAGEN Kit. Cycling parameters of standard PCR were as follows: an initial denaturation step for 15 min at 95°C, 35 cycles of 1 min at 95°C, 50s at 55°C and 1min at 72°C and a final incubation step for 7 min at 72°C. Positive PCR products were sequenced using BigDye® terminator chemistry on

Table 1. Evalation of IMP-lysate, combined-disk and double-synergy tests for detection of VIM MBL-producing isolates of *P.aeruginosa*.

Isolates	Date of isolation	Site of location	Phenotypic screening			Molecular screening	
	Day/ Month/ Year		Method A	Method B	Method C	VIMPCR	SHV 2a PCR
Ps 27	11/13/2007	ICU	Positive	Negative	Positive	Positive	Positive
Ps 30	6/7/2008	ICU	Positive	Positive	Negative	Positive	Negative
Ps 44	10/18/2008	ICU	Positive	Positive	Positive	Positive	Negative
Ps 48	12/12/2008	S	Positive	Positive	Positive	Positive	Positive
Ps 62	10/16/2009	S	Positive	Positive	Positive	Positive	Positive
Ps 63	10/16/2009	ICU	Positive	Positive	Positive	Positive	Positive
Ps 64	10/17/2009	ICU	Positive	Positive	Positive	Positive	Positive
Ps 65	10/22/2009	NN	Positive	Positive	Positive	Positive	Positive
Ps 66	5/11/2011	ENT	Positive	Positive	Positive	Positive	Positive
Ps 67	5/15/2011	Or	Positive	Positive	Positive	Positive	Positive
Ps 69	8/13/2008	ICU	Positive	Positive	Positive	Positive	Positive
Ps 70	8/18/2008	ICU	Positive	Positive	Positive	Positive	Positive
Ps 22	7/30/2005	ICU	Negative	Negative	Positive	Negative	Positive
Ps 28	6/4/2008	U	Positive	Negative	Negative	Negative	Positive
Ps 35	8/25/2008	ICU	Negative	Negative	Negative	Negative	Positive
Ps 50	1/23/2009	PNE	Negative	Negative	Negative	Negative	Positive
Ps 6	12/3/2004	ICU	Positive	Positive	Negative	Negative	Positive
Ps 11	1/5/2005	ICU	Positive	Positive	Negative	Negative	Positive
Ps 17	7/4/2005	ID	Positive	Negative	Negative	Negative	Positive
Ps 20	7/23/2005	ICU	Positive	Negative	Negative	Negative	Positive
Ps21	7/24/2005	ICU	Positive	Negative	Positive	Negative	Positive
Ps24	3/28/2006	ICU	Positive	Negative	Negative	Negative	Positive
Ps29	6/7/2008	ICU	Positive	Positive	Negative	Negative	Positive
Ps31	6/17/2008	ICU	Positive	Negative	Negative	Negative	Positive
Ps38	9/6/2008	ICU	Positive	Positive	Positive	Negative	Positive
PsCOL1	-	-	Positive	Positive	Positive	Positive	Negative
PsATCC27853	-	-	Negative	Negative	Negative	Negative	Negative

Ps, strains from Monastir hospital; Ps, strains from Mahdia hospital; ENT, ear,nose and throat; ICU, intensive care unit; NN, neonatal; S, surgery; Or, orthopedics; ID, I nfectious disease; U, urology; PNE, pneumology; Method A, CDT; Method B, DDST; Method C, Imp-lysate test.

an automated ABI 3730 sequencer (PE Applied Biosystems, Foster City, CA).

MBL hydrolytic activity test (method C)

Test organisms were inoculated onto blood agar plate (90 mm diameter) and incubated overnight at 37°C. Half of plate was resuspended in 1.5 ml sodium phosphate buffer (pH 7). The cells were subsequently lysed by cycling between (-20°C) and room temperature (RT) and a vortex (30 s) for a total of five times. The lysed cells were separated from the other debris by centrifugation (10 min, 3.200xg, 4°C) and filtration through a 0.22 µm syringe filter (Minisart, Sartorius Stedim Biotech, Goettingen, German). About 1 ml of filtrate was recuperated each time. Instead of concentrating the filtrate through a microcon device as described by Tan et al. (2008), it was divided equally into two tubes, one of which contained 25 µl of 0.5 M EDTA at pH 8. The two samples were incubated with 10 µg imipenem per ml for 20 min at 37°C and then 15 µl from each tube was transferred into 8 mm blank disks (spaced by 6 cm) in Mueller Hinton agar plates with indicator isolate *Escherichia coli* ATCC 25922 spread on the surface. On the same plate the study tested *P. aeruginosa* ATCC27853 (harboring no resistance mechanism) as a negative control and a blank disk with 15 µl of 10 µg imipenem per milliliter solution. The diameter of inhibition zones were measured after overnight incubation at 37°C. The IMP-lysate MBL hydrolytic activity assay was confirmed by comparing the sizes of zone inhibitions for three disks; the lysate-IMP disk impregnated with lysates from *P. aeruginosa* strain and IMP, the lysate-IMP-EDTA disk with the same lysates incubated with IMP and EDTA and the third IMP disk with imipenem solution. Negative and positive controls must be tested each time. The inhibition zone from the disk (IMP) provided a reference for comparison; it was about 20 mm (data not shown). The diminution of inhibition zone around lysate-IMP disk, compared to the IMP disk, proved the hydrolysis of IMP by the lysate solution. The increase of the zone around the lysate-IMP-EDTA disk compared to the lysate-IMP disk proved that the enzyme hydrolysing IMP was inhibited by EDTA was therefore a MBL.

Statistical method

The Youden's Index (YI)

The YI is the difference between the true positive rate and the false

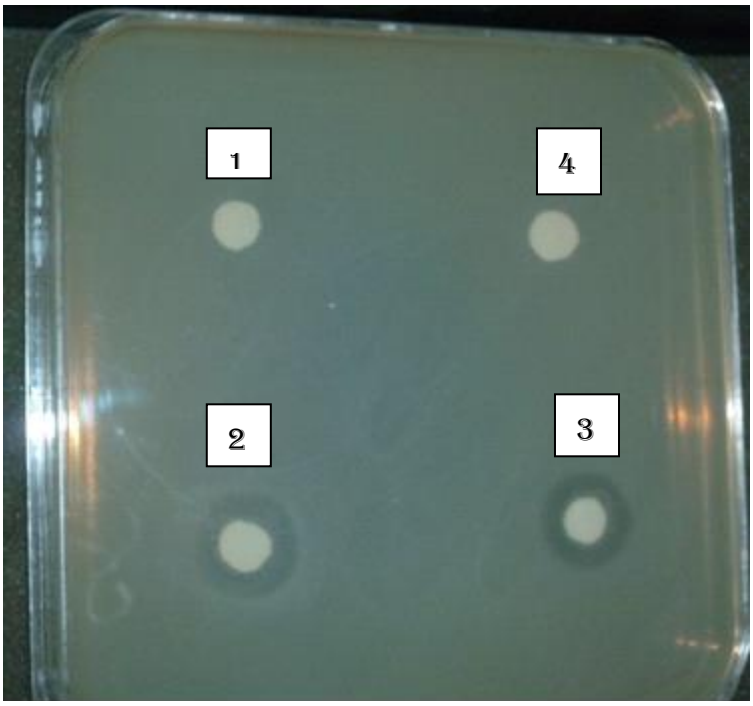

Figure 1. Results for IMP-lysate MBL hydrolytic activity test using disk 1 with lysates from *P.aeruginosa* COL-1 strain incubated with imipenem (IMP) at 10 µg per ml, disk 2 with the same lysates incubated with IMP and EDTA (0.5 M), disk 3 negative control with lysates from *P. aeruginosa* ATCC27853 incubated with IMP and disk 4 with EDTA (0.5) alone.

positive rate. It is a commonly used measure of overall diagnostic effectiveness. This index ranges between 0 and 1, with values close to 1 indicating that the biomarker's effectiveness is relatively large and values close to 0 indicating limited effectiveness (Schisterman et al., 2005) YI=sensibility+specificity-1.

RESULTS

The strains used in this study were unrelated; they were collected from two different hospitals, different medical and surgical wards, and at different time periods (Table 1). The positive control sample showed with method C no inhibition zone around disk (lysate-IMP) and 15 mm inhibition zone around disk (lysate-IMP-EDTA) (Figure 1). *P. aeruginosa* ATCC27853 sample (harbouring no resistance mechanism) showed, under the study experimental conditions, 16.87±1.76 inhibition zone around the disk (lysate-IMP).

Several tests were carried out on the negative control strain (*P. aeruginosa* ATCC27853). The lysate-IMP disk showed no upper than 5 mm decrease compared to the IMP disk, which represents the upper bound of MBL-negative strain and obviously the lower bound of MBL-positive strain. In fact, a decrease in the inhibition zone of >5 mm represents a strong argument for judging a positive strain by this assay. Disks impregnated with EDTA (0.5M) alone and lysate alone showed no inhibition zone with the indicator strain (Figure1).

Method C was compared to the two phenotypic methods considered in this study (method A and method B) and to the molecular method (PCR) as a reference method. Among the three phenotypic methods considered in this study, method A showed 100% of sensitivity. Method B and method C showed 91.66% of sensitivity. The highest level of specificity was shown by method C (76.92%), followed by method B (69.23%) than method A (23.07%) (Table 1). To evaluate efficiencies of methods, the study noted that the highest Youden Index (YI) was shown by method C (0.7), followed by method B (0.6) than method A (0.2).

DISCUSSION

There is an urgent need for an early detection of MBL-producing organisms for their prevention of their inter and intra hospital dissemination. Currently, the most widely accepted standardized MBL functional screen is the MBL E-test. However, this method suffers from high cost and unavailability of E-test strips. Both CDT and DDST have been reported to be reliable in screening for MBL production in *P. aeruginosa* (Yan et al., 2004). It has

been reported that CDT and DDST were simple, inexpensive phenotypic resources for detection of MBL that could be easily incorporated into the routines of clinical laboratories. In Tunisian clinical laboratories, for its high cost, the MBL E-test is not frequently used. Generally this test is used for research purposes and not for routine screening of MBL.

Although, MBL E-test has been evaluated to be a sensitive method for detection of MBL production in *P. aeruginosa* (Walsh et al., 2002). Qu et al. (2009) reported that several MBL-producing strains could not be detected by the MBL E-test. Several studies have been interested in evaluation and comparison of phenotypic tests (Yan et al., 2004; Picao et al., 2008; Qu et al., 2009). Variable results have been reported. Yan et al. (2004) found that the DDST was most sensitive for all bacterial species tested (Yan et al., 2004). However, one of the major disadvantages of the DDST is the subjective interpretation of results that depends upon the technician's expertise to discriminate true synergism from the intersection of inhibition zones (Picao et al., 2008; Qu et al., 2009). Other studies evaluated the CDT as most sensitive method (Berges et al., 2007; Picao et al., 2008). In this study, DDST was evaluated as more sensitive than CDT. Thus, it has been suggested that the selection of the best MBL screening method should be based on the isolated species, the local prevalence of MBL producers, and the ability of specialized technicians to correctly interpret MBL inhibition (Yan et al., 2004; Picao et al., 2008).

False detection of MBL in *P. aeruginosa* by E-test, CDT and DDST depend on EDTA susceptibility (Chu et al., 2005). It is known that EDTA may increase bacterial cell wall permeability and so it can increase the susceptibility of *P. aeruginosa* to various antimicrobials, including IMP (Ayres et al., 1999). Tan et al. (2008) proposed an IMP-lysate MBL assay that overcomes the major disadvantage of the three phenotypic methods; the direct bactericidal EDTA effect on the test strain (Tan et al., 2008). It provides a simple, inexpensive and reproducible functional screen for MBL-producing *P. aeruginosa*. However, that technique requires special equipment, specifically the Microcon Device. Due to the cost and the scarcity of the device, it is typically not available in laboratories. Thus, the study modified the technique to adapt it to laboratory's conditions. After the elimination of the step of enzyme-concentration from the original protocol, screening of MBL bla_{VIM} producing *P. aeruginosa* is still simple and easy. Importantly, EDTA still has little effect on the indicator strain.

In this study, method C showed 91.66% of sensitivity and 76.92% of specificity, and referring to Youden test, method C was more efficient than method A and B.

Conclusion

Since MBL-Etest and PCR were expensive and not adaptable for extension use in clinical microbiology laboratories, a modified IMP-lysate MBL hydrolytic activity can be chosen by laboratories with limited resources as an inexpensive, simple, and accurate test to detect *P. aeruginosa* producing bla_{VIM} type enzyme.

ACKNOWLEDGEMENTS

The authors would like to thank the leaders of the "Unité de Recherche en Maladies Infectieuses et Tropicales Emergentes (URMITE) Aix-Marseille France" for allowing them to identify strains by MALDI-TOF.

Conflict of interests

The author(s) did not declare any conflict of interest.

REFERENCES

Andrade SS, Picao RC, Campana EH, Nicoletti AG, Pignatari AC, Gales AC (2007). Influence of disk preparation on detection of metallo-beta-lactamase-producing isolates by the combined disk assay. J. Clin. Microbiol. 45:2058-2060

Aubron C, Poirel L, Fortineau N, Nicolas P, Collet L, Nordmann P (2005). Nosocomial spread of *Pseudomonas aeruginos*a isolates expressing the metallo-beta-lactamase VIM-2 in a hematology unit of a French hospital. Microb. Drug Resist. 11:254-259

Ayres HM, Furr JR, Russell AD (1999). Effect of permeabilizers on antibiotic sensitivity of *Pseudomonas aeruginosa*. Lett. Appl. Microbiol. 28:13-16

Berges L, Rodriguez-Villalobos H, Deplano A, Struelens MJ (2007). Prospective evaluation of imipenem/EDTA combined disc and Etest for detection of metallo-beta-lactamase-producing *Pseudomonas aeruginosa*. J. Antimicrob. Chemother. 59:812-813

Chu YW, Cheung TK, Ngan JY, Kam KM (2005). EDTA susceptibility leading to false detection of metallo-beta-lactamase in *Pseudomonas aeruginosa* by Etest and an imipenem-EDTA disk method. Int. J. Antimicrob. Agents 26:340-341

Conejo MC, Garcia I, Martinez-Martinez L, Picabea L, Pascual A (2003). Zinc eluted from siliconized latex urinary catheters decreases OprD expression, causing carbapenem resistance in *Pseudomonas aeruginosa*. Antimicrob. Agents Chemother. 47:2313-2315

Hammami S, Boutiba-Ben B, I, Ghozzi R, Saidani M, Amine S, Ben RS (2011). Nosocomial outbreak of imipenem-resistant *Pseudomonas aeruginosa* producing VIM-2 metallo-beta-lactamase in a kidney transplantation unit. Diagn. Pathol. 6:106

Hammami S, Gautier V, Ghozzi R, Da CA, Ben-Redjeb S, Arlet G (2010). Diversity in VIM-2-encoding class 1 integrons and occasional bla_{SHV-2a} carriage in isolates of a persistent, multidrug-resistant *Pseudomonas aeruginosa* clone from Tunis. Clin. Microbiol. Infect. 16:189-193

Jacobson RK, Minenza N, Nicol M, Bamford C (2012). VIM-2 metallo-beta-lactamase-producing *Pseudomonas aeruginosa* causing an outbreak in South Africa. J. Antimicrob. Chemother. 67:1797-1798

Kaye KS, Pogue JM (2015). Infections Caused by Resistant Gram-Negative Bacteria: Epidemiology and Management. Pharmacotherapy 35:949-962.

Ktari S, Mnif B, Znazen A, Rekik M, Mezghani S, Mahjoubi-Rhimi F, Hammami A (2011). Diversity of beta-lactamases in Pseudomonas aeruginosa isolates producing metallo-beta-lactamase in two Tunisian hospitals. Microb. Drug Resist. 17:25-30

Lee K, Chong Y, Shin HB, Kim YA, Yong D, Yum JH (2001). Modified Hodge and EDTA-disk synergy tests to screen metallo-beta-lactamase-producing strains of Pseudomonas and Acinetobacter

species. Clin. Microbiol. Infect. 7:88-91
Lee K, Lim YS, Yong D, Yum JH, Chong Y (2003). Evaluation of the Hodge test and the imipenem-EDTA double-disk synergy test for differentiating metallo-beta-lactamase-producing isolates of *Pseudomonas* spp. and *Acinetobacter* spp. J. Clin. Microbiol. 41:4623-4629
Liu Q, Li X, Li W, Du X, He JQ, Tao C, Feng Y (2015). Influence of carbapenem resistance on mortality of patients with *Pseudomonas aeruginosa* infection: a meta-analysis. Sci. Rep. 5:11715
Maltezou HC (2009). Metallo-beta-lactamases in Gram-negative bacteria: introducing the era of pan-resistance? Int. J. Antimicrob. Agents 33:405-407
Mansour W, Poirel L, Bettaieb D, Bouallegue O, Boujaafar N, Nordmann P (2009). Metallo-beta-lactamase-producing *Pseudomonas aeruginosa* isolates in Tunisia. Diagn. Microbiol. Infect. Dis. 64:458-461
Mazzariol A, Mammina C, Koncan R, Di G, V, Di CP, Cipolla D, Corsello G, Cornaglia G (2011). A novel VIM-type metallo-beta-lactamase (VIM-14) in a *Pseudomonas aeruginosa* clinical isolate from a neonatal intensive care unit. Clin. Microbiol. Infect. 17:722-724
Oliver A, Mulet X, Lopez-Causape C, Juan C (2015). The increasing threat of *Pseudomonas aeruginosa* high-risk clones. Drug Resist. Updat. 21-22:41-59
Peter S, Lacher A, Marschal M, Holzl F, Buhl M, Autenrieth I, Kaase M, Willmann M (2014). Evaluation of phenotypic detection methods for metallo-beta-lactamases (MBLs) in clinical isolates of *Pseudomonas aeruginosa*. Eur. J. Clin. Microbiol. Infect. Dis. 33(7):1133-1141.
Picao RC, Andrade SS, Nicoletti AG, Campana EH, Moraes GC, Mendes RE, Gales AC (2008). Metallo-beta-lactamase detection: comparative evaluation of double-disk synergy versus combined disk tests for IMP-, GIM-, SIM-, SPM-, or VIM-producing isolates. J. Clin. Microbiol. 46:2028-2037
Pitout JD, Revathi G, Chow BL, Kabera B, Kariuki S, Nordmann P, Poirel L (2008). Metallo-beta-lactamase-producing *Pseudomonas aeruginosa* isolated from a large tertiary centre in Kenya. Clin Microbiol. Infect. 14:755-759.
Qu TT, Zhang JL, Wang J, Tao J, Yu YS, Chen YG, Zhou JY, Li LJ (2009). Evaluation of phenotypic tests for detection of metallo-beta-lactamase-producing *Pseudomonas aeruginosa* strains in China. J. Clin. Microbiol. 47:1136-1142.
Sardelic S, Bedenic B, Colinon-Dupuich C, Orhanovic S, Bosnjak Z, Plecko V, Cournoyer B, Rossolini GM (2012). Infrequent finding of metallo-beta-lactamase VIM-2 in carbapenem-resistant *Pseudomonas aeruginosa* strains from Croatia. Antimicrob. Agents Chemother. 56:2746-2749.
Schisterman EF, Perkins NJ, Liu A, Bondell H (2005). Optimal cut-point and its corresponding Youden Index to discriminate individuals using pooled blood samples. Epidemiology 16:73-81.
Seng P, Drancourt M, Gouriet F, La SB, Fournier PE, Rolain JM, Raoult D (2009). Ongoing revolution in bacteriology: routine identification of bacteria by matrix-assisted laser desorption ionization time-of-flight mass spectrometry. Clin. Infect. Dis. 49:543-551
Tan J, Pitout JD, Guttman DS (2008). New and sensitive assay for determining *Pseudomonas aeruginosa* metallo-beta-lactamase resistance to imipenem. J. Clin. Microbiol. 46:1870-1872
Touati M, Diene SM, Dekhil M, Djahoudi A, Racherache A, Rolain JM (2013). Dissemination of a class I integron carrying VIM-2 carbapenemase in *Pseudomonas aeruginosa* clinical isolates from a hospital intensive care unit in Annaba, Algeria. Antimicrob. Agents Chemother. 57:2426-2427
Viedma E, Juan C, Villa J, Barrado L, Orellana MA, Sanz F, Otero JR, Oliver A, Chaves F (2012). VIM-2-producing multidrug-resistant *Pseudomonas aeruginosa* ST175 clone, Spain. Emerg. Infect. Dis 18:1235-1241
Walsh TR, Bolmstrom A, Qwarnstrom A, Gales A (2002). Evaluation of a new Etest for detecting metallo-beta-lactamases in routine clinical testing. J. Clin. Microbiol. 40:2755-2759.
Watanabe M, Iyobe S, Inoue M, Mitsuhashi S (1991). Transferable imipenem resistance in Pseudomonas aeruginosa. Antimicrob. Agents Chemother. 35:147-151
Yagi T, Kurokawa H, Shibata N, Shibayama K, Arakawa Y (2000). A preliminary survey of extended-spectrum beta-lactamases (ESBLs) in clinical isolates of *Klebsiella pneumoniae* and Escherichia coli in Japan. FEMS Microbiol. Lett. 184:53-56
Yan JJ, Wu JJ, Tsai SH, Chuang CL (2004). Comparison of the double-disk, combined disk, and Etest methods for detecting metallo-beta-lactamases in gram-negative bacilli. Diagn. Microbiol. Infect. Dis. 49:5-11
Yong D, Lee K, Yum JH, Shin HB, Rossolini GM, Chong Y (2002). Imipenem-EDTA disk method for differentiation of metallo-beta-lactamase-producing clinical isolates of *Pseudomonas spp*. and *Acinetobacter spp*. J. Clin. Microbiol. 40:3798-3801.

African Journal of Biotechnology

Related Journals Published by Academic Journals

Biotechnology and Molecular Biology Reviews
African Journal of Microbiology Research African Journal of Biochemistry Research African Journal of Environmental Science and Technology
African Journal of Food Science
African Journal of Plant Science
Journal of Bioinformatics and Sequence Analysis
International Journal of Biodiversity and Conservation

academicJournals